Eawag_06820

Diss. ETH N° 19289

Toxicity of Diazinon in *Daphnia magna* - a Mechanistic Effect Model Based on Time-resolved Quantification of Bioconcentration, Biotransformation and Enzyme Inhibition

A dissertation submitted to

ETH ZURICH

for the degree of
Doctor of Sciences

presented by

ANDREAS CHRISTOPHER KRETSCHMANN
Dipl. Chemiker (Friedrich-Alexander Universität Erlangen-Nürnberg)

born on August 5, 1979 in Nürnberg
Citizen of Germany

accepted on the recommendation of
PD Dr. Beate I. Escher, examiner
Prof. Dr. Juliane Hollender, co-examiner
Prof. Dr. Jukka Jokela, co-examiner
Dr. Tjalling Jager, co-examiner

Zurich, 2010

Table of Contents

Summary.....I

Zusammenfassung.....IV

Chapter 1: General Introduction.....1

Chapter 2: General Introduction to TK and TD processes of organophosphates in (aquatic) organisms and on TKTD modeling..... ..7

Chapter 3: Mechanistic Toxicodynamic Model for Receptor-mediated Toxicity of Diazoxon, the Active Metabolite of Diazinon, in *Daphnia magna*..... 21

Supporting information for chapter 3.....35

Chapter 4: Mechanistic Effect Model for Receptor-mediated Toxicity of Diazinon in *Daphnia magna*..... 57

Supporting information for chapter 4.....73

Chapter 5: Mechanistic Effect Model for Diazinon in *Daphnia magna*..... 97

Chapter 6: Conclusions and Outlook.....115

References.....119

Danksagung - Acknowledgements.....127

Curriculum Vitae.....129

Summary

Understanding the fate of a xenobiotic inside an aquatic organism is crucial to predict its hazardous effects under environmental conditions. The severity of a toxic effect caused by an environmental pollutant is determined by toxicokinetic (TK) and toxicodynamic (TD) processes. TK processes determine the time course of a toxicant's uptake, elimination, metabolism and distribution within an organism, TD processes describe the interaction of the active form of the chemical with the molecular target site in an organism and its link to the observed effect. TKTD models combine both TK and TD processes and relate concentrations of chemicals detected in the environment with the final effect.

The overall goal of this PhD thesis was to develop a time-resolved TKTD model for the water flea *Daphnia magna* to predict toxic effects of organophosphorus insecticides. A detailed kinetic and mechanistic analysis of TK processes as well as of the TD interaction with the target site was performed in *in vivo* and *in vitro* studies and the derived TK and TD parameters incorporated in the model. The model specifically considers the role played by active and inactive metabolites formed inside the organism and links the effect on molecular scale with the effect on organism scale. The phosphorothionate insecticide diazinon served as model compound.

In the first part of this thesis the TD phase of diazinon in *D. magna* was systematically analyzed using *in vitro* and *in vivo* experiments. The TD phase consists of the inhibition of the target site acetylcholinesterase (AChE) by the active metabolite diazoxon, which triggers the toxic effect on organism level (immobilization, mortality). In enzymatic experiments with diazoxon and enzymatically active extract of *D. magna* the underlying inhibition mechanism of AChE was elucidated and the kinetics of inhibition determined. Inhibition was demonstrated to be an irreversible reaction with the AChE in two steps via an intermediate enzyme-inhibitor complex. Comparison of the kinetic parameters with literature values for different species revealed a very high affinity of diazoxon towards daphnids` AChE. This is in accordance with the in general high sensitivity of this species towards organophosphorus compounds. In addition to inhibition, restoration of AChE activity i.e. when exposed animals are transfered into toxicant free medium was considered in the TD model and analyzed *in vivo*. Although recovery from the molecular effect appeared to be possible, no return from immobilization to normal condition was observed once daphnids' mobility was affected and death was inevitable. The confirmed inhibition mechanism, the corresponding inhibition rate constants and the kinetics describing recovery of enzyme activity were combined in a process-based TD model. This model, which assumes death to occur as a chance process (hazard model) as soon as AChE activity falls below a certain threshold value, accurately described the *in vivo* time course of immobilization/ mortality in dependence of the AChE activity during exposure to diazinon. A special feature of the TD model is that it was parameterized with both, *in vitro* and *in vivo* data and that it enabled the calculation of the absolute amount of the toxic metabolite directly present at the target site.

The second part of this thesis deals with the TK phase considering the processes passive uptake and elimination of diazinon into and out of the organism, enzymatic activation to its toxic metabolite

diazoxon as well as enzymatic detoxification processes including dearylation of diazinon to its metabolite pyrimidinol. In *in vivo* experiments *D. magna* were exposed to diazinon with and without inhibition of the activation step. After different exposure times the internal concentrations of the parent compound as well as of the metabolites were measured with HPLC-MS/MS. The rate constants of the different TK steps were obtained by modeling the time course of the internal concentrations with a one-compartment first-order kinetics model. The results confirmed that diazinon is biotransformed extensively in *D. magna*. The major elimination step of diazinon was found to be its detoxification to pyrimidinol. Activation to its toxic metabolite diazoxon amounted to only 8 % of the total elimination. Although activation has only a minor quantitative role this is of course the relevant step leading to TD. Detected diazoxon concentrations in the organism were in general too low for a clear identification and quantification. This observation can be explained by (a) a low activation rate and/ or (b) elimination processes that are very fast compared to the activation rate, e.g. a fast reaction with the target site AChE.

Internal concentrations in aquatic organisms are usually normalized to the wet weight of the organism. Since the rather lipophilic diazinon is likely to accumulate mainly in the lipid phase in *D. magna*, the influence of the lipid content on bioconcentration kinetics was also evaluated. As recommended in standard toxicity test guidelines our daphnids were not fed during the exposure experiments. Under these conditions a decline in lipid content was observed. For a short exposure duration (20 h) the lipid content had only a minor influence compared to the variability between the experiments. Since after 48 h the lipid content was reduced by approx. 50 %, while in parallel the wet weight increased, the time course of lipid content might indeed play an important role for longer exposure times. That factor is hardly considered in present bioconcentration studies with *Daphnia* and warrants further research.

As a last step all TK and TD parameters derived *in vivo* and *in vitro* were combined to a comprehensive time-resolved effect model for receptor-mediated toxicity in *D. magna*. This TKTD model could accurately predict the time course of active AChE and immobilization/mortality in dependence of the internal concentrations of diazinon and its metabolites during exposure to diazinon. A misfit of the internal diazoxon concentration, which was especially pronounced at low diazinon exposure concentrations, indicates a probable induction of the activating enzyme cytochrome P450 monooxygenase, which was not considered in the proposed model. A comparison of the TD and TK data revealed that despite the low activation rate from diazinon to diazoxon the extremely high sensitivity of the target site AChE is responsible for the high toxicity of diazinon towards *D. magna*. Recovery of AChE activity after exposure to diazinon was found to be very slow in relation to the TK processes. TD processes are therefore rate limiting for the overall process leading to the observed toxicity. This is an important finding since subsequent pulses of diazinon might lead to an accumulation of internal damage to critical levels although bioconcentration kinetics would predict complete recovery.

The developed process-based effect model, which takes account of internally formed metabolites and the effect on a molecular scale, allows insight in the complex interaction of biochemical processes

combining the initial exposure with the final effect. The model features time resolution and is therefore a useful tool for the prediction of toxic effects of xenobiotics under fluctuating and time-variable exposure conditions, which will ultimately inform risk assessment.

Zusammenfassung

Um schädliche Effekte einer Chemikalie in einem aquatischen Organismus unter Umweltbedingungen abschätzen zu können, ist es essentiel, die zugrunde liegenden Mechanismen und Prozesse zu verstehen. Toxikokinetische (TK) und toxikodynamische (TD) Prozesse bestimmen das Ausmass eines toxischen Effekts, der durch einen Schadstoff in einem Organismus verursacht wird. TK Prozesse beschreiben den zeitlichen Verlauf der Aufnahme einer Chemikalie in den Organismus, der Elimination, der Metabolisierung und Verteilung innerhalb eines Organismus. TD Prozesse beschreiben die Wechselwirkung der aktiven Form einer Chemikalie mit dem molekularem Zielort und dessen Link mit dem beobachteten Effekt. Modelle, die TK und TD Prozesse kombinieren und in der Umwelt gemessene Chemikalienkonzentrationen mit dem beobachtbaren Effekt in Beziehung setzen können, sind TKTD Modelle.

Das Ziel dieser Doktorarbeit war die Entwicklung eines zeitaufgelösten TKTD Modells für den Wasserfloh *D. magna*, das die Vorhersage von toxischen Effekten von Organophosphat-Insektiziden ermöglicht. Eine detailierte kinetische und mechanistische Analyse von TK Prozessen und der TD Wechselwirkung mit dem Zielort wurde mit Hilfe von *in vitro* und *in vivo* Experimenten durchgeführt und die abgeleiteten TK und TD Parameter in das Modell eingefügt. Das Modell berücksichtigt explizit die Bildung von aktiven und inaktiven Metaboliten im Organismus und verbindet den Effekt auf molekularer Ebene mit dem Effekt auf organisatorischer Ebene des Organismus. Als Modellchemikalie wurde das Insektizid Diazinon ausgewählt, welches zur Gruppe der Thiophosphorsäureester gehört.

Im ersten Teil dieser Arbeit wurde die TD Phase von Diazinon in *D. magna* mit *in vitro* und *in vivo* Experimenten systematisch analysiert. Die TD Phase besteht aus der Inhibition des Zielorts Acetylcholinesterase (AChE) durch den aktiven Metaboliten Diazoxon, welche den toxischen Effekt auf Organismenebene (Immobilisation, Mortalität) verursacht. In Experimenten mit Diazoxon und enzymatisch aktiven Extrakten von *D. magna* wurde der der AChE Inhibition zugrunde liegende Mechanismus und die entsprechende Kinetik untersucht. Hier wurde eine irreversible Inhibition, welche in zwei Schritten über einen intermediären Enzym-Inhibitor Komplex verläuft, nachgewiesen. Ein Vergleich der kinetischen Parameter mit Literaturwerten für unterschiedliche Organismen zeigte eine extrem hohe Affinität von Diazoxon zu der AChE von *D. magna*. Dies ist in Uebereinstimmung mit einer generell hohen Sensitivität von Wasserflöhen gegenüber Organophosphatverbindungen. Neben Inhibition wurde auch die Erholung und Wiederzunahme der AChE-Aktivität, z.B. wenn Tiere nach Exposition zu Diazinon in sauberes Medium gesetzt wurden, im Modell berücksichtigt und *in vivo* untersucht. Obwohl eine Erholung vom molekularen Effekt beobachtet werden konnte, war dies nicht der Fall für die Immobilisierung: Waren die Daphnien einmal immobilisiert, war keine Rückkehr zum Normalzustand möglich und Mortalität war unausweichlich. Der nachgewiesene Inhibitonsmechanismus wurde zusammen mit den ermittelten kinetischen Parametern für Inhibition und Erholung in einem prozess-orientierten TD Modell vereinigt. Dieses Modell, welches das Eintreten von Mortalität, sobald ein bestimmter Schwellenwert für AChE Aktivität unterschritten ist, als einen stochastischen Prozess annimmt, war in der Lage, den zeitlichen Verlauf des Anteils überlebender

Tiere während Exposition zu Diazinon korrekt zu beschreiben. Eine Besonderheit dieses Modells ist seine Parameterisierung mit einer Kombination aus *in vivo* und *in vitro* Daten. Dies ermöglichte die Berechnung des absoluten Betrags an toxischem Metabolit unmittelbar präsent am Zielort AChE.

Der zweite Teil dieser Arbeit behandelt die TK Phase unter Berücksichtigung von Prozessen wie passive Aufnahme von Diazinon in den Wasserfloh und Elimination in die umgebende Wasserphase, enzymatische Aktivierung zum toxischen Metaboliten Diazoxon und enzymatische Detoxifizierungsprozesse, wie z.B. Dearylierung von Diazinon zum Metaboliten Pyrimidinol. In *in vivo* Experimenten wurde *D. magna* Diazinon ausgesetzt und die Aufnahmekinetik mit bzw. ohne gleichzeitiger Inhibition des Aktivierungsschrittes untersucht. Nach unterschiedlichen Expositionszeiten wurden die internen Konzentrationen der Ausgangssubstanz und deren Metabolite mit HPLC-MS/MS gemessen. Die Geschwindigkeitskonstanten der unterschiedlichen TK Schritte wurden durch Beschreibung des zeitlichen Verlaufs der internen Konzentrationen mittels einem Modell ermittelt, das auf einem Kompartiment mit Kinetik erster Ordnung beruhte. Die Ergebnisse zeigen, das Diazinon in *D. magna* in hohem Masse metabolisch umgesetzt wird. Hierbei wird Diazinon zum Grossteil durch Detoxifizierung zu Pyrimidinol eliminiert. Die Aktivierung zum toxischen Metaboliten betrug nur 8 % der Gesamtelimination. Obwohl dieser Prozess quantitativ gesehen eine untergeordnete Rolle spielt, ist dies der entscheidende Schritt, welcher zu TD führt. Diazoxonkonzentrationen im Organismus waren im Allgemeinen zu niedrig für eine klare Identifizierung und Quantifizierung. Mögliche Erklärungen sind (a) die niedrige Aktivierungsrate und (b) Eliminationsprozesse, die im Vergleich zur Ausgangssubstanz Diazinon sehr schnell ablaufen, z.B. eine schnelle Reaktion mit AChE.

Interne Konzentrationen werden für aquatische Organismen in der Regel auf das Nassgewicht bezogen. Da sich das lipophile Diazinon mit hoher Wahrscheinlichkeit in der Lipidphase von *D. magna* anreichert, wurde untersucht, inwieweit der Fettgehalt die Biokonzentrationskinetiken beeinflusst. Unter Bedingungen, die für Standard-Toxizitätstests empfohlen werden (keine Fütterung der Daphnien), konnte eine Abnahme des Lipidgehalts beobachtet werden. Für Expositionszeiten unter 20 h hatte dies nur eine geringe Auswirkung auf die Variabilität, die zwischen den einzelnen Expositionsexperimenten beobachtet wurde. Da der Lipidgehalt nach 48 h auf 50 % reduziert war und gleichzeitig das Nassgewichts zunahm, kann die zeitliche Abnahme des Lipidgehalts für längere Expositionszeiten in der Tat eine wichtige Rolle spielen. Dieser Umstand wurde bisher in Biokonzentrationsstudien mit Daphnien kaum berücksichtigt.

In einem letzten Schritt wurden alle beschriebenen *in vivo* und *in vitro* TK und TD Prozesse vereinigt zu einem zeitlich aufgelösten Modell zur Beschreibung von auf Rezeptorwechselwirkung basierenden toxischen Effekten in *D. magna*. Der zeitliche Verlauf von aktiver AChE und Immobilisation/ Mortalität in Abhängigkeit der internen Diazinon- und Metabolitkonzentrationen während Exposition zu Diazinon konnten mit diesem Modell akkurat simuliert werden. Keine gute Uebereinstimmung wurde für Diazoxon gefunden, insbesondere für niedrige Expositionskonzentrationen, was auf eine mögliche Induktion von Cytochrom P450 Monooxygenase hindeutet, die wiederum in unserem Modell nicht berücksichtigt wurde.

Ein Vergleich der TK und TD Daten identifizierte die hohe Sensitivität der AChE, im Gegensatz zur niedrigen Aktivierungsrate, als ausschlaggebenden Faktor für die hohe Toxizität von Diazinon gegenüber *D. magna*. Der Wiederanstieg der AChE-Aktivität nach Exposition zu Diazinon wurde als sehr langsam im Vergleich zur Elimination von Diazinon und Diazoxon nachgewiesen. TD Prozesse sind demnach geschwindigkeitsbestimmend für den letzlich beobachteten Effekt. Dies ist eine wichtige Erkenntnis, da demnach der interne Schaden nach aufeinanderfolgenden Diazinonpulsen sich bis zu kritischen Werten aufsummieren kann, obwohl Biokonzentrationskinetiken isoliert betrachtet eine vollständige Erholung der Organismen vorhersagen.

Das entwickelte, prozess-basierte Effektmodell, welches ausdrücklich intern gebildete Metaboliten und den Effekt auf molekularer Ebene berücksichtigt, ermöglicht einen Einblick in das komplexe Wechselspiel von biochemischen Prozessen, welche die Exposition mit dem biologischen Effekt verbinden. Seine zeitliche Auflösung macht das Modell zu einem nützlichen Instrument für die Vorhersage von toxischen Effekten von Umweltschadstoffen unter fluktuierenden und zeitlich variablen Expositionsbedingungen.

Chapter 1

General introduction

General introduction

Toxicity is the property of a chemical that causes a harmful effect upon a biological system (Landis and Yu 1995). Mechanistic toxicology describes the processes, which lead from initial exposure to a toxicant to the resulting toxic injury in an organism. The underlying mechanism of the toxic effect consists of various causal and sequential processes on the molecular scale (Boelsterli 2007).

All events between exposure and effect can be divided into two groups: Toxicokinetic (TK) and toxicodynamic (TD) processes (see Figure 1.1). Toxicokinetics describe the time course of a chemical in an organism and consist of processes like uptake, distribution, biotransformation and (passive) elimination. In other words toxicokinetics describe "what the organism does to the chemical" (Rozman and Doull 2000; Boelsterli 2007). In contrast TD processes describe the dynamic interaction of a compound with the biological target site and the successive biological effects ("what a chemical does to the organism"). Toxicodynamics include accrual of damage as well as recovery from damage e.g. by repair mechanisms, reversibility of the toxic effect and/ or adaption of the organism. The ratio of injury to recovery governs the time course of the toxic effect. In summary toxicity can be regarded as function of exposure (dose and exposure time), toxicokinetics and toxicodynamics (McCarty and Mackay 1993; Rozman and Doull 2000; Boelsterli 2007).

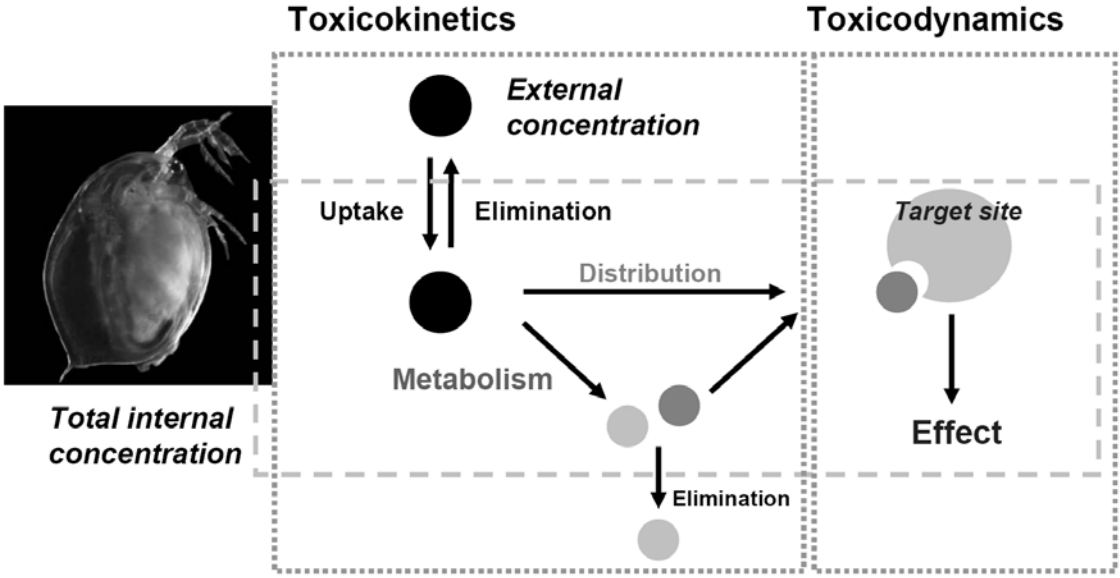

Figure 1.1. *Schematic illustration of toxicokinetic and toxicodynamic events, which lead from initial exposure to a toxicant to the final effect.*

According to (Verhaar et al. 1992; Escher and Hermens 2002) chemicals can be classified in different mode of actions based on their underlying mechanism of interaction with the target site. In general sites of toxic action can be cellular membranes, proteins and/ or DNA. Narcotic chemicals cause a reversible toxic response by partitioning into cell membranes which leads to a nonspecific disturbance of the membrane structure and function (Van Wezel and Opperhuizen 1995). The potency of narcotics depends solely on their bioconcentration potential as effective internal concentrations are constant and independent of the

type of chemical. This mode of action is exerted by any chemical (called minimum or baseline toxicity) but is often masked by a more potent specific mode of action. Reactive compounds possess enhanced toxicity compared to baseline toxicity and are chemicals, which react selectively or unselectively with functional groups of biomolecules under formation of a covalent bond (Hermens 1990; Verhaar et al. 1992). Toxicants with a specific mode of action interact with certain receptor molecules in a reversible or irreversible way e.g. the interaction with enzymes, which leads to inhibiton of the enzymatic activity, or binding to receptors leading to activation or deactivation of the associated pathway. The toxicity of reactive and specific acting compounds is typically 10 - 10^4 times higher than predicted with Quantitative Structure Activity Relationship (QSAR) for baseline toxicity (Verhaar et al. 1992).

The toxic response of an organism therefore depends on the type of the target site, the type of interaction of the toxicant with the target site and the concentration at the target site. In case of specific receptor mediated effects the intrinsic potency of a compound also depends on the affinity of the toxicant to the receptor (Escher and Hermens 2002). For the predicition of the overall toxic response exhibited by an organism it is therefore essential to know and quantify the underlying processes, which determine the target site concentration (toxicokinetics) and the interaction with the target site (toxicodynamcis). Since TK and TD processes are compound and species specific this knowledge is also important for the understanding of species selectivity and sensitivity (Escher and Hermens 2002).

A well known example for specifically acting compounds are organophosphorus compounds (OPs). Within the last decades these compounds became the dominant class of insecticides worldwide (e.g. 70 % of total insecticide use in U.S. 2001 (EPA 2004)) because of their high insecticidal efficiency and their usually low persistence in the environment with a half life of several hours to maximally several weeks (Chambers 1992; Racke 1992; Boelsterli 2007). A major drawback is their high acute toxicity also to non-target organisms and their associated risk of secondary poisoning (Elliott et al. 1997; Mineau et al. 1999). Especially aquatic organisms are at risk due to water runoff from agricultural fields after rainevents (Holmes and de Vlaming 2003; Pedersen et al. 2006; EPA 2008). Comparison of acute effect concentrations of organophosphorus pesticides for different aquatic species reveals an extremely large variation of up to six orders of magnitude. Especially daphnids are among the most sensitive species (Vaal et al. 1997b). Acute toxic effects of organophosphorus compounds are mainly, if not entirely, related to inhibition of the enzyme acetylcholinesterase (AChE) (Chambers 1992). AChE is responsible for the fast breakdown of the neurotransmitter acetylcholine present in the central nervous system and the peripheral nervous system in various organs (Boelsterli 2007).

A large group of OP insecticides belong to the class of phosphorothionates e.g. diazinon, parathion and chlorpyrifos. These chemicals are poor AChE inhibitors itself and have to be metabolically activated by cytochrome P450-dependent monooxygenases to their respective oxon analogues in order to exhibit their toxic potency (Forsyth and Chambers 1989; Keizer et al. 1995). In contrast to activation phosphorothionates and their oxons can also be metabolically detoxified by several oxidative and hydrolytic

reactions (Chambers et al. 1994; Tang and Chambers 1999; Poet et al. 2003) or also by binding to non-critical enzymes like carboxylesterase (Maxwell 1992; Barata et al. 2004). The complex interaction of TK and TD processes as it is the case for OP compounds lead to a pronounced species selectivity and time dependency of OP toxicity (Chambers and Carr 1995; Legierse et al. 1999). For example a decrease of LC_{50} values with increasing exposure times, even after steady state between the exposure concentration and the concentration inside the organism is reached, was observed for aquatic organism exposed to OPs due to rate determining TD processes (Legierse et al. 1999).

In current environmental risk assessment methodology chemicals are commonly assessed by determining effect levels after exposure of aquatic organisms to constant concentrations over a fixed period of time (e.g. 48 h LC_{50} values, lethal concentration after 48 h for 50 % of the organisms tested). This approach does not account for time dependency of toxicity and cannot mechanistically explain observed differences in species sensitivities (Jager et al. 2006).

Tools for the prediction of toxic effects, which are capable to deal with such complex toxic mechanisms as it is the case for organothiophosphates and explicitely account for the time dependency of toxicity, are process-based TK and TD models (Jager et al. 2006; Ashauer et al. 2010). TK and TD models link toxicokinetic and toxicodynamic processes and are able to translate time-variable exposure to toxicants into time course of effects. Existing models are for example the threshold damage assessment model (TDM) (Ashauer et al. 2007a), the critical target occupation model (CTO) (Legierse et al. 1999) and the DEBtox receptor kinetics model (Jager and Kooijman 2005). The TDM is designed to deal with a broad range of chemicals and different modes of action, the latter two were designed especially for receptor mediated toxicity by OPs. In the TDM the internal damage and the corresponding kinetic parameters are not further specified. The latter two models make an a priori assumption about the inhibition mechanism. Within these models biotransformation processes are not considered or are based on assumption since they were not verified and quantified via measured metabolite concentrations. The TD part (internal damage) is parameterized solely via *in vivo* data on the external effect (survival).

The goal of this work was therefore to develop a time-resolved TKTD model for the prediction of toxic effects of OP insecticides, which provides a coherent and mechanistic picture from initial exposure to the final effect, as it is shown in Figure 1.1. In contrast to the above mentioned models it explicitely links measured active and inactive metabolites formed during the TK phase and measured AChE activity with the observed external effect in dependence of time. The underlying inhibition mechanism is explicitely elucidated with *in vitro* experiments. In our study the freshwater crustacean *D. magna* served as model organism and the phosphorothionate insecticide diazinon as model compound.

In the first part of this work (chapter 3) we analysed the TD phase of diazinon in *D. magna* to answer the question “what does diazinon do to *D. magna*?”. Questions of interest were: What is the underlying mechanism and the respective kinetics of the inhibition of AChE by the toxic metabolite diazoxon? How is the intrinsic effect (AChE inhibition) linked to the external effect (immobilization, mortality) on a time scale?

Is recovery from AChE inhibition and/ or from immobilization possible? To answer these questions the mechanism and kinetics of AChE inhibition were analyzed with *in vitro* experiments with diazoxon and the time course of enzyme activity and immobilization/ survival monitored during exposure to acute concentrations of diazinon *in vivo*.

The second part (chapter 4) elucidated the TK processes to answer the question „what does *D. magna* do to diazinon?“. Here it was analyzed, how fast diazinon is taken up and eliminated, to what extent it is biotransformed to active or non-active products and what processes determine the time course of the toxic metabolite diazoxon. For this purpose internal concentrations of diazinon and its metabolites were measured in extracts of *D. magna* during *in vivo* exposure to diazinon. A further topic was how the lipid content in *D. magna* influences the TK parameters.

In chapter 5 all the obtained TK and TD parameter were combined in a comprehensive effect model. Within the developed model the basic structure of the above mentioned TKTD models was applied and extended/ modified in order to account for biotransformation processes and inhibition of the target site AChE.

Finally (chapter 6) the potential for application of the developed model in environmental risk assessment is discussed and future research directions are suggested.

Chapter 2

General introduction to TK and TD processes of organophosphates in (aquatic) organisms and on TKTD modeling

Model compound and model organism

Diazinon and the water flea *D. magna*

Diazinon was first produced commercially in 1952 by the Swiss Company Ciba-Geigy (later Novartis, afterwards Syngenta) (Larkin and Tjeerdema 2000). It belongs to the class of phosphorothionate insecticides. It is applied worldwide against pests and vermins in agriculture, households and gardens. E.g. in U.S. it has been one of the most widely used insecticides (13 million pounds used anually on agricultural sites, state 2008 (EPA 2008)). Although its use was constricted in the last years (since 2004 all residential use of diazinon cancelled in U.S.) due to its high risk to humans and to ecological systems (particularly mammals, birds, bees, fish and aquatic invertebrates) (EPA 2005; EPA 2008) it still can be detected regularly in the environment. Diazinon was for example detected in Swiss surface waters, often above the Swiss quality standard for biocidal compounds in surface waters (100 $ng \cdot L^{-1}$) and in single peaks in concentrations as high as 2.7 $\mu g \cdot L^{-1}$ (Wittmer et al. 2010).

In aquatic risk assessment the three species algae, water flea and fish play a key role in aquatic risk assessment. Especially acute and chronic toxicity tests with daphnids are performed most frequently in ecotoxicology because of their easy handling and culturing and the short reproduction times (Fent 1998). For this project the water flea *D. magna* Straus was chosen as model organism (recommended for toxicity testing in the OECD guideline 202, guideline for testing of chemicals; acute immobilisation test (OECD 2004)). This species is very sensitive to organophosphorous insecticides, the LC_{50}(48 h) for diazinon amounts to 0.8 $\mu g \cdot L^{-1}$ (Ankley et al. 1991). A single clone, called clone 5, was obtained from the Institute of Environmental Science at the RWTH Aachen and reared in our laboratories.

Acetylcholinesterase and its inhibition by organophosphorus compounds

Esterases catalyze the hydrolysis of a wide range of esters (Walker and Thompson 1991). In general esterases which are inhibited by OPs are classified as „B“ esterases whereas those which hydrolyze OP compounds and are not inhibited by them are termed „A“ esterases , (Aldridge 1953b; Walker and Thompson 1991). „B“ esterases consist of two major groups: the cholinesterases (ChEs) and the carboxylesterases (CbEs). CbEs hydrolyze a wide range of esters (Walker and Thompson 1991). ChEs hydrolyze preferentially cholinesters. Again ChEs can be divided in two subclasses: Acetylcholinesterase (AChE) and buturylcholinesterase (BuChE or pseudocholinesterase) (Eto 1974).

AChE occurs mainly in nervous tissues of the central nervous system, ganglia and motor end-plate (Eto 1974), where it is located e.g. on the presynaptic and postsynaptic membrane (Boelsterli 2007). It is responsible for the hydrolysis of the neurotransmitter acetylcholine (ACh) (Boelsterli 2007). During the degradation process of ACh it binds to a serine hydroxyl group in the active center under release of choline. AChE is rapidly reactivated by hydrolysis of the acetylated serine group (Landis and Yu 1995). The kinetics of this reaction can be described by the Michaelis-Menten equation:

$$v = \frac{v_{max} \cdot S}{K_m + S} \quad (2.1)$$

v and v_{max} in $nmol \cdot mg_{protein}^{-1} \cdot min^{-1}$ are the velocity and the maximal velocity of substrate hydrolysis, respectively, S (M) the substrate concentration, K_m (M) the Michaelis-Menten constant (Bisswanger 2008).

Aldridge et al. proposed a reversible formation of an enzyme-inhibitor complex followed by an irreversible formation of inhibited enzyme as molecular mechanism for the inhibition of AChE by organophosphates (Aldridge 1950). In Figure 2.1 the assumed inhibition mechanism of AChE by diazoxon, the activated metabolite of diazinon, is depicted. It is believed that the first step consists of the reversible formation of a rather loose Michaelis-type complex between the nucleophilic serine hydroxyl group and the OP with the central P atom being the acceptor of electron pairs. This step is characterized by the association constant K_a (M^{-1}). The second step consists of the formation of a covalent bond between the serine hydroxyl group and the phosphate moiety under release of the leaving group, in case of diazoxon 2-Isopropyl-6-methyl-4-pyrimidinol (pyrimidinol). This phosphorylation reaction, which is characterized by the phosphorylation rate constant k_p (min^{-1}), inactivates the enzyme. Similar to the acetylated AChE also the phosphorylated enzyme can be reactivated (spontaneous reactivation) but this hydrolysis is slow (Wallace 1992; Landis and Yu 1995; Boelsterli 2007). A permanent inactivation of the enzyme is achieved by dealkylation of the phosphate adduct (aging) (Wallace 1992; Carletti et al. 2008).

According to Wallace (Wallace 1992) OP toxicity can be explained as a TD phenomenon and is mainly driven by TD parameters like the inhibition parameters K_a and k_p.. K_a can be regarded as a measure for the affinity of the OP compound for the receptor. k_p is an estimate for the reactivity of the organophosphorus ester towards the serine hydroxyl group of the enzyme.

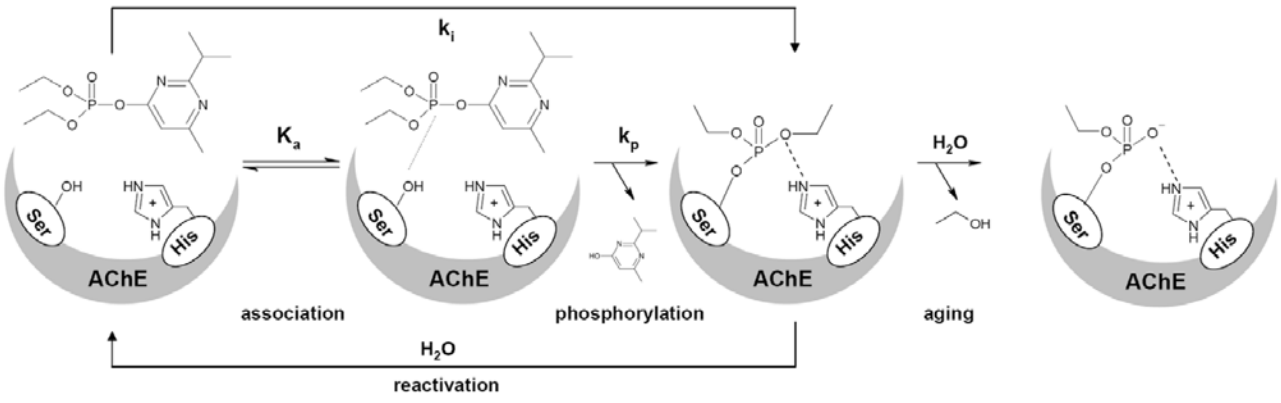

Figure 2.1. *Simplified schmeme of the assumed reaction of diazoxon (active metabolite of diazinon) with the active site of acetylcholinesterase (AChE) (adapted from (Landis and Yu 1995; Carletti et al. 2008)): K_a: association constant, k_p: phosphorylation constant, k_i: bimolecular reaction constant, Ser-OH: serine hydroxyl group (esteratic site), His-R: Histidine imidazolium group*

The overall inhibitory potency of an organophosphorus compound for a certain species is represented by the bimolecular inhibition reaction constant k_i ($min^{-1} \cdot M^{-1}$) which contains information about the association as well as the phosphorylation step (Fukuto 1990). This constant is the product of K_a and k_p:

$$k_i = K_a \cdot k_p \qquad (2.2)$$

Both K_a and k_p are compound and species specific. They depend on the electrophilicity and nucleophilicity of the central phosphorus atom of the OP compound and the active site (serine hydroxyl group) of the enzyme, respectively. Furthermore the reactivity (k_p) of the inhibitor is governed by the strength of the P-OX bond, where OX is the leaving group. The bond strength depends on the electronic properties/ stability of the leaving group itself and of the other substituents on the P atom. Steric hindrance which is a function of the molecular volume of the OP compound and the finite dimensions of the esteratic site plays an important role for the association of the inhibitor to the active site (K_a) (Fukuto and Metcalf 1956; Fukuto 1990; Wallace and Kemp 1991). In general, the shorter or less branched alkyl/ alkoxy groups are (Fukuto and Metcalf 1959; Wallace and Kemp 1991), the more electron withdrawing the leaving group is (Fukuto and Metcalf 1956), the bigger the dimensions of the active site and the higher the nucleophilicity of the esteratic site are (Kemp and Wallace 1990) the higher is the inhibitory potency.

Table 2.1 shows the influence of increasing alkyl chain length on the inhibitory potency (k_i) of dialkyl-p-nitrophenyl phosphates for AChE from trout and chicken (values taken from (Kemp and Wallace 1990)). For AChE from both species an decrease in inhibitory potency with increasing chain length was observed (Kemp and Wallace 1990). For chicken this was attributed to an increased steric hindrance with increasing chain length, since mainly the association constant K_a was lowered. In trout primarily k_p was affected. Here, the determining factor was assumed to be primarily the decreasing electrophilicity of the central phosphorous atom with increasing alkyl chain length. The different influence of chain length on the phosphorylation step was explained by differences in the nucleophilicity of the esteratic site (weak nucleophilic site in trout AChE, strong nucleophilic site in chicken AChE). In general low K_a values of trout AChE compared to chicken lead to the assumption of a greater steric hindrance due to a relatively small active site present in trout (Kemp and Wallace 1990; Wallace and Kemp 1991).

Table 2.1. *Inhibition parameters k_p, K_a, k_i according to the inhibiton mechanism as shown in Figure 2.1 for dialkyl-p-nitorphenyl phosphates and AChE from trout and hen. T, pH: used temperature and pH in experiments. Values taken from (Kemp and Wallace 1990). Arrows indicate the direction of decreasing inhibitory potency with increasing alkyl chain length.*

OP compound	Species	Source of AChE	k_p (min^{-1})	K_a (M^{-1})	k_i ($min^{-1}M^{-1}$)	T (°C)	pH
Dialkyl-p-nitrophenyl phosphates:							
Dimethyl	Hen	Brain	2.04E+00	4.03E+05	8.28E+05	37	8.0
Diethyl			2.48E+00	4.52E+05	1.14E+06		
Di-n-propyl			2.23E+00	8.23E+04	1.83E+05		
Di-n-butyl			2.71E+00	2.79E+04	7.90E+04		
Di-i-propyl			1.75E+00	8.26E+03	1.60E+04		
Dimethyl	Trout	Brain	9.80E+00	5.46E+02	5.37E+03	11	8.0
Diethyl			3.10E-01	1.18E+03	3.75E+02		
Di-n-propyl			6.40E-02	5.20E+02	4.20E+01		
Di-n-butyl			2.70E-01	9.65E+01	2.70E+01		
Di-i-propyl			5.30E-03	6.73E+01	1.30E+00		

The velocity of spontaneous reactivation of inhibited AChE is compound dependent and also differs strongly among species (Wallace and Herzberg 1988) (e.g. regain of enzymatic activity for paraoxon and rat 1.48 ± 0.07 $\%\cdot h^{-1}$, for paraoxon and catfish no reactivation found (Carr and Chambers 1996)). In general spontaneous reactivation occurs faster for dimethylated OP compounds than diethylated ones (Chambers 1992). Since hydrolysis of phosphorylated AChE (reactivation) is exceedingly slow compared to acetylated AChE the catalytic function of the enzyme is practically lost (Fukuto and Metcalf 1956; Habig and Giulio 1991; Chambers 1992). OPs are thus considered as irreversible inhibitors, but in some cases, when aging is very slow and hydrolysis of the inhibited complex is possible, they can appear as reversible inhibitors. Recovery from AChE inhibition is in principal possible by two processes: Spontaneous reactivation of phosphorylated AChE and/ or *de novo* synthesis of active enzyme (Benke and Murphy 1974; Wallace 1992; Boelsterli 2007).

Many studies report the occurence of detrimental effects only after a certain fraction of inhibited AChE is exceeded. This threshold value is species dependent (Fulton and Key 2001). For example for estuarine fish species mortality was correlated with inhibition levels of brain AChE higher than 70 % (Fulton and Key 2001). For the invertebrate *D. magna* and the OP insecticides malathion and chlorpyrifos survival was affected if whole body AChE inhibition levels exceeded 50 % (Barata et al. 2004).

Although acute toxic effects of OPs are commonly related to AChE inhibition OP compounds are capable of binding also to other macromolecular sites like pseudo-ChEs, CbEs and neurotransmitter receptors (Aldridge 1953b; Chambers 1992; Maxwell 1992; Tang and Chambers 1999) and as reviewed in (Pope et al. 2005). Binding to these macromolecular sites might influence toxic effects of OPs due to AChE inhibition. For *D. magna* and for mosquitofish a higher or at least a similar affinity of the oxons of parathion and chlorpyrifos for non-critical CbE than for ChEs was suggested (Boone and Chambers 1996; Barata et al.

2004). CbEs were assumed to protect against OP poisoning binding the oxons before they can inhibit the critical target site AChE (Maxwell 1992; Boone and Chambers 1996; Barata et al. 2004). For *D. magna* and the OP acephate other binding sites than AChE were assumed to be involved in acute toxicity since high levels of AChE inhibition were not directly related to immobilization (Printes and Callaghan 2004). For some OPs toxicity might therefore be associated with secondary modes of action (Printes and Callaghan 2004).

Bioconcentration and biotransformation

Bioconcentration of xenobiotics in aquatic organisms

Aquatic organisms can in general take up xenobiotics from the surrounding water by different routes. Figure 2.2 illustrates the possible uptake and also clearance routes of a xenobiotic in daphnids. These include uptake via passive diffusion, uptake via the diet, elimination via passive diffusion and biotransformation and egestion.

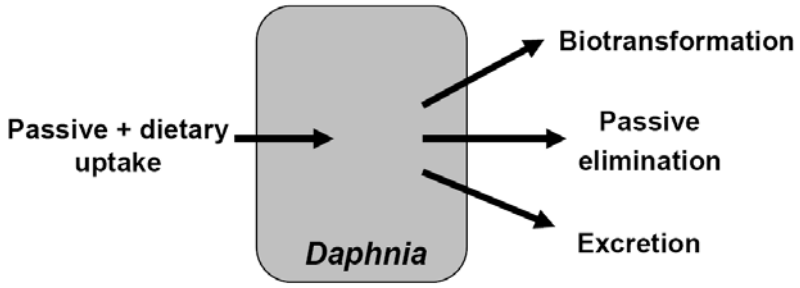

Figure 2.2. *Pathways of xenobiotic uptake and clearance for Daphnia species (adapted and modified from (Mackay and Fraser 2000))*

Bioconcentration (bioaccumulation) describes the accumulation solely via nondietary routes i.e. uptake via gills or skin. Biomagnification describes the uptake of xenobiotica solely via the food and their enrichment from lower to higher trophic levels within the food chain (Schwarzenbach et al. 2003).

The bioconcentration factor (BCF) describes the extent of bioconcentration and is defined as the ratio between the concentration in the organism c_{int} and in the water c_{ext} under steady state conditions (Spacie 1983):

$$BCF = \frac{c_{int}^{ss}}{c_{ext}} \qquad (2.3)$$

The internal concentration is defined as the amount of a chemical per g wet weight of the organism ($mol \cdot g_{ww}^{-1}$). c_{ext} has the units M and the BCF $L \cdot g_{ww}^{-1}$.

If the organism is regarded as a single homogenous compartment and first-order kinetics are assumed for uptake and elimination of a compound into and out of the organism the time course of the internal concentration can be described by a simple one-compartment first-order kinetics model (Spacie 1983; Hawker and Connell 1986):

$$\frac{dc_{int}(t)}{dt} = k_{in} \cdot c_{ext}(t) - k_{el,tot} \cdot c_{int}(t) \quad (2.4)$$

k_{in} ($L \cdot g_{ww}^{-1} \cdot h^{-1}$) and $k_{el,tot}$ (h^{-1}) are the rate constants for uptake and elimination of the chemical, respectively. With this model the BCF can be expressed as:

$$BCF = \frac{k_{in}}{k_{el,tot}} \quad (2.5)$$

For lipophilic compounds the lipoid tissues of an aquatic organism can be regarded as the primary storage compartment (Mackay and Fraser 2000). If the partitioning between the aqueous and the lipid phase is approximated via the octanol-water partitioning coefficient K_{ow} the BCF for *D. magna* can be estimated with the following relationship (QSAR) (Geyer et al. 1991)

$$\log BCF = 0.850 \cdot \log K_{ow} - 1.100 \quad (2.6)$$

Such a relationship is applicable to inert and neutral chemicals with a $\log K_{ow}$ between approximately 2 and 6 (Hawker and Connell 1986).

Equation 2.6 is an approximate estimation of the BCF and valid in absence of biotransformation. Besides the hydrophobicity of a compound also physiological parameters (e.g. lipid content and body size) and biochemical parameters (e.g. biotransformation capacity) of the animal as well as additional physicochemical properties of the chemical (e.g. steric properties and reactivity) influence the uptake and elimination process (Barron 1990). For example for *D. magna* differences in lipid content had a significant influence on bioconcentration: Animals with a low amount of stored lipids (visible in this species as oil droplets within the carapace) exhibited a low BCF (based on wet weight) compared to animals with a high lipid content (Dauble et al. 1985). Furthermore, some organophosphorous pesticides in fish showed a faster elimination (lower BCF) than expected according to their K_{ow} due to biotransformation of the chemicals (de Bruijn and Hermens 1991). In this case $k_{el,tot}$ in equation 2.5 can be written as (de Wolf et al. 1992):

$$k_{el,tot} = k_{el} + k_{met} \quad (2.7)$$

k_{el} (h^{-1}) describes the physicochemical loss of the unchanged parent compound e.g. by diffusion processes and k_{met} (h^{-1}) the loss via biotransformation (de Wolf et al. 1992). Hereby, k_{met} is a cumulative first order rate constant summarizing all relevant biotransformation pathways (Spacie 1983).

Biotransformation processes

Biotransformation generally transforms lipophilic compounds into more water soluble compounds in order to facilitate their excretion. In most cases the degradation products are less toxic than the parent compound. These processes, which are catalyzed by different enzymes, can be divided into two major pathways: phase I and phase II reactions. Phase I reactions like oxidation, reduction or hydrolysis lead to introduction/ formation of functional groups like hydroxyl, amino, carboxyl, thiol groups. In phase II functional groups are conjugated with endogenous substrates like sulfate, glucuronic acid, acetate and

glutathione (Landis and Yu 1995; Boelsterli 2007). In the following the main biotransformation processes and the associated enzymes, which play a role for OPs, are listed.

Cytochrome P450 monooxygenase:

The most important enzymes, which catalyze a variety of oxidative reactions in phase I belong to the cytochrome P450 system (P450) (Landis and Yu 1995). In mammals P450 are located in the smooth endoplasmatic reticulum of cells of most tissues, particularly in the liver (Landis and Yu 1995).

A number of studies examined biotransformation processes of phosphorothionate insecticides catalyzed by these enzymes in mammals (Levi et al. 1988; Forsyth and Chambers 1989; Fabrizi et al. 1999; Kappers et al. 2001; Mutch and Williams 2006). Phosphorothionates (e.g. diazinon, parathion, fenitrothion) are metabolically detoxified by oxidative dearylation (Levi et al. 1988; Fabrizi et al. 1999). In case of diazinon diethyl thiophosphate and the phenol derivate 2-isopropyl-4-methyl-6-pyrimidinol (pyrimidinol) are formed (Fabrizi et al. 1999). What causes actually the toxicity of phosphorothionates is an oxidative desulfuration reaction catalyzed by the same enzyme class. The resulting oxons are very potent AChE inhibitors in comparison to their parent compounds (Levi et al. 1988; Forsyth and Chambers 1989; Keizer et al. 1995). Oxidative desulfuration and oxidative dearylation are supposed to proceed via the same intermediate, a phosphooxythiiran (Chambers 1992). The ratio of these two reactions is governed by the different isoforms of P450 involved (Levi et al. 1988; Fabrizi et al. 1999; Mutch and Williams 2006) and varies between different compounds (Chambers et al. 1994; Mutch and Williams 2006). For example the major transformation pathway of diazinon in enterocyte and hepatic microsomes from rat *in vitro* was the oxidative dearylation to pyrimidinol. Activation to diazoxon only played a minor role (Poet et al. 2003).

In aquatic species reactions of phosphorothionate insecticides catalyzed by P450 were evaluated in analogy to mammals: In *in vitro* studies with cell preparations from fish liver diazinon was oxidatively transformed to diazoxon, pyrimidinol, diethyl thiophosphate and diethyl phosphate (oxidative activation and dearylation) (Hogan and Knowles 1972; Keizer et al. 1995). In *in vivo* exposure studies with fenitrothion and fish, snail and crustaceans (*D. pulex*, shrimp, blue crab) the oxon analog fenitrooxon could be detected (Johnston and Corbett 1986; Takimoto et al. 1987a; Takimoto et al. 1987b; Takimoto et al. 1987c), presumably formed by P450 activation (Johnston and Corbett 1986). *In vivo* experiments with the polycyclic aromatic hydrocarbon pyrene confirmed the participation of P450 in metabolic processes in *D. magna* (Akkanen and Kukkonen 2003; Ikenaka et al. 2006). Hereby, the *Daphnia* species appears to possess multiple cytochrome P450 enzymes (Baldwin and Leblanc 1994; David et al. 2003). Therefore the occurence of both oxidative desulfuration and dearylation of phosphorothionates can also be assumed to occur in this species.

A-esterases:

A-esterases only hydrolyze phosphate triesters (oxons) but not their sulfur analogs (phosphorothionates) (Kasai et al. 1992). This ester hydrolysis leads in general to detoxification of organophosphates (Li et al. 1995). Diazoxon for example is cleaved to diethylphosphate and pyrimidinol during this reaction (Poet et al. 2003). A-esterase activity towards diazoxon was observed e.g. *in vitro* in intestine and liver of rat (Poet et al. 2003) and in liver of fish (Keizer et al. 1995). For guppy and zebra fish this activity was only very low compared to diazoxon formation by P450 and it was absent in trout (Keizer et al. 1995). In comparison to mammals, birds showed only a very low A-esterase activity (Brealey et al. 1980). Insects seem to lack the ability to hydrolyze OPs by A-esterases completely (Mackness et al. 1983).

Glutathione S-transferases:

Glutathione S-transferase (GST) is a superfamily of enzymes which catalyze the conjugation of a variety of xenobiotics with the tripeptide glutathione (GSH) (Boelsterli 2007). This reaction involves the nucleophilic attack of the cystein thiol group of GSH at an electrophilic center of a xenobiotic (Fukami 1980). *In vitro*, and possibly also *in vivo*, dialkylaryl thiophosphates and their oxon analoga are detoxified by dealkylation and dearylation under formation of S-alkyl and S-arylglutathione (Abel et al. 2004; Fujioka and Casida 2007). For mammals and insects the major metabolites of diazinon and diazoxon found *in vitro* were diethylthiophosphate, diethylphosphate and the GSH conjugate of pyrimidinol (Shishido et al. 1972; Fujioka and Casida 2007). GST activity towards OPs was found to be present not only in mammals but also in fish (Keizer et al. 1995) and in crustacean species (Escartin and Porte 1996). In *D. magna* multiple isoforms of GST were identified (Leblanc and Cochrane 1987). Although a number of *in vitro* studies exist the role of GSH conjugation on the toxicity of organophosphates *in vivo* is not very clear (Sultatos 1992).

Conjugation with sulfate, glucoside, and glucuronide:

Conjugation with sulfate, glucoside, and glucuronide affects in general metabolites formed during phase I. These conjugation reactions are catalyzed by sulfotranferases, glucosyltransferases, and UDP-glucuronosyltransferase (Boelsterli 2007). Different aquatic species (fish, crustaceans, molluscs) exposed *in vivo* to fenitrothion formed sulfate, glucoside, and glucuronide conjugates of the phase I metabolite 3-methyl-4-nitrophenol. The extent of conjugation with different substrates was strongly dependent on the species: In the crustacean *D. pulex* only 3-methyl-4-nitrophenyl sulfate could be detected, in blue crab 3-methyl-4-nitrophenyl sulfate and glucoside (Johnston and Corbett 1986; Takimoto et al. 1987a; Takimoto et al. 1987b; Takimoto et al. 1987c). In *D. magna* exposed to pyrene and pentachlorophenol *in vivo* conjugation with sulfate was found to be the major phase II pathway (Kukkonen and Oikari 1988; Ikenaka et al. 2006).

Toxicokinetic phase of diazinon in *D. magna*

The following toxicokinetic model for diazinon and *D. magna* was designed after the literature analysis above (see Figure 2.3):

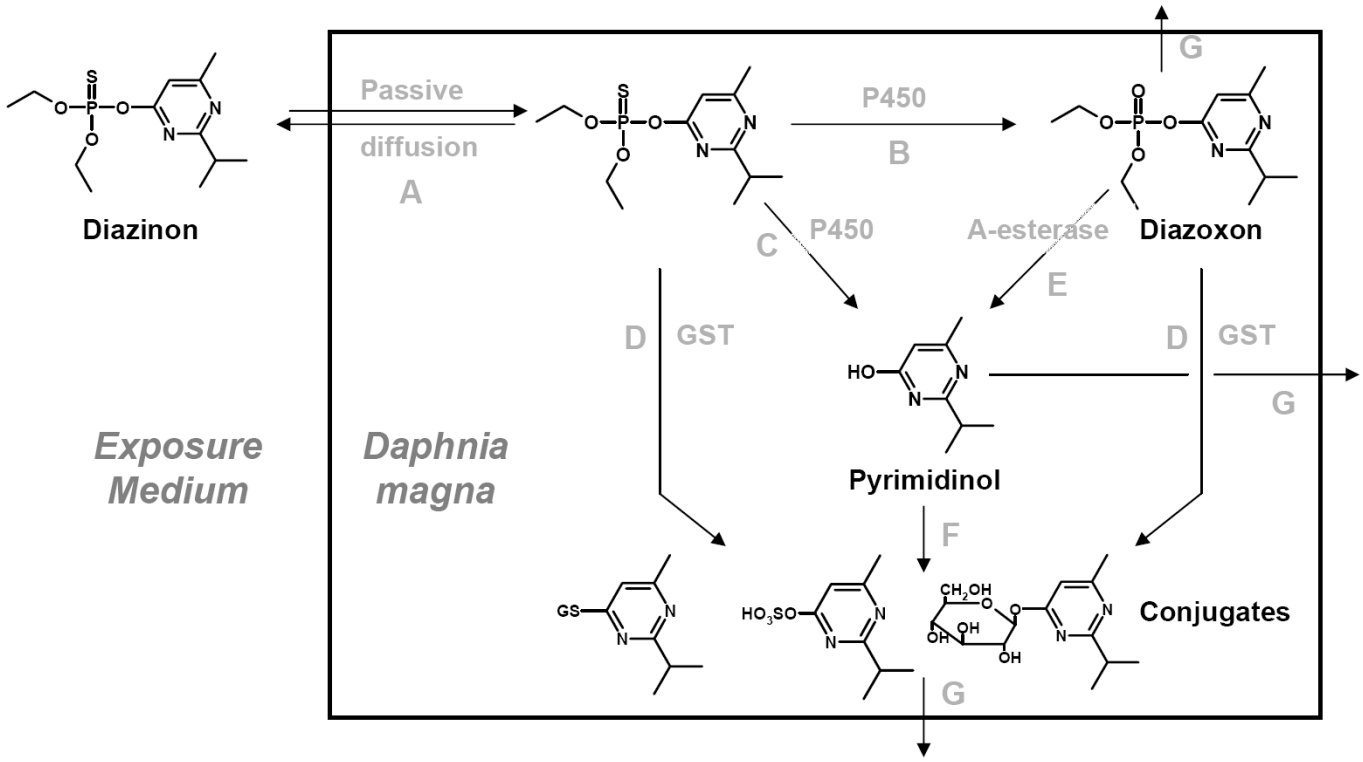

Figure 2.3. *Assumed toxicokinetic phase of diazinon in D. magna. Explanation of each pathway and abbreviations are in the text.*

D. magna is regarded as a single compartment. Uptake from the water phase and elimination of the unchanged compound occurs via passive diffusion (pathway A). Inside the organism diazinon is activated to diazoxon and/or degraded to pyrimidinol by cytochrome P450 via oxidative desulfuration and oxidative dearylation, respectively (pathway B and C, respectively). Both diazinon and diazoxon are cleaved by GST under formation of S-pyrimidinylglutathione, diethyl thiophosphate and diethyl phosphate, respectively (pathway D). Diazoxon can be hydrolyzed by A-esterases to pyrimidinol and diethylphosphate (pathway E). Furthermore pyrimidinol is conjugated e.g. with sulfate and glucose (pathway F). Each metabolite can itself be eliminated out of the organism via passive diffusion (pathway G).

Toxicokinetic and toxicodynamic (TKTD) models

If a binary response (only two possible outcomes: effect occurs or not, e.g. mortality or immobilisation) of an individual exposed to a toxicant is regarded and the cumulative effect (% of positive response) is plotted as continuum against the (logarithmic-) dose or concentration usually a sigmoidal curve results. The number of animals showing the effect in addition to the preceeding dose/ concentration is log-normally distributed (Landis and Yu 1995). Two hypotheses may explain this effect (here mortality as representative

effect): The individual effective dose (IED) or individual tolerance distribution concept assumes that an individual dies instantaneously as soon as a certain threshold dose or concentration (Gaddum 1953; Zhao and Newman 2007) is exceeded (deterministic death). The IED is often assumed to be log-normally distributed among the individuals of a population (Gaddum 1933; Zhao and Newman 2007), that means that animals differ in their sensitivity towards a toxicant. In the second theory individuals are regarded as equally sensitive (equal threshold dose or concentration) and death is assumed to be stochastic. If the threshold is exceeded the probability of dying increases with increasing dose (Newman and McCloskey 2000).

Experiments performed to test if the individual tolerance distribution or the stochastic theory might best explain the variation of various observed individual responses indicated that neither is the sole determinant and rather a mixture of both concepts applies (Newman and McCloskey 2000; Zhao and Newman 2007). The relative contribution of these concepts is dependent on the toxicant, the organism and the exposure intensities (Newman and McCloskey 2000; Zhao and Newman 2007).

In the following a short overview of a selection of (process-based) ecotoxicological models developed for the prediction of survival or other quantal effects as function of TK and/ or TD processes is given. The critical body residue (CBR) approach (Mackay et al. 1992; Verhaar et al. 1999), the critical area under the curve (CAUC) model (Verhaar et al. 1999) and the critical target occupation (CTO) model (Legierse et al. 1999) are based on the individual tolerance distribution concept (Ashauer and Brown 2008). The dynamic energy budget toxicity (DEBtox) model for receptor kinetics (Jager and Kooijman 2005) and the threshold damage assessment model (TDM) (Ashauer et al. 2007a) assume death to be a chance process. For a detailed compilation and discussion of these models the reader is refered to (Ashauer et al. 2006) and (Ashauer and Brown 2008).

In these models the TK part (time course of the internal concentration of a chemical in an organism) is described by a one compartment first-order kinetics model:

$$\frac{dc_{int}(t)}{dt} = k_{in} \cdot c_{ext}(t) - k_{el} \cdot c_{int}(t) \qquad (2.3)$$

c_{int} ($mol \cdot g_{ww}^{-1}$) is the whole body concentration, which serves as surrogate for the concentration at the site of toxic action. c_{ext} (M) is the concentration in the exposure medium. k_{in} ($L \cdot g_{ww}^{-1} \cdot h^{-1}$) and k_{el} (h^{-1}) are the rate constants for uptake and elimination of the chemical inside/ out of the organism, respectively.

According to the CBR concept 50 % of a population die when the internal whole body concentration reaches a critical value, the critical body residue (Mackay et al. 1992; Verhaar et al. 1999):

$$CBR = BCF \cdot LC_{50}(t) \cdot (1 - e^{-k_{el} \cdot t}) = const \qquad (2.4)$$

with BCF ($L \cdot g_{ww}$) is the bioconcentration factor of the respective compound and LC_{50} (M) the external concentration at which 50 % of the animals are dying. The CBR is assumed to be a constant value, independent of the chemical and of exposure time (Verhaar et al. 1999). The interaction with the target site is instantaneous and the toxic action completely and instantaneously reversible (Ashauer and Brown 2008).

Here TK processes are rate limiting. This concept holds true e.g. for narcotic compounds. The $LC_{50}(t)$ value reaches its incipient value as soon as the bioconcentration kinetics (equation 2.3) are in steady state.

For reactive compounds or compounds with a specific mode of action not the internal concentration but the amount of affected target molecules is related to the toxic effect. If the reaction with the target molecule is irreversible and instantaneous the integrated internal concentration over time serves as a dose metric. Mortality occurs as soon as a critical threshold value is exceeded, called the critical area under the curve (CAUC, $mol \cdot h \cdot g_{ww}^{-1}$) (Verhaar et al. 1999):

$$CAUC = \int_0^t BCF \cdot c_{ext}(t) \cdot \left(1 - e^{k_{el} \cdot t}\right) dt = c_{int}(t) dt = const \qquad (2.5)$$

The critical area under the curve is compound dependent. The time dependency of the LC_{50} is given by:

$$LC_{50}(t) = \frac{CAUC / BCF}{t - (1 - e^{-k_{el} \cdot t}) / k_{el}} + LC_{50}(\infty) \qquad (2.6)$$

In contrast to the CBR concept the LC_{50} declines with increasing exposure time also after TKs have reached steady-state and approaches the incipient LC_{50} for $t \rightarrow \infty$. The $LC_{50}(\infty)$ value accounts for repair/ reactivation mechanisms of occupied target sites (Verhaar et al. 1999). As in the CBR theory also the CAUC model assumes that interactions with the target site are fast. Therefore the toxic effect can be directly linked to the (integrated) internal (whole body) concentration.

Based on the CAUC model Legierse et al. (Legierse et al. 1999) developed a model for acute toxicity of phosphorothionate pesticides to aquatic organisms. Mortality is assumed to be related with a critical amount of irreversible inhibited AChE, the critical target occupation CTO. This amount is proportional to the time integrated concentration of the activated oxon analogue in the target tissue until time of death ($CAUC_{oxon}$):

$$CTO = k_{inh} \cdot \int_0^{t_{death}} c_{oxon}(t) dt = k_{inh} \cdot CAUC_{oxon} \qquad (2.7)$$

CTO ($mol \cdot g_{ww}^{-1}$) and $CAUC_{oxon}$ ($mol \cdot h \cdot g_{ww}^{-1}$) are concentrations normalized to the amount of target tissue. k_{inh} (h^{-1}) is the overall inhibition rate constant. The AChE amount in the target tissue is assumed to be constant. If the whole body concentration serves as surrogate for the concentration in the target tissue then the critical area under the curve of the parent compound $CAUC_{wb}$ ($mol \cdot h \cdot g_{ww}^{-1}$) can be directly related to the whole body concentration of inhibited AChE ($mol \cdot g_{ww}^{-1}$):

$$CTO_{wb} = k_{inh} \cdot k_{act} \cdot CAUC_{wb} \qquad (2.8)$$

k_{act} (h^{-1}) is the first order rate constant for the activation process of the phosphorothionate to the oxon analogue. The time dependent LC_{50} can be derived if we use equation 2.6 of the CAUC model and insert $CAUC_{wb}$ of equation 2.8. Here the incipient $LC_{50}(\infty)$ accounts for compensating mechanisms of deactivated AChE, like *de novo* synthesis of active enzyme.

Model approaches, which assume death as a stochastic process are for example so called hazard rate models. They are able to simulate survival in a population over time (Ashauer and Brown 2008). These models link the internal toxicant concentration with survival via the hazard rate, the probability of an organism dying at a given time (Ashauer et al. 2007a).

In contrast to the before mentioned CBR and CTO model for narcotic or specifically acting chemicals the threshold damage assessment model (TDM) developed by Ashauer et al. (Ashauer et al. 2007a) describes the TDs in a more general way making it applicable to a broad range of chemicals with different modes of action. Here the toxicant in the organism causes a certain internal damage which leads to reduced health of the organism (Ashauer and Brown 2008). The TK part of this approach is described by equation 2.3. The time course of damage is determined by accrual of and also repair from damage, both following first-order kinetics (Ashauer et al. 2007a):

$$\frac{d}{dt}D(t) = k_{kill} \cdot c_{int}(t) - k_{rec} \cdot D(t) \qquad (2.9)$$

Damage D (dimensionless) stands for any hazardous effect on molecular level. k_{kil} is called the killing rate constant ($g_{ww} \cdot pmol^{-1} \cdot h^{-1}$), k_{rec} (h^{-1}) the recovery rate constant. The hazard rate (h^{-1}), increases after damage exceeds a certain threshold (Ashauer and Brown 2008):

$$h(t) = \frac{dH(t)}{dt} = \theta \cdot \max\left[D(t) - \text{threshold}, 0\right] \qquad (2.10)$$

The cumulative hazard H is linked to the probability of surviving until a given time t via an exponential function.

$$S(t) = \exp\left[-H(t)\right] \qquad (2.11)$$

The DEBtox receptor kinetics model has in principle the same structure as the TDM. Instead of an unspecified damage this model implements the occupation of receptor molecules, e.g. the inhibition of AChE by organophosphates. It is based on the DEBtox method extended by receptor inhibition kinetics (Jager and Kooijman 2005). The bioconcentration kinetics is analog to equation 2.3 but the internal concentration is scaled ($c_{int,\,scaled}$, $mol \cdot L^{-1}$) by dividing by the BCF.

$$\frac{d}{dt}c_{int,scaled}(t) = \frac{k_{el}}{l(t)} \cdot \left[c_{ext}(t) - c_{int,scaled}(t)\right] - c_{int,scaled}(t) \cdot \frac{d}{dt}\ln l(t)^3 \qquad (2.12)$$

The effect of growth on the elimination rate (area to volume ratio) and on the toxicant concentration (growth dilution) are taken into account. l is the scaled body length of the organism (l/l_{max}). The total number of target molecules (e.g. AChE in case of OP poisoning) is the sum of functional (non-occupied) and non-functional (occupied) receptors:

$$N_{tot}(t) = N_f(t) + N_n(t) = N_{tot,max} \cdot l(t)^3 \qquad (2.13)$$

N_{tot} is increasing with increasing body volume until a maximum value for a fully grown organism (l = 1) is reached. The inhibition reaction is assumed to be of second-order kinetics. The possibility of recovery from

inhibition e.g. by spontaneous reactivation is included via a first-order reaction. The time course of non-functional, inhibited target sites follows equation 2.14:

$$\frac{d}{dt}N_n(t) = k_{inh2} \cdot c_{int,scaled}(t) \cdot N_f(t) - k_{rec2} \cdot N_n(t) \quad (2.14)$$

k_{inh2} is called the "knock-out" rate ($mol^{-1} \cdot h^{-1}$). k_{rec2} is the specific recovery rate constant (h^{-1}). With $f_n = N_n/N_{tot}$ is the fraction of non-functional receptors, equation 2.14 can be transformed into:

$$\frac{d}{dt}f_n(t) = k_{inh2} \cdot c_{int,scaled}(t) - \left[k_{rec2} + k_{inh2} \cdot c_{int,scaled}(t) + \frac{d}{dt}\ln l(t)^3 \right] \cdot f_n(t) \quad (2.15)$$

The last term in brackets accounts for dilution of occupied target sites caused by body growth. The receptor deactivation is linked with the effect endpoint via the hazard rate h (h^{-1}):

$$h(t) = \frac{dH(t)}{dt} = k_{kill2} \cdot \max\left[f_n(t) - c_0, 0\right] \quad (2.16)$$

where c_0 is the no effect concentration (NEC) expressed as fraction of occupied receptor molecules. k_{kill2} is the killing rate (h^{-1}). The link of receptor occupation with survival is equal to the TDM. In general the DEBtox receptor kinetics model is suitable to predict survival for reversible ($k_{rec2} \neq 0$) as well as irreversible ($k_{rec2} = 0$) interaction of the toxicant with the target site (Jager and Kooijman 2005).

Chapter 3

Mechanistic Toxicodynamic Model for Receptor-mediated Toxicity of Diazoxon, the Active Metabolite of Diazinon, in *Daphnia magna*

Kretschmann, A.; Ashauer, R.; Hitzfeld, K.; Spaak, P.; Hollender, J.; Escher, B. I.
Mechanistic toxicodynamic model for receptor-mediated toxicity of diazoxon, the active metabolite of diazinon, in *Daphnia magna*. *Environmental Science & Technology*, **submitted**

Introduction

Toxicity can be described as a function of exposure to a chemical in combination with toxicokinetic (TK) and toxicodynamic (TD) processes (Rozman and Doull 2000). Toxicokinetics describe the time course of a toxicant inside an organism and include bioconcentration, distribution and biotransformation processes. TD processes link the internal concentration of a toxicant with the toxic effect observed on organism level by describing the time dependent build up and recovery of injury on molecular, organ and organism level. As soon as the active compound reaches the target site it initiates a cascade of detrimental molecular and physiological reactions, which propagate to toxic effects on the organism level. Compensating molecular mechanisms leading to recovery of an organism are also part of the TD (Rozman and Doull 2000; Ashauer et al. 2007a; Boelsterli 2007).

A group of chemicals, for which the effects on molecular as well as on organism level are well studied are organophosphorus insecticides (OPs), which belong to the class of phosphorothionates (e.g. diazinon). A major concern of these insecticides is their high acute toxicity to non-target organisms e.g. in aquatic systems, especially crustacean species like daphnids (Vaal et al. 2000).

Acute toxic effects of phosphorothionates are mainly, if not entirely, related to inhibition of the enzyme acetylcholinesterase (AChE) by their respective oxon analogues (e.g. diazoxon, the active metabolite of diazinon) (Forsyth and Chambers 1989; Maxwell et al. 2006). As mechanism of inhibition a reversible formation of a Michaelis-Menten type enzyme-inhibitor complex followed by an irreversible formation of inhibited enzyme (phosphorylation) (Aldridge 1950) is widely accepted and has been applied in most kinetic *in vitro* inhibition studies in the last decades (e.g. (Main 1964; Carr and Chambers 1996)). But also other (kinetic) mechanisms are possible like irreversible inhibition in one step as it was found e.g. for inhibition of AChE by diisopropyl fluorophosphate (Baici et al. 2009). Recovery from AChE inhibition is possible by spontaneous reactivation of inhibited AChE and/ or *de novo* synthesis of active enzyme (Wallace 1992).

A number of *in vivo* studies determined the impact of OP insecticides on AChE activity in non-target aquatic organisms either in dependence of exposure concentration or duration (Sancho et al. 1997; Xuereb et al. 2007). Furthermore the relationship between AChE inhibition and sublethal (e.g. immobilization) or lethal effects was analysed, although mainly for constant exposure conditions, for example by relating standard effect concentrations eliciting 50% of maximum effect (EC_{50}) for immobilization to percentage of enzyme inhibition measured *in vivo* (Sturm and Hansen 1999; Printes and Callaghan 2004). Only a few studies quantified both, the effect on molecular as well as on individual level on a temporal scale in order to derive information about their kinetic behaviour and their time dependent relationship to each other (Barata et al. 2004).

Mechanistic approaches, which are able to link the internal damage as function of exposure with the effect on organism level and explicitly account for the time dependency of toxicity, are TKTD models (Jager and Kooijman 2005; Ashauer et al. 2007a; Ashauer et al. 2010). In current TKTD models applied for OP toxicity

in aquatic organisms either the internal damage is not further specified or the inhibition mechanism and kinetic parameters were not further verified e.g. with mechanistic *in vitro* studies or via *in vivo* measurement of the internal effect (AChE inhibition) (Jager and Kooijman 2005; Ashauer et al. 2007a; Ashauer et al. 2010).

The goal of this study was to develop a mechanistic TD model using the organothiophosphate diazinon as model compound and the water flea *Daphnia magna* as model organism. This model can predict the time course of the *in vivo* effect observed on organism level, here immobilization and mortality, as function of the *in vivo* effect on molecular scale, here the inhibition of AChE, and the internal concentration of the active metabolite diazoxon. The inhibition mechanism of AChE inhibition was elucidated and the relevant kinetic parameters determined *in vitro* using diazoxon and enzyme extracts of *D. magna*. The time course of enzyme activity and immobilization/ mortality during exposure to diazinon and potential recovery from AChE inhibition and immobilization were analyzed within *in vivo* studies. The TD model was then parameterized with both *in vitro* and *in vivo* data sets.

Theory

In vitro elucidation of inhibition mechanism and determination of inhibition parameters

Figure 3.1 shows the different reaction pathways for AChE inhibition along with the corresponding kinetic parameters as considered in the current *in vitro* study with diazoxon and analyzed according to (Baici et al. 2009). Only inhibition of the competitive type was considered, where inhibitor or substrate can bind only to the free enzyme.

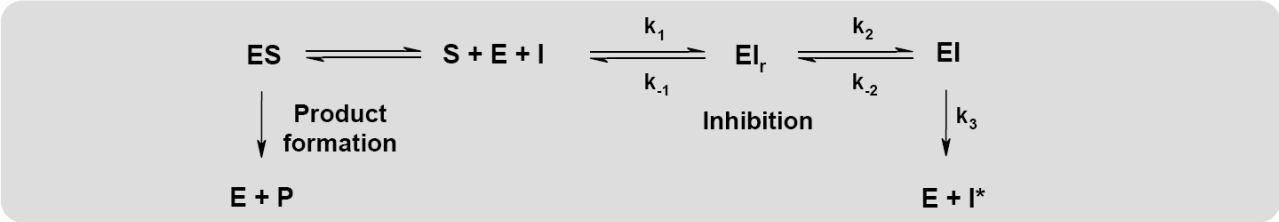

Figure 3.1. *A. Overview of considered reaction pathways in AChE inhibition in the presence of substrate (competitive type, adapted from (Baici et al. 2009) with modifications). E: enzyme, I: inhibitor, S: substrate, ES: Michaelis-Menten complex, EI_r: associative enzyme inhibitor complex, EI: covalently bound enzyme-inhibitor complex, I*: non-active degradation product of inhibitor.*

Irreversible inhibition may occur in two steps or in one step. In the first case a slow irreversible formation of an inactive complex EI, in which the inhibitor I is bound covalently to the enzyme (phosphorylation of the enzyme), is proceeded by a fast and reversible generation of an associative enzyme-inhibitor complex EI_r. Irreversible inhibition in two steps degenerates to irreversible inhibition in one step if the concentration of the intermediate complex EI_r is very low in steady state. Further variations of these mechanisms arise if the covalent enzyme-inhibitor complex EI can degrade to free enzyme plus an inactive form of the inhibitor (spontaneous reactivation of phosphorylated AChE). Here the enzyme is only temporarily inhibited. In addition to irreversible modifications also reversible, slow-binding enzyme inhibition in two steps or in one step were considered.

Differentiation between the different inhibition mechanisms and derivation of the respective kinetic parameters was performed *in vitro* by incubating AChE from *D. magna* with different diazoxon concentrations in presence of the substrate acetylthiocholine ATCh (as surrogate for the neurotransmitter acetylcholine ACh) and recording the formation of product thiocholine P over time. The details of this analysis are given in the supporting information (SI). In the following only the most likely mechanism, which is irreversible inhibition in two steps, is described.

The reversible formation of EI_r is described by the association constant K_a (M^{-1}) = k_{-1}/k_1 or its reciprocal value K_i (M), the dissociation constant. The irreversible formation of EI is described by the phosphorylation constant k_p (min^{-1}) = k_2. The product/ ratio of both is the bimolecular (inhibition) reaction constant k_i ($min^{-1}M^{-1}$) (Main 1964):

$$k_i = \frac{k_p}{K_i} = K_a \cdot k_p \qquad (3.1)$$

Development of TD model

The proposed model shall describe the time dependent accrual of damage on molecular level (here: AChE inhibition) and link this intrinsic effect with the effect observed on organism level (here: survival). Our TD model is based on the concept of hazard modeling: death is stochastic at the level of individuals. Existing TKTD models based on hazard modeling are for example the threshold damage model TDM (Ashauer et al. 2007a; Ashauer et al. 2010) and the DEBtox receptor kinetics model (Jager and Kooijman 2005). The proposed model is structured in analogy to the DEBtox receptor kinetics model (Jager and Kooijman 2005), but instead of the fraction of non-functional receptors the measured absolute amount of active AChE is implemented as dose metric. Furthermore the explicit rate law for the underlying inhibition mechanism and the respective inhibition parameters determined *in vitro* are implemented in the model (for details, see SI).

The *in vivo* time course of active AChE E_a in presence of inhibitor I can be described by equation 3.2:

$$\frac{dE_a(t)}{dt} = -k_p \cdot K_a \cdot I(t) \cdot E_a(t) + k_{rec} \cdot \left[E_0 - E_a(t)\right] \quad (3.2)$$

Enzyme (complex) or inhibitor concentrations are expressed in pmol·g_{ww}^{-1}, K_a in g_{ww}·$pmol^{-1}$ and k_p in h^{-1} (ww: wet weight of organisms; transformation of units from M into pmol·g_{ww}^{-1} is described in the SI). The first term on the right side of equation 3.2 describes the decline of enzyme activity due to irreversible occupation of the target site AChE. The inhibition parameters k_p and K_a were determined *in vitro*. The second term describes the *in vivo* recovery of enzyme activity due to (induced) *de novo* synthesis of free enzyme or spontaneous reactivation of the enzyme-inhibitor complex. In analogy to the TDM or the receptor kinetics model the rate of recovery k_{rec} (h^{-1}) is assumed to be dependent of existing damage (first-order kinetics). k_{rec} was determined *in vivo*. The total enzyme amount E_0 is assumed to be constant.

If k_p and K_a and the amount of E_a at time point t_i are known then I at time point t_i can be approximated with equation 3.3:

$$I(t_i) = \frac{k_{rec} \quad \left[E_0 - E_a(t_i)\right] - \frac{\Delta E_a(t_i)}{\Delta t}}{k_p \cdot K_A \cdot E_a(t_i)} \quad (3.3)$$

with $\Delta t = t_i - t_{i-1}$ (3.4)

and $\Delta E_a(t_i) = E_a(t_i) - E_a(t_{i-1})$ (3.5)

The active enzyme form is linked to survival via the hazard rate h. The probability that an organism dies increases as soon as the amount of E_a falls below a certain threshold value $E_{a,threshold}$ of active AChE.

$$h(t) = \frac{dH(t)}{dt} = k_{kill} \cdot \max\left[E_{a,threshold} - E_a(t), 0\right] \quad (3.6)$$

k_{kill} (g_{ww}·$pmol^{-1}h^{-1}$) is called the killing rate constant. The integration of the hazard rate over time yields the cumulative hazard H(t), which is linked to the probability of surviving until a given time t as follows (Jager and Kooijman 2005; Ashauer et al. 2007a):

$$S(t) = \exp\left[-H(t)\right] \quad (3.7)$$

Material and methods

Chemicals, culturing of *D. magna* and data analysis

A list with the chemicals used can be found in the SI. Nominal concentrations given in the *in vitro* experiments were corrected by the purity of the chemicals, *in vivo* exposure concentrations were measured with LC-MS/MS. *D. magna* (Clone 5) with an age of 5 - 6 d were used for experiments. Linear and nonlinear regression and statistical tests were performed with the program GraphPad Prism version 4.03 for Windows (GraphPad Software, San Diego California USA, www.graphpad.com). Parameter estimation of the TD model was performed using ModelMaker version 4.0 (Cherwell Scientific Ltd, Oxford UK, www.modelkinetix.com).

Measurement of cholinesterase activity and protein content in extracts of *D. magna*

The protein content in S10 extracts of *D. magna* was determined with the Lowry method (Lowry et al. 1951). The measurement of cholinesterase (ChE) activity in S10 extracts of *D. magna* was performed with the Ellman method (Ellman et al. 1961). ATCh iodide was used as substrate. For determination of the Michaelis-Menten kinetics refer to SI.

In vitro experiments

Experiments were performed in a 96 well plate. Inhibitor concentrations in the wells are given with respect to the final volume of 290 µL. The daphnid tissue concentration was approximately 3 mg_{ww} per well.

Relative contribution of different processes to the measured ChE activity

The relative contribution of enzymatic and non-enzymatic processes to the measured activity towards ATCh was analysed by incubation of S10 extract with iso-OMPA as selective inhibitor of buturylcholinesterase (BuChE, also termed pseudo-cholinesterase) and eserine sulfate as selective inhibitor of the cholinesterases AChE and BuChE. For comparison also inhibition with diazoxon was performed. Enzyme activity is expressed (also in further experiments) as the ratio of treatment to (solvent) control (both in min^{-1}) in % activity of control. In the following experiments the measured AChE activity was corrected by an eserine sulfate control.

Determination of AChE amount in D. magna

For the determination of the absolute AChE amount present in *D. magna* S10 extracts were incubated with 0, 0.04, 0.08, 0.12, 0.17 and 0.21 nM diazoxon (linear decrease of AChE activity, see SI). The amount of active AChE centers in nM was obtained by plotting activity vs. the diazoxon concentration and calculating the intercept of the linear regression line with the x-axis (activity = 0%). For the transformation in mass units the weight of one subunit of tetrameric AChE from electric eel was used (80 kDa, one active site per

subunit (Dudai and Silman 1974)). Nominal diazoxon concentrations were checked with LC-MS/MS and amounted to 81 % of the measured concentrations. Nominal concentrations were used for data analysis.

Elucidation of inhibition mechanism and determination of inhibition parameters

S10 extract of *D. magna* was incubated with different diazoxon concentrations (0.2, 0.4, 0.6, 0.8 and 1.0 µM) in presence of ATCh and the formation of the product thiocholine was recorded over time using the color reaction of the Ellman test (reaction progress curves). Measurements were performed in triplicate. Reaction progress curves were analyzed according to Baici et al. (Baici et al. 2009) (details see SI).

***In vivo* exposure to diazinon**

The degree of immobilization and mortality during exposure to different diazinon concentrations (5.3, 13.1 and 26.3 nM) for approximately three days was investigated in a pre-experiment. Immobilization in the early stage was characterized by an intense and fast convulsive movement of the second antennae, which disabled the daphnids to conduct normal locomotion. Especially for high concentrations the frequency of this movement decreased until no movement at all was detectable with the bare eye. Nevertheless, even for the highest exposure concentration (100% immobilization after one day) the majority of the daphnids were still alive after three days of exposure (e.g. heartbeat still observable under the microscope). Based on the pre-experiment, daphnids, for which no movement was visible anymore with the naked eye, were counted as immobilized.

During the actual *in vivo* experiments *D. magna* was exposed to 9.2 nM diazinon (exposure phase, all organisms affected over approx. 40 h but still remaining in the early stage of immobilization) and the time course of ChE activity and % immobilization recorded. Measurements were continued after transferring the exposed daphnids into clean medium (0.008% acetone, elimination phase). Two separate experiments were performed: Exposure for 13 h and 21 h and subsequent transfer into clean medium (experiment I and II, respectively). Animals from experiment I were also exposed up to 37 h without a subsequent elimination phase. Experiments were performed at 20 ±1 °C in the dark without feeding according to the OECD Guideline 202 (OECD 2004). Two replicates with 20 animals each per treatment and for each solvent control (0.008% acetone) were used. After different exposure times ChE activity was measured (all daphnids collected). Activity expressed in % activity of the solvent control activity at the respective sampling time was transformed into absolute amounts ($pmol \cdot g_{ww}^{-1}$) using the absolute amount of active AChE determined *in vitro* (see SI). The first-order rate constant of enzyme restoration k_{rec} (h^{-1}) was determined by fitting equation 3.2 to the enzyme activity during the elimination phase with the assumption that diazoxon is completely eliminated from the organism, i.e. I(t) = 0.

The diazoxon concentration present at the target site was predicted via the measured AChE activity according to equation 3.3. Immobilization over time in dependence of the measured AChE activity was described by fitting equation 3.6 and 3.7 (here used for immobilization instead of mortality) to the *in vivo*

immobilization data. In ModelMaker differential equations were solved with the Runge-Kutta method; best fit values for k_{kill} and $E_{a,threshold}$ were obtained by least-square optimization using the Levenberg-Marquardt method.

Results and discussion

In vitro experiments

Relative contribution of different processes to the measured AChE activity

A comparison of the maximal inhibition levels of AChE activity after incubation with the inhibitors diazoxon, eserine sulfate and iso-OMPA (82 %, 77 %, and 6 % inhibition, respectively) showed that the main part of the observed activity towards hydrolysis of the substrate ATCh is caused by AChE. The residual activity in case of eserine sulfate (approx. 20%) was presumably composed of several processes other than ChE hydrolysis (e.g. non enzymatic hydrolysis of ATCh, see also SI). As data were corrected via an eserine sulfate control, these effects are eliminated from the measured activity and the observed rate of ATCh hydrolysis was therefore expressed as AChE activity.

Determination of AChE amount in D. magna

For the tested diazoxon concentration range (0 to 0.21 nM) a linear decrease of AChE activity from 100 % down to approx. 70 % with increasing diazoxon concentration was observed. If it is assumed that one molecule of diazoxon inhibits one molecule of AChE, the intercept of the regression line with the x-axis equals the amount of AChE present in S10 extract. This extrapolation yielded 0.7 nM (95 % CI: 0.6 to 0.9 nM) active AChE or 0.02 % of the total protein in the S10 extract.

Elucidation of inhibition mechanism and determination of inhibition parameters

Comparison of the different inhibition mechanisms *in vitro* (as detailed in the SI) led to the conclusion that in case of *D. magna* AChE is inhibited by diazoxon irreversibly in two steps. The inhibition parameters were determined as 0.75 min^{-1} (95% CI: 0.69 to 0.81) for k_p and 5.85 nM (95% CI: 4.42 to 7.29) for K_i. The bimolecular reaction constant k_i describing the overall inhibition process amounts to 0.13 $nM^{-1} \cdot min^{-1}$.

Under *in vivo* conditions the calculated diazoxon concentration (see below Figure 3.2 b, maximum value 4.2 $pmol \cdot g_{ww}^{-1}$) is much smaller than the dissociation constant K_i (566 $pmol \cdot g_{ww}^{-1}$). Therefore the concentration of the associative complex EI_r is kinetically not significant and irreversible inhibition occurs exclusively in one step (Baici et al. 2009). The inhibition rate law (see equation 3.2) indeed corresponds to an irreversible inhibition in one step following second order kinetics but the constant k_i still includes both the phosphorylation (k_p) and the association step (K_a). k_p, K_a and k_i values derived here and literature values for different species and diethylphenyl phosphates are listed in Table 3.1.

Table 3.1. *Inhibition parameters k_p, K_a, k_i according to an irreversible inhibition in two steps for different diethylphenyl phosphates and AChE from several species. T, pH: temperature and pH in experiments.*

OP compound	Species	Source of AChE	k_p (min^{-1})	K_a (M^{-1})	k_i ($min^{-1}M^{-1}$)	T (°C)	pH	Ref.
Diazoxon	*D. magna*	Whole body	7.53E-01	1.71E+08	1.29E+08	19-20	7.2	This study
Chlorpyrifos-oxon	Rat	Brain	3.0E-01	2.41E+07	7.53E+06	37	7.4	*(Carr and Chambers 1996)*
	Catfish	Brain	4.3E-01	2.27E+06	9.59E+05	37	7.4	
Paraoxon	Rat	Brain	3.96E-01	2.05E+06	8.55E+05	37	7.4	*(Carr and Chambers 1996)*
	Catfish	Brain	5.50E-01	5.24E+04	3.27E+04	37	7.4	
	Electric eel		1.98E+01	5.88E+03	1.91E+03	22	6.9	*(Forsberg and Puu 1984)*
	Rat	Brain	3.82E+01	4.61E+04	1.76E+06	22	8	*(Wang and Murphy 1982)*
	Chicken	Brain	2.53E+01	1.57E+05	3.98E+06	22	8	
	Catfish	Brain	2.22E+01	4.93E+03	1.09E+05	22	8	

In comparison to *in vitro* data from rat, chicken and fish the phosphorylation rate constant k_p determined for *D. magna* and diazoxon is relatively low, but the association constant K_a ($1.71 \cdot 10^8$ M^{-1}) and k_i = $1.01 \cdot 10^8$ $M^{-1}min^{-1}$ are by at least a factor of 10 higher than for the listed vertebrates. Such high k_i values have only been found for extremely potent OP compounds like VX (k_i = $1.4 \cdot 10^8$ $M^{-1}min^{-1}$, rat brain synaptosomal AChE) (Maxwell 1992). The observed very high enzyme-inhibitor affinity is reflected by a very high overall sensitivity of *D. magna* AChE towards inhibition by diazoxon. This is consistent with the high toxicity of diazinon towards this species with LC_{50}(48 h) = 0.8 µg·L^{-1}. Diazinon is much less toxic in fish: The LC_{50}(96 h) for guppy and zebrafish are 0.8 ± 0.5 mg L^{-1} and 8 ± 1 mg L^{-1}, respectively (Keizer et al. 1991), the LC_{50}(48 h) for killifish 4.4 mg L^{-1} (Tsuda et al. 1997). This aligns well with the generally low k_i values found for fish AChE (see Table 3.1).

In our study whole body homogenates were used. Since organophosphates are capable of binding also to non-critical pseudo-cholinesterases and carboxylesterases (Chambers 1992; Maxwell 1992) the inhibition parameters might also be influenced by other binding sites than AChE. Consequently the absolute amount of AChE determined in our study constitutes an upper level of this enzyme present in the water flea.

***In vivo* experiments**

Exposure to diazinon and modeling of the time course of AChE activity and survival

During *in vivo* experiments no immobilization or mortality occurred in the solvent controls. In Figure 3.2 a the AChE activity and immobilization during exposure to 9.1 nM diazinon is plotted as a function of the exposure time (experiment I). After an initial time period of low response AChE activity and immobilization decreased and increased, respectively. Within an exposure period of 36.9 h 100% of the organisms were immobilized and AChE activity declined to a minimum value of 5.5 % of solvent control activity.

The TD model (equations 3.6 and 3.7, $r^2 = 0.97$) fitted to the time course of immobilization during exposure to diazinon (experiment I) is shown in Figure 3.2 a. The best fit value for the killing rate k_{kill} is 0.0163 ± 0.0004 $g_{ww} \cdot pmol^{-1} h^{-1}$ and the threshold value $E_{a,threshold}$ equates to 23.0 ± 2.3 $pmol \cdot g_{ww}^{-1}$, which corresponds to approximately 40 % of control AChE activity. Figure 3.2 b shows the internal diazoxon concentration calculated according to equation 3.3 via the measured AChE activity applying the inhibition parameters k_p and K_a determined *in vitro* and the recovery rate k_{rec} determined *in vivo* (see below). Diazoxon follows an exponential curve inversely related to the AChE activity with only a slow increase in the first hours.

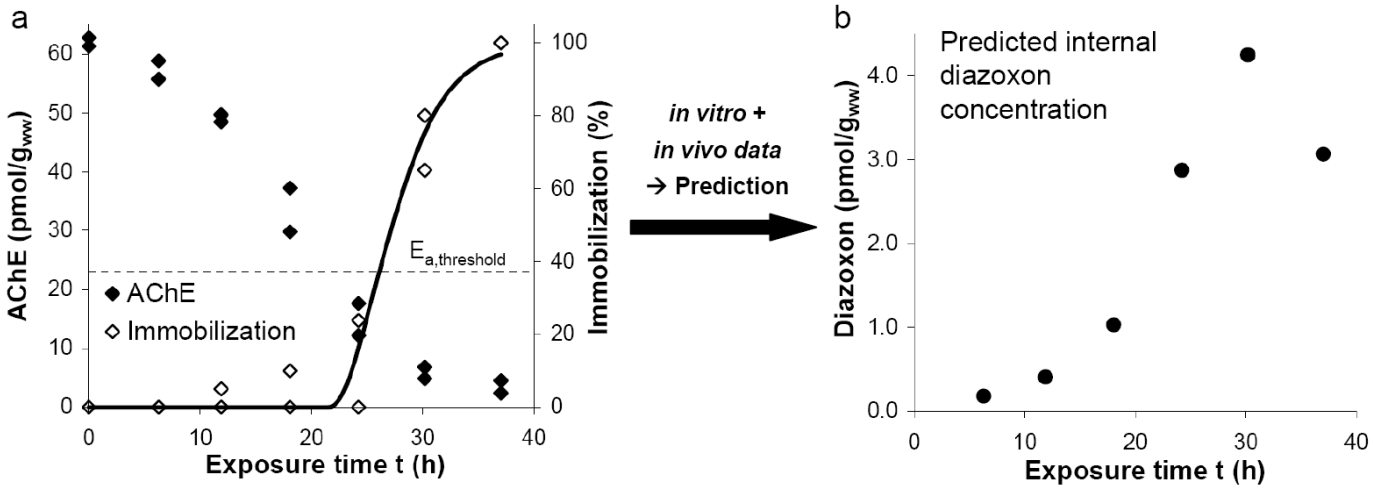

Figure 3.2. *Experiment I: (a) Time course of active AChE and immobilization during exposure to 9.1 nM diazinon. Solid line: TD model (equations 6 and 7) fitted to the immobilization data. (b) Time course of diazoxon concentration present at the target site calculated with equation 3.3.*

Linking the internal diazoxon concentration with the intrinsic effect

The predicted diazoxon concentration represents the concentration, which the target enzyme AChE actually must have encountered to cause the observed time course of inhibition. The slow increase during exposure to diazinon in the first hours may be explained by a delay from uptake of diazinon into the organism, activation of diazinon to the toxic metabolite diazoxon and distribution to the target site (TK processes). Since AChE in *D. magna* was shown to be very sensitive towards diazoxon, the reaction of the active compound with the target molecule was assumed to happen instantaneously. The time course of AChE inhibition therefore parallels the time course of the internal diazoxon concentration at the target site. Maximum inhibition velocity is reached when the product of the amount of diazoxon present at the target site and amount of active enzyme is maximal. Since receptor sites are saturable the velocity of inhibition levels off with continued exposure. *In vivo* studies with OPs and aquatic organisms support our findings: For *D. magna* exposed to malathion and chlorpyrifos an accelerating decline in AChE activity with increasing exposure time was preceded by a period without response. The length of this period was dependent on the exposure concentration: For high concentrations inhibition set in already shortly after the beginning of exposure (Barata et al. 2004).

Linking the intrinsic with the external effect

The determined threshold for AChE activity means, that for more than 60 % inhibition of control levels immobilization (according to our TD model the probability for immobilization) increases with decreasing activity. Similarly to the internal concentration of diazoxon and target activity, the time course of AChE activity and immobilization also seem to be directly related, but not before this threshold is reached (see Figure 3.2 a). Studies with *Gammarus pulex* and *D. magna* exposed to OP compounds revealed similar threshold values. Here lethal effects occurred at inhibition levels higher than 50 % (Barata et al. 2004; Xuereb et al. 2007). The actual reason why immobilization arises is accumulation of the neurotransmitter ACh as soon as AChE is inhibited to a certain percentage leading to overstimulation of ACh receptors (Boelsterli 2007). Consequently time dependent ACh accumulation might explain the observed time delay between enzyme inhibition and immobilization. Such an alternative concept to the threshold approach is applied in pharmacology and explains the time lag between the internal concentration (or internal effect) and an external effect by an indirect response mechanism, e.g. a time consuming production of an endogenous substrate (Derendorf and Meibohm 1999). This concept was for example applied to model the time course of muscular response in patients after application of an AChE inhibitor (Jusko and Ko 1994). Compared to the hazard rate the implementation of the neurotransmitter ACh in our model would provide a mechanistic link of the intrinsic and the extrinsic effect.

Linking immobilization with mortality

In the preexperiment, even for the highest diazinon concentration (26.3 nM) mortality seemed to occur days after immobilization set in. In agreement with this observation, also in a study with *D. pulex* exposed to chlorpyrifos (Van der Hoeven and Gerritsen 1997) mortality (no movements of antennae, legs, heart and intestines observable under the microscope) occurred at a later time point than immobilization. This time interval between immobilization and death seemed to be independent of the applied chlorpyrifos concentration and of prolonged exposure. It was proposed that a secondary factor, e.g. starvation, is causing death of immobilized animals (Van der Hoeven and Gerritsen 1997). In contrast to the direct relationship (on a time scale) of enzyme activity with immobilization AChE inhibition seems not to be directly linked to mortality. As immobilization was shown to be irreversible in our exposure experiments (see next section) it can be set equal to mortality. Therefore it is justified to translate immobilization into survival in the proposed TD model.

Recovery from damage on molecular and organism scale

When daphnids were transfered into diazinon free medium in experiment I and II AChE inhibition continued initially but then AChE activity increased again with continued depuration (see Figure 3.3). Fit of equation 3.2 to the measured AChE activity during the depuration phase from 24.2 h to 61.4 h and from 31.3 h to 79.2 h (diazoxon assumed to be completely eliminated) in experiment I and II, respectively, yielded 0.008 ± 0.002 h^{-1} (r^2 = 0.75) for the first order recovery rate constant k_{rec}. If the measured activity at time point 68.4 and 79.2 h of the depuration phase of experiment II, where activity seems to decline again after an initial increase, were excluded the k_{rec} was 0.014 ± 0.003 h^{-1} (r^2 = 0.81).

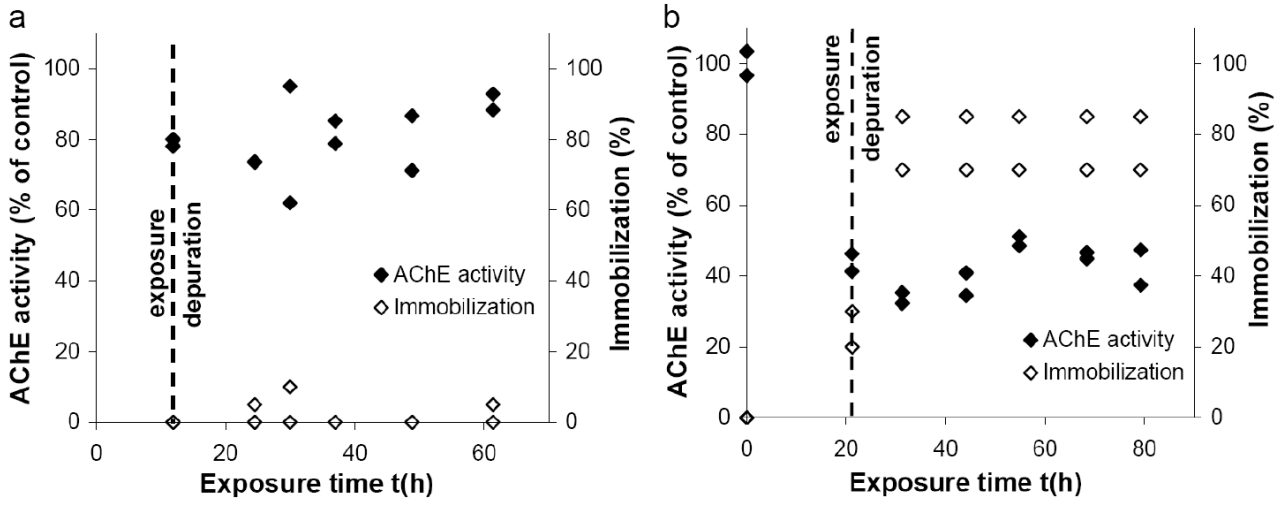

Figure 3.3. *Experiment I (a) and II (b): Time course of AChE activity and immobilization during the elimination phase after 13 h of exposure to 9.1 nM diazinon and 21 h of exposure to 9.2 nM diazinon, respectively, and subsequent transfer into diazinon free medium. In b the time course of immobilization of one duplicate sample, which was continously recorded, is shown.*

According to our model recovery from the threshold activity for immobilization (60 % inhibition) to 95 % of control activity would take place within approx. 13 d (7 d if last two samples in experiment II are excluded). As this regain in activity is measured against non-exposed animals (controls) it is likely to be due to *de novo* synthesis induced by diazoxon or spontaneous reactivation of inhibited enzyme. Similar to our study a study with paraoxon-methyl found that recovery of AChE activity in *D. magna* is a relatively fast process compared to other species: A regain of ≥ 30 % (relative to cholinesterase activity) took place within 48 h (Duquesne 2006).

For *G. pulex* the time needed to recover from exposure to diazinon was predicted as 28 d (here, recovery from a not further specified internal damage, which lumps all processes causing a dentrimental effect in an organism, is regarded) (Ashauer et al. 2010). This is in line with slow restoration of AChE activity in *Gammarus* after OP poisoning, which was found to take up to several weeks (Kuhn and Streit 1994). Slow recovery was assumed to be due to slow *de novo* synthesis of AChE (Benke and Murphy 1974). For *D. magna* and diazinon at least a fast reactivation can be excluded since within our mechanistic analysis *in vitro* (duration of experiment 30 min) inhibition was found to be persistent.

Recovery from immobilization was assessed in experiment II (25 % immobilization at time point of transfer). In Figure 3.3 b the time course of immobilization of one duplicate sample, which was used for AChE measurement in the end of the experiment, is shown. Here, immobilization was continuously recorded from the beginning till the end of the experiment in order to show potential recovery from immobilization of one consistent sample. A maximum immobilization of 78 % was reached at 31.3 h after beginning of the experiment. Further depuration until 79.2 h did not lead to any further change in percentage of immobilized animals. Recovery of affected animals could not be observed; in contrast, the vitality appeared to decrease with time and mortality was inevitable. A possible explanation might be that with ongoing immobilization health is reduced, which might impair vital functions of the organism like *de novo* synthesis of enzymes. The decline of AChE activity compared to controls after an initial restoration period in toxicant free medium (data at 68.4 and 79.2 h in experiment II, see Figure 3.3 b) is in accordance with this assumption. This might be due to a lack of food. However, for *D. pulex* which were fed during exposure to chlorpyrifos and subsequently transferred into non-contaminated medium also no recovery from immobilization was detectable (Van der Hoeven and Gerritsen 1997).

Outlook

The proposed TD model combines all the mechanistic information about the toxic action of diazoxon and enables to link and predict the time course of the effect on molecular level with the effect on organism level as function of the internal concentration of the active compound. In contrast to current TKTD models (Jager and Kooijman 2005; Ashauer et al. 2007b) the TD model was explicitly parameterized by *in vitro* and *in vivo* measurements on the interaction with the target site and the resulting effect on molecular scale. Since the inhibition parameters K_a and k_p are direct descriptors of species sensitivity (Wallace 1992) specific

information about the interaction with the target site obtained *in vitro* is important to include in effect modeling e.g. if differences in toxicity between different species need to be explained.

Supporting information for chapter 3

Additional information on Theory

In vitro elucidation of inhibition mechanism and determination of inhibition parameters

Figure 3.1 summarizes all potential inhibition mechanisms that were evaluated in this study.

Irreversible inhibition may occur in two steps (mechanism I(2)) or in one step (mechanism I(1)). In mechanism I(2) a slow irreversible formation of an inactive complex EI, in which the inhibitor is bound covalently to the enzyme (phosphorylation of the enzyme), is proceeded by a fast and reversible generation of an associative enzyme-inhibitor complex EI_r. I(2) degenerates to I(1) if the concentration of the intermediate complex EI_r is very low in steady state. Further variations of these mechanisms arise if the covalent enzyme-inhibitor complex EI_i can degrade to free enzyme plus an inactive form of the inhibitor (I(1,r); I(2,r)). This pathway is equivalent to the spontaneous reactivation of phosphorylated AChE. Here the enzyme is only temporarily inhibited. In addition to irreversible modifications also reversible, slow-binding enzyme inhibition in two steps R(1) or in one step R(2) are considered. In the first case the reversible formation of an associative enzyme-inhibitor complex (EI_r) is followed by a slower step, in which a reversible enzyme-inhibitor complex is formed. For both, R(1) and I(1) the concentration of the associative complex EI_r is negligible in steady state (Baici et al. 2009).

In case of mechanism I(2) the reaction progress curve describing product formation with time is given by equation S-3.1:

$$P(t) = \frac{v_z}{\lambda} \cdot (1 - e^{-\lambda t}) \qquad \text{(S-3.1)}$$

Equation S-3.1 is fitted to the reaction progress curves by nonlinear regression for a series of experiments with varying inhibitor concentration. v_z ($M \cdot min^{-1}$) is the velocity of product formation at time point zero and λ (min^{-1}) the first order rate constant. In a next step the best fit values for λ and v_z are plotted against the inhibitor concentration (equation S-3.2 and S-3.3). The fit of the corresponding mathematical expressions of these parameters results in best fit values for the inhibition parameters of I(2) (Baici et al. 2009).

$$v_z = \frac{V_{max} \cdot S}{K_m\left(1 + \frac{I}{K_i}\right) + S} \quad \text{(S-3.2)} \qquad \lambda = \frac{k_2 \cdot I}{K_i\left(1 + \frac{S}{K_m}\right) + I} \quad \text{(S-3.3)} \qquad \text{with } K_i = \frac{k_{-1}}{k_1} = \frac{1}{K_a} \quad \text{(S-3.4)}$$

K_i (M) is the dissociation constant, K_a (M^{-1}) its reciprocal value, the association constant. $k_2 = k_p$ is the phosphorylation constant (min^{-1}). I (M) is the inhibitor concentration.

The product of K_a and k_p is the bimolecular (inhibition) reaction constant k_i ($min^{-1}M^{-1}$) (Main 1964):

$$k_i = K_a \cdot k_p \qquad \text{(S-3.5)}$$

To test if a different mechanism than I(2) applies measured reaction progress curves are processed in an analogous way as described for meachnism I(2) but with the mathematical expressions of the respective mechanism. Additional parameters like the velocity of product formation in steady state and the velocity of product formation for $t \rightarrow \infty$ v_s and v_∞, respectively (all in $M \cdot min^{-1}$) are regarded. The respective best fit values for λ and v_z obtained for the different mechanisms are plotted against the inhibitor concentration. A

hyperbolic dependency of λ and v_z vs. I indicates the presence of an inhibition in two steps (see graphic distinction of mechanisms in Figure S-3.1). If λ is linearly dependent and v_z indenpendent (horizontal line) on the inhibitor concentration an inhibition in one step can be concluded. A further subdivision in reversible and irreversible inhibition is possible by analysis of the slope of the progress curves in steady state and the y-intercept of the regression curve through λ vs. I: A value > 0 for slope and intercept indicates a reversible reaction, a value = 0 an irreversible reaction, respectively. The graphical findings are supported by the best fit values of the kinetic rate constants for the different reaction pathways and their relativ significance to each other (see Figure S-3.1) (Baici et al. 2009). For a compilation of equations for the different inhibition mechanisms and of the respective simulated curves the reader is referred to (Baici et al. 2009).

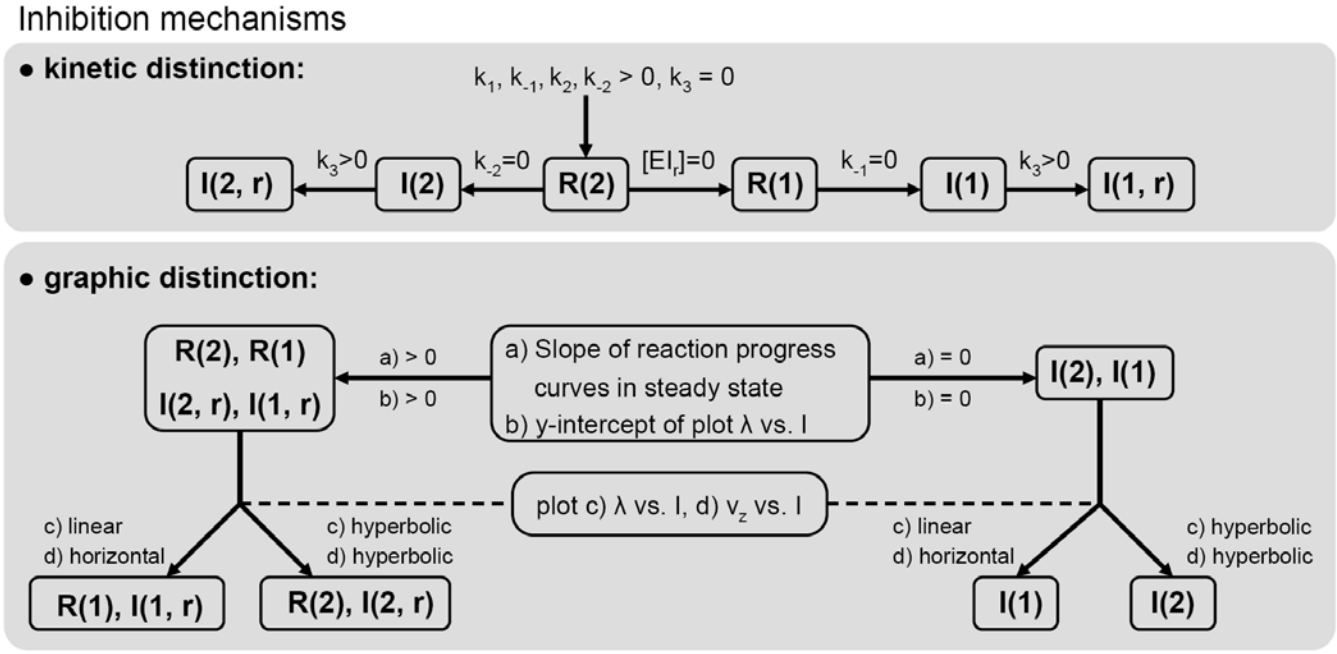

Figure S-3.1. *Distinction of inhibition mechanisms by comparison of kinetic rate constants, graphical analysis of reaction progress curves and plots of λ and v_z vs. the inhibitor concentration according to (Baici et al. 2009). Abbreviations indicating inhibition mechanism: I(...): irreversible inhibition, R(...): reversible inhibition, 1: in one step, 2: in two steps, r: spontaneous reactivation of covalent enzyme-inhibitor complex. >0 and =0 indicate if values of the kinetic rate constants or the concentration of the associative complex are significantly different from zero or negligible small/ equal to zero.*

Development of TD model

The derivation of the rate equation for mechanism I(2) under *in vitro* conditions is described in (Bisswanger 2008) and (Main 1964). Since the concentration of the neurotransmitter acetylcholine (ACh) in living *D. magna* is not known, we rely on an expression established for inhibition in the absence of substrate. In the following enzyme (complex) or inhibitor concentrations are expressed in $pmol \cdot g_{ww}^{-1}$, K_a in $g_{ww} \cdot pmol^{-1}$ and k_p in h^{-1}. The rate-determining step during the inhibition reaction is the phosphorylation step. The rate of the inhibiton reaction is therefore given by:

$$\frac{dEI_i(t)}{dt} = k_p \cdot EI_r(t) \qquad \text{(S-3.6)}$$

If high substrate concentrations are applied, the inhibitor in the reversible enzyme-inhibitor complex can be replaced by the substrate. With this assumption the active enzyme form E_a equals the sum of free enzyme E and associative complex EI_r. Since for the *in vitro* measurement of the AChE activity in extracts of daphnids exposed *in vivo* high concentrations of acetylthiocholine (ATCh) as surrogate for the neurotransmitter ACh are used, the activity can be refered to the active enzyme form E_a. The total amount of enzyme E_0 (initial amount of free enzyme) is composed by the free enzyme in the system, the reversibly formed intermediate and the inactivated enzyme:

$$E_0 = E + EI_r + EI_i = E_a + EI_i \qquad \text{(S-3.7)}$$

If we assume that the association step happens instantaneously the equilibrium constant K_a is given by:

$$K_a = \frac{EI_r}{E \cdot I} \qquad \text{(S-3.8)}$$

Here, I is the concentration of the toxicant at the target site. From inserting equation S-3.8 in S-3.7, it follows that:

$$E_a = E + EI_r = \frac{EI_r}{K_a \cdot I} + EI_r \qquad \text{(S-3.9)} \qquad \text{and} \qquad EI_r = \frac{E_a \cdot K_a \cdot I}{1 + K_a \cdot I} \qquad \text{(S-3.10)}$$

Insertion of equation S-3.10 in S-3.6 and the assumption that E_0 is constant gives the decline of the active enzyme with time:

$$\frac{dEI_i(t)}{dt} = \frac{d\left[E_0 - E_a(t)\right]}{dt} = -\frac{dE_a(t)}{dt} = \frac{k_p \cdot K_a \cdot I(t)}{1 + K_a \cdot I(t)} \cdot E_a(t) \qquad \text{(S-3.11)}$$

In vivo the inhibitor concentration at the target site I is likely to be very small ($K_a \cdot I << 1$). Equation S-3.11 simplifies to equation S-3.12, which describes the decline of enzyme activity due to irreversible occupation of the target site AChE. The inhibition parameters k_p and K_a can be determined *in vitro*.

$$\frac{dE_a(t)}{dt} = -k_p \cdot K_a \cdot I(t) \cdot E_a(t) \qquad \text{(S-3.12)}$$

An additional second term needs to be implemented into equation S-3.12 to describe the recovery of enzyme activity due to (induced) *de novo* synthesis of free enzyme or spontaneous reactivation of the enzyme-inhibitor complex.

$$\frac{dE_a(t)}{dt} = -k_p \cdot K_a \cdot I(t) \cdot E_a(t) + k_{rec} \cdot \left[E_0 - E_a(t)\right] \qquad \text{(S-3.13)}$$

The first-order rate constant k_{rec} (h^{-1}) has to be determined with *in vivo* data as *in vitro de novo* synthesis is not possible. The total enzyme amount E_0 is assumed to be constant.

Relative contribution of different processes to the measured AChE activity

AChE activity present e.g. in animal tissue extracts can be measured *in vitro* with the method developed by Ellman et al. (Ellman et al. 1961). Here, ATCh served as surrogate for ACh. The hydrolysis product thiocholine (TCh) reacts with 5,5′-Dithiobis(2-nitrobenzoic acid) (DTNB) to form a yellow anion which is detected photometrically. The observed activity towards ATCh is comprised of several processes (Figure

S-3.2): Enzymatic hydrolysis by AChE as well as buturylcholinesterase (BuChE, also termed pseudo-cholinesterase); non-enzymatic hydrolysis of ATCh; reaction of DTNB with thiol groups; (enzymatic) degradation of the formed dye. In order to apportion the relative contribution of these processes to the observed activity, extracts were incubated with different enzyme inhibitors. Eserine sulfate was used as selective inhibitor of the cholinesterases AChE and BuChE and iso-OMPA as selective inhibitor of only BuChE.

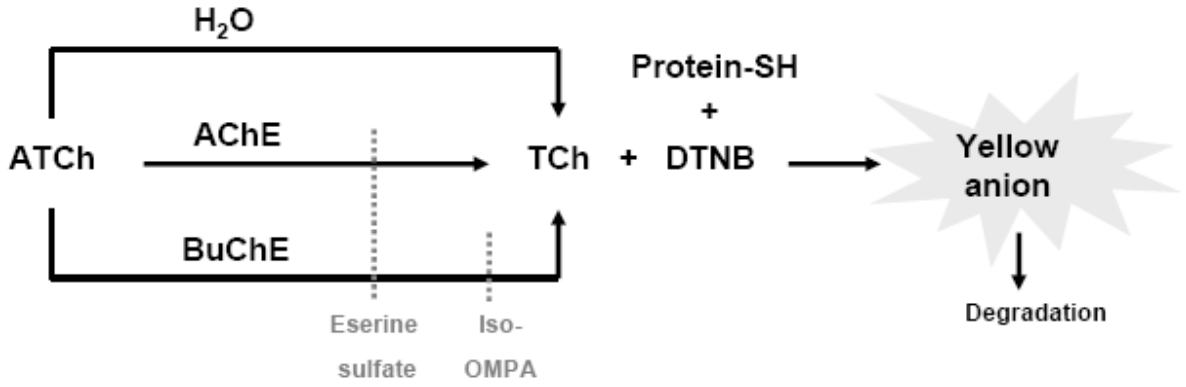

Figure S-3.2. *Enzymatic and non-enzymatic processes contributing to the measured activity towards the substrate acetylthiocholine (ATCh) in extracts of animal tissues.*

Determination of AChE amount in D. magna

In many species AChE has been reported to exist in oligomeric form e.g. as a dimer or up to a hexamer composed of subunits. The molecular weight of one subunit (80 kDa) of tetrameric AChE from electric eel used for our calculations is similar to values found in other aquatic organisms. Authors report molecular weights of one subunit ranging from approximately 40 to 80 kDa (Dudai and Silman 1974; Engels et al. 1978; Forget et al. 2002). In the copepod *Eurytemora affinis* AChE is present in dimeric form with a molecular weight of 70 kDa per subunit (Forget et al. 2002). In the sea mussel *Mytilus edulis* even a hexameric form was detected with each subunit possessing a molecular weight of about 41 kDa (Engels et al. 1978). If the stoichiometry of inhibition is known (e.g. one monomeric AChE contains one binding site) and if the OP molecule is assumed to bind irreversibly, the absolute amount of AChE present in *D. magna* can be determinded by titration of the active sites with organophophorous compounds. The amount of inhibitor necessary to cause 100 % inhibition is equal to the amount of enzyme. Organophosphorous compounds can not only bind to AChE but also to other enzymes like BuChE and carboxylesterases (CbE) (Aldridge 1953b; Walker and Thompson 1991; Chambers 1992; Maxwell 1992; Tang and Chambers 1999). Therefore the AChE concentration measured in extracts of *D. magna* by titration of the active sites might also include other types of enzymes.

Additional information on Materials and Methods

Chemicals used

Diazinon was purchased from Ultra Scientific (CAS 333-41-5, 99.5 % purity, N. Kingstown RI, USA). Diazoxon (CAS 962-58-3, 99.5 % purity) was obtained from Wako Pure Chemical Industries, Ltd. (Osaka, Japan). 5,5′-Dithiobis(2-nitrobenzoic acid) (DTNB, CAS 69-78-3, 99 % purity), acetylthiocholine (ATCh) iodide (CAS 1866-15-5, 98 % purity), eserine hemisulfate salt (CAS 64-47-1, 98 % purity), tetraisopropyl pyrophosphoramide (iso-OMPA, CAS 513-00-8, 98 % purity), the Folin & Ciocalteu's phenol reagent 2N, bovine serum albumin (BSA, CAS 9048-46-8, 98 % purity), and chemicals used for Lowry protein determination (see (Lowry et al. 1951), purity ≥ 98%) were purchased from Sigma-Aldrich (Buchs, Switzerland).

For preparation of the M4 medium according to (OECD 2004) only chemicals of analytical grade were used (Sigma-Aldrich, Buchs, Switzerland). All solvents used were of analytical grade (Acros Organics, New Jersey, USA; Merck, Darmstadt, Germany; Sigma Aldrich, Buchs, Switzerland). For preparation of solutions and M4 medium ultrapure water from a Milli-Q® system (Millipore AG, Zug, Switzerland) was taken.

Preparation of stock solutions and dilutions

For all experiments a phosphate buffer (0.1 M, pH = 7.2) was used as buffer. ATCh iodide was dissolved in water. The concentration of the stock solution was 60 mM. A DTNB stock solution was prepared by dissolving DTNB together with $NaHCO_3$ (31 mM) in water. Stock solutions were subdivided in small portions and stored at -20°C. For determination of K_m and V_{max} 0.58 mL of the ATCh stock solution were diluted with 1.42 mL phosphate buffer resulting in a concentration of 17.0 mM and 3.42 mL of the DTNB stock solution with 0.58 mL water resulting in a concentration of 8.5 mM. For all other experiments an ATCh/ DTNB mixture (8.5 mM/ 8.5 mM) was prepared by mixing 3.42 ml of the DTNB stock solution with 0.58 mL of the ATCh stock solution. These dilutions were prepared shortly before the experiments.

A stock solution of diazinon (22.5 mM) was prepared in methanol. For the *in vivo* experiments the stock solution was diluted with acetone to a final concentration of 90.1 µM (0.6 % methanol). Diazoxon was dissolved in acetone (3.6 mM) and diluted with acetone to 0.36 mM and 35.8 µM. For in vitro experiments the stock solutions were diluted with phosphate buffer.

An eserine hemisulfate salt and iso-OMPA stock solution was prepared in water (1.9 mM) and ethanol (2.8 mM), respectively, and each of the stock solution diluted to 9.6 µM and 9.8 µM, respectively, with phosphate buffer. For controls analog solutions in buffer but without the active compounds were prepared (in case of eserine sulfate only buffer was used).

LC-MS/MS Analysis

Diazinon and diazoxon were analyzed with online-SPE HPLC-ESI-MS/MS using a TSQ (Triple Stage Quadrupole) Quantum Ultra mass spectrometer from Thermo Fisher Scientific. Extraction was performed on ENV+ (hydroxylated polystyrene divinylbenzene, mean particle size 40-70 µm, average pore size 60 Å) from International Sorbent Technology Ltd as sorbent. For separation of compounds an Atlantis T3 column (3.0x150mm, C18, particle size 3 µm, pore size 100 Å) from Waters was used. A linear gradient with MeOH and water (2 mM NH_4Ac) was applied (total flow 400 $\mu L \cdot min^{-1}$). For quantification of diazinon and diazoxon diazinon-diethyl-d10 served as internal standard, respectively. Data were evaluated with Xcalibur (Thermo Scientific, U.S.) in the Qual and Quan Browser.

Culturing of D. magna

D. magna STRAUS 1820 clone 5 was originally obtained from the Institute for Environmental Research at the RWTH Aachen University. Animals were cultured in artificial M4 medium (according to (OECD 2004)) at a temperature of 20 ± 2 °C and with a 16 h light and 8 h dark cycle.

Mothers were kept in glass beakers each containing 20 animals and approximately 1.5 L of M4 medium. The main culture was divided according to the age of the daphnids: Up to one, two, three and four week old animals (1st, 2nd, 3rd and 4th week, respectively) were kept separately in beakers. Neonates from the 3rd and 4th week adults were separated at least three times a week. The M4 medium was renewed once a week. Every week the order of the culture was changed: The former 1st week became the new 2nd week, the former 2nd week the new 3rd week etc.. Neonates from the 4th week formed the new 1st week. The 4th week itself was dismissed. Once a week the culture was checked for males. If there were any present these were separated from the culture and discarded. The basic method of culturing was obtained from the Institute for Environmental Research at the RWTH Aachen University (Preuss Institute for Environmental Research, RWTH Aachen University). As food source the green algae Scenedesmus obliquus cultured in a chemostat was used. In the 1st week 0.05 mg(particulated organic carbon, POC)$\cdot daphnid^{-1} \cdot d^{-1}$ were supplied, in the 2nd to 4th week 0.1 mg(POC)$\cdot daphnid^{-1} \cdot d^{-1}$.

For experiments neonates ≤ 24h were separated from the 3rd and 4th week of the main culture. These were raised for 5 days under the same conditions as the main culture apart from one beaker containing 40 animals, which were fed with 0.025 mg(POC)$\cdot daphnid^{-1} \cdot d^{-1}$. Prior to the experiments daphnids were transferred into clean M4 medium for 1 - 3 h. The wet weight (ww) was determined and daphnids checked for ovaries, eggs or males under the microscope. For subsequent in vitro experiments animals were sieved, washed with water, snap frozen in liquid nitrogen and stored at -80°C until further analysis. In case of *in vivo* exposure animals were directly transfered into the exposure medium. After exposure daphnids were processed the same way as mentioned for *in vitro* experiments.

Determination of the wet weight of D. magna

The wet weight of *D. magna* was determined at the beginning of the *in vivo* exposure or before freezing daphnids for the *in vitro* experiments. Three to four replicate measurements were performed. Five daphnids per replicate were put on a paper tissue with a pipette in order to remove excess water from the outside of the carapace. Afterwards daphnids were transfered with a tweezers into an aluminium cup and weighted with an ultra-micro balance (XP2U, Mettler-Toledo, Switzerland, readability: 0.1 µg). In Table S-3.2 the mean values ± standard derivation are shown.

Preparation of S10 extract of D. magna and determination of protein content and ChE activity

Extracts were prepared as described in (Barata et al. 2004; Xuereb et al. 2007) modified as follows. *D. magna*, which were stored at -80°C, were homogenized with an ultrasonic homogenizer Labsonic® M, Sartorius Stedim Biotech (3x 30 s with an amplitude of 100% and a cycle of 1.0 with 15-30 s break in between). For *in vivo* and *in vitro* experiments 20 and 40 daphnids, respectively, were homogenized in 750 µL phosphate buffer plus 0.1% v/v Triton X-100. In case of *in vitro* experiments the homogenates were diluted with phosphate buffer (0.1% v/v Triton X-100) to a final concentration of approximately 30 $g_{ww} \cdot L^{-1}$. During the whole work-up process samples were cooled on ice. The obtained homogenates were centrifuged at 10000 g at 4 °C for 10 min. Supernatants were collected and stored on ice until further analysis. 100 µL of S10 extract was added to each well. The final volume in the wells was 290 µL.

Measurements were performed with a Tecan Infinite® 200 microplate reader set to λ = 750 nm for the protein determination and λ = 420 nm for the ChE assay (details of ChE measurement see Table S-3.1).

a) ChE measurement

Cholinesterase (ChE) activity in S10 extracts of *D. magna* was determined with the Ellman method (Ellman et al. 1961) and adapted to 96 well plate according to (Hamers et al. 2000) with modifications. If not otherwise stated ATCh concentrations in the final solutions in the wells were 1.5 mM each. The ATCh concentration is approx. 200x the Michaelis-Menten constant Km to assure that all experiments were conducted at maximum velocity of substrate hydrolysis vmax.

ChE activity (velocity of ATCh hydrolysis in min^{-1}) was determined by linear regression of measured absorbance (optical density, OD) as a function of time. Obtained OD vs. t curves were corrected with an eserine sulfate control, if available. The linear portion of the measured OD vs. t curve was chosen by comparison of residuals and distribution of data points along the regression line for different time intervals. Data points should be equally distributed and the residuals as small as possible. In most cases correction of data via an eserine sulfate control lead to an improvement of linearity. Absorbance was transformed into $mol \cdot L^{-1}$ product concentration via the Lambert-Beer law (equation S-3.14)

$$\text{Absorbance} = OD = \varepsilon \cdot c \cdot d \qquad \text{(S-3.14)}$$

with an extinction coefficient for the yellow anion of 1.36 $L \cdot mol^{-1} \cdot cm^{-1}$ and a path length of 0.81 cm in case of the used 96 well plate containing a volume of 290 µL per well. The resulting concentration units of M

were transformed into mol·mg(protein)$^{-1}$ considering a well volume of 290 µL and the measured protein content per well.

Table S-3.1. *Parameters of AChE activity measurement with a photometer. Experiment A: Determination of K_m and v_{max}, B: Inhibition of ChE activity with diazoxon, eserine sulfate and iso-OMPA, C: Determination of AChE amount, D: Elucidation of inhibition mechanism, E: in vivo experiment I, F: in vivo experiment II. Temperatures during plate measurement: Data not marked with an asterix - temperature was measured inside the photometer. Data marked with an asterix - room temperature*

Experiment		**A**	**B**	**C**	**D**	**E**	**F**
Temperature							
During plate preparation/ incubation	(°C)	20	20	20	22	20	20
During plate measurement	(°C)	20-21	21*	22-23	20-21	20*	20-21
Wavelength λ	(nm)	420	420	420	420	420	420
Duration	(min)	15	15	30	30	25	30
Time intervall Δt	(s)	15	15	20	20	15	20
Curve part used for evalutation	(min)	0.33 - 2.00	0.00 - 2.00	0.00 - 30.00	0.00 - 30.00	0.00 - 4.00	0.00 - 4.00

b) Protein measurement

The protein content of S10 extracts of *D. magna* was quantified using the Lowry method (Lowry et al. 1951) in a 96-well plate format with bovine serum albumine as reference. This was performed in triplicate with the same S10 extracts as prepared for ChE activity measurement. 100 µL of the extracts were diluted with 150 µL phosphate buffer (Triton® X-100 0.1% v/v) and 250 µL 0.1 M NaOH. In triplicate, 20 µL of the diluted extract together with 200 µL of Lowry reagent (0.5 mL 1% w/v CuSO4 in H2O, 0.5 mL 2% w/v K-Na-tartrate in H2O and 25 mL 1% w/v Na_2CO_3 in 0.1 M NaOH) were spiked to a 96 well microplate and mixed with a pipette. After 5 min 20 µL 1N Folin & Ciocalteu's phenol reagent were added and the solution mixed again with a pipette. Measurement of absorbance (λ = 750 nm) was started after 30 min of incubation. Calibration solutions were prepared by mixing a BSA stock solution (5 mg·mL^{-1} in H_2O) with phosphate buffer resulting in concentrations of 0.15 to 0.90 mg·mL^{-1} and subsequent dilution 1:1 with phosphate buffer (Triton® X-100 0.2 % v/v). The BSA solutions were further processed the same way as the daphnid extracts. Since the surfactant Triton® X-100 might cause interferences calibration solutions with (0.1 % v/v) and without Triton® X-100 were compared. The slopes and y-intercepts of the two calibration curves were not significantly different (P = 0.58 for slopes, P = 0.72 for y-intercepts), a disturbance by Triton® X-100 was therefore excluded.

Table S-3.2. *Wet weight and protein content of Daphnia magna used for in vitro and in vivo experiments. For in vivo experiments data were determined from unexposed daphnids at the beginning of the experiments. *Three separately prepared S10 extracts (S10/A,B,C). **Three separately prepared extract dilutions for protein measurement (S10/1,2,3)*

Experiment	Wet weight	Sample	Protein content
	mg_{ww}·daphnid^{-1}		µg·daphnid^{-1}
	mean ± SD (n = 3,4)		mean ± SD (n = 3)
***In vivo* experiments**			
Experiment I	1.54±0.09	D-0/A	41.6±2.9
		D-0/B	50.8±1.1
Experiment II	1.11±0.06	D-0/A	37.7±1.8
		D-0/B	38.6±1.4
***In vitro* experiments**			
Determination of K_m and v_{max}*	1.06±0.04	S-10/A	32.7±1.0
		S-10/B	32.6±0.4
		S-10/C	32.2±1.3
Inhibition of ChE activity	1.10±0.12		54.6±1.4
Determination of AChE amount	see determination of K_m and v_{max}		see determination of K_m and v_{max}
Elucidation of inhibition	1.13±0.17	S-10/1	42.2±0.2
		S-10/2	40.3±0.3
		S-10/3	41.4±0.7

Determination of K_m and v_{max}

For the determination of the Michaelis-Menten constant K_m (M) and the maximum velocity of substrate hydrolysis v_{max} (nmol·$mg_{protein}^{-1}$·min^{-1}) the enzyme activity was measured for increasing ATCh concentrations following a geometrical dilution series ranging from 1.4 µM to 3.0 mM. This experiment was performed in triplicate with three separately prepared S10 extracts (S10-A, S10-B, S10-C). K_m and v_{max} were obtained from separate fits of the Michaelis-Menten equation ($v = v_{max}·S/(K_m+S)$ with S is the substrate concentration (Bisswanger 2008)) to three replicate experiments.

(Detailed procedure: In a 96 well plate 50 µL phosphate buffer were added to wells 2 to 12 of one row. 50 µL of an ATCh solution (17.0 mM) were spiked in the first and second well mixed with a pipette. 50 µL from the second well were then transfered into the third well, mixed and 50 µL transfered into the fourth well and so on in order to give a geometrical dilution series. From the 12th well 50 µL of the mixture were disposed. In a next step 90 µL phosphate buffer, 50 µL DTNB solution (8.5 mM) and 100 µL S10 extract were added to all wells. Absorbance was immediately measured after mixing the solutions with a pipette (see details Table S-3.1)).

Relative contribution of different processes to the measured AChE activity

In the following inhibitor concentrations are defined with respect to a final volume of 290 µL. S10 extract of *D. magna* was spiked to a geometrical dilution series of inhibitor and incubated for 45 min at 20°C (volume in wells 240 µL). After incubation, ATCh and DTNB were added and the product formation with time measured. The concentrations of diazoxon ranged from 0.01 to 2.0 nM, of eserine sulfate and iso-OMPA from 0.4 nM to 0.8 µM. As controls (100% activity) buffer (for eserine sulfate) or solutions of acetone and ethanol in buffer (for diazoxon and iso-OMPA, respectively) were spiked to wells instead of inhibitor solutions. Inhibition assays are based on (Hamers et al. 2000; Xuereb et al. 2007) and were modified to our requirements.

(Detailed procedure: A 236 nM diazoxon dilution in buffer was prepared using the 35.8 µM acetone stock solution. To a 96 well plate 50 µL phosphate buffer was added in all wells of three rows. Subsequently, 50 µL of the 236 nM diazoxon, 10 µM iso-OMPA or 10 µM eserine hemisulfate salt solution were spiked to the first well of each row and mixed with a pipette. 50 µL from the first well were then transfered into the second well, mixed and 50 µL transfered into the third well and so on in order to give a geometrical dilution series. From the 12th well 50 µL of the mixture were disposed. In a next step 90 µL phosphate buffer and 100 µl S10 extract were added to all wells and mixed with a pipette. The mixtures were incubated for 45 min at 20 °C. Afterwards 50 µL of the 8.5 mM ATCh/ 8.5 mM DTNB mixture were added. After mixing the solutions with a pipette absorbance was measured immediately (Table S-3.1). As control (100% enzyme activity) the same procedure was performed but instead of the diazoxon, iso-OMPA and eserine sulfate solution 50 µL of the acetone/buffer, ethanol/ buffer solution and buffer, respectively, were applied.)

Determination of AChE amount in D. magna

For the determination of the absolute AChE amount present in *D. magna* S10 extracts were incubated with diazoxon applying the analog experimental approach as described in the previous section. Diazoxon concentrations were (0, 0.04, 0.08, 0.12, 0.17 and 0.21 nM). The measurement was performed in triplicate with three separately prepared S10 extracts. For correction of processes others than hydrolysis of ATCh by cholinesterases, the S10 extract was treated with eserine sulfate (1.7 µM) instead of diazoxon.

(Detailed procedure: A 0.58 nM diazoxon dilution in buffer was prepared using the 35.8 µM acetone stock solution. This experiment was performed in triplicate. Three separate S10 extracts were prepared. To a 96 well plate certain volumes of phosphate buffer were added to result in an incubation volume of 240 µL per well. To wells in one row 0, 20, 40, 60, 80 and 100 µL of the diazoxon dilution were spiked. Subsequently, 100 µL S10 extract were added, mixed with a pipette and incubated for 45 min at 20 °C. Afterwards 50 µl of the 8.5 mM ATCh/ 8.5 mM DTNB mixture were added. After mixing the solutions with a pipette absorbance was measured immediately (see details Table S-3.1). For correction of processes

others than hydrolysis of ATCh by cholinesterases 50 µL eserine hemisulfate salt solution 10 µM were applied instead of diazoxon.)

Elucidation of AChE inhibition mechanism, determination of inhibition parameters

For correction of processes others than hydrolysis of ATCh by cholinesterases S10 extract was incubated for 15 min with eserine sulfate (1.7 µM) prior to addition of ATCh and DTNB (see above). As reference for 100% activity S10 extract was incubated to the highest amount of acetone as present in the diazoxon treatments. For elucidation of the inhibition mechanism eserine corrected OD vs. t curves were set to 0 for t = 0. In general, for K_m the best-fit value from determination of the Michaelis-Menten parameters was used, as K_m is specific for the enzyme-substrate system and should remain constant for all experiments. In contrast, for v_{max} the best-fit value of v_z of the acetone control was taken because the protein content in daphnid extracts may vary due to variability in the work-up method or variability in the organism itself. In case of I(2) K_i was obtained as best fit value of equation S-3.2. During the fit of equation S-3.3 K_i was kept constant and the best fit value of k_p calculated.

(Detailed description: Diazoxon dilutions in phosphate buffer with a concentration of 1.2, 2.4, 3.6, 4.8, 6.0 µM were prepared using the 0.36 mM stock solution. Measurements were performed in triplicate. To wells of a 96 well plate 90 µL phosphate buffer, 50 µL of the respective diazoxon solution and 50 µL of the 8.5 mM ATCh/ 8.5 mM DTNB mixture were added. After spiking of 100 µL S10 extract the solutions were immediately mixed with a pipette and absorbance measured. As (solvent) control (100% enzyme activity) the same procedure was performed with either pure buffer and an acetone/ buffer solution with the same acetone content as the highest inhibitor concentration instead of diazoxon. For correction of processes others than hydrolysis of ATCh by cholinesterases 90 µL phosphate buffer, 50 µL of the 10 µM eserine hemisulfate salt solution and 100 µL S10 extract were spiked to wells and preincubated for 15 min at 22 °C prior to addition of 50 µL of a 8.5 mM ATCh/ 8.5 mM DTNB mixture.)

In vivo exposure experiments

The degree of immobilization and mortality during exposure to different diazinon concentrations (5.3, 13.1 and 26.3 nM) for approximately three days was investigated in a preexperiment. The preexperiment consisted of a solvent control (M4 medium containing 0.01 % acetone) and three different diazinon concentrations. Per treatment duplicate samples with 20 daphnids per 200 mL exposure medium were used and the occurance of immobilisation and mortality as function of time was analysed.

The exposure medium of the actual exposure experiments was prepared by adding 375 µL of diazinon solution (0.13 mM in acetone) and M4 medium (freshly prepared and aerated before the experiment) into a 5 L glass flask and subsequent thorough shaking. Medium for solvent controls and the depuration phase was prepared the same way with pure acetone instead of diazinon solution. The maximum acetone fraction was 0.008% v/v (recommended maximum solvent concentration by OECD: 0.01 % v/v (OECD 2000)).

At the beginning of the experiment 20 daphnids (age: 5 - 6 d) were transferred in 250 mL Schott bottles containing 200 mL of exposure medium or solvent control medium. Two separate experiments were performed: In experiment I daphnids were sampled after 0, 6, 12, 18, 24, 30 and 37 h during the exposure phase. Elimination phase was initiated by transferring dapnhids out of exposure medium into clean medium (0.008% acetone) after 13 h. Here, daphnids were sampled after 25, 30, 37, 49 and 61 h. In experiment II animals were transferred into clean medium (0.008% acetone) after 21 h of exposure and sampled after 0 and 21h of exposure (exposure phase) and after 31, 44, 55, 69 and 79 h out of clean medium (elimination phase). Oxygen content, pH and diazinon concentrations were measured in the exposure/elimination medium and in solvent controls at the beginning and the end of the experiment.

Measurement of AChE activity in exposed daphnids were performed in triplicate. 140 µL phosphate buffer, 100 µL S10 extract and 50 µL 8.5 mM ATCh/ 8.5 mM DTNB mixture were added to microplate wells and mixed with a pipette. As positive control (100% inhibition) 100 µL S10 extract of daphnids sampled at t = 0 h was mixed with 90 µL phosphate buffer and 50 µL 10 µM eserine hemisulfate salt solution and incubated for 15 - 30 min prior to addition of 50 µL of a 8.5 mM ATCh/ 8.5 mM DTNB mixture. As control activity the mean value of two replicate solvent controls was used. Immobilization is presented in % of total number of animals per sample.

Prior to modeling units describing AChE activity were transformed into $pmol \cdot g_{ww}^{-1}$. The enzyme amount at time point zero (100 % activity, E_0 in equation 3.2) was calculated by multiplying the determined AChE amount (in $pmol \cdot mg_{protein}^{-1}$) with the protein content ($mg_{protein} \cdot g_{ww}^{-1}$) of daphnids at the beginning (t = 0) of the respective experiment. The enzyme activity at time point t (in % of control) was subsequently multiplied with the calculated value for E_0. K_i (nM) was transfered into $pmol \cdot g_{ww}$ via the volume and wet weight applied per well of the 96 well plate.

Additional information on Results and Discussion

Determination of K_m and v_{max}

The best fit results of each experiment and the corresponding 95% confidence intervals are shown in Table S-3.3.

Table S-3.3. *Values for maximum velocity of substrate hydrolysis v_{max} and Michaelis-Menten constant K_m and 95% CI for three replicate S10 extracts (S10-A, S10-B, S10-C)*

Sample name	S10-A	S10-B	S10-C	mean	stdev
v_{max} (nmol·$mg_{protein}^{-1}$· min^{-1})	3.2	4.2	4.3	3.9	0.6
95% CI	3.1 to 3.3	4.1 to 4.4	4.2 to 4.5		
Km (µM)	8.0	6.7	5.0	6.6	1.5
95% CI	7.0 to 9.0	5.6 to 7.8	4.1 to 5.9		

The maximum velocity of substrate hydrolysis of the S10 extracts and the Michaelis-Menten constant were 3.9 ± 0.6 nmol·$mg_{protein}^{-1}$$min^{-1}$ and 6.6 ± 1.5 µM, respectively. K_m found in our study is in accordance with values determined for other crustacean species: K_m values range from 4.28 ± 0.07 µM (Diamantino et al. 2003) for *D. magna*, *95* µM for the blue crab (Habig et al. 1988) to 106.5 ± 11.6 µM for *Gammarus pulex* (Xuereb et al. 2007). The specific activity towards hydrolysis of ATCh (v_{max}) determined in our study is lower by at least a factor of two compared to literature values for *D. magna*: One study found an specific activitiy towards the substrate ATCh of 8.51 ± 0.17 nmol·$mg_{protein}^{-1}$*min^{-1} (Diamantino et al. 2003), a comparison of five different clones from *D. magna* revealed values ranging from 14.9 ± 4.9 to 62.3 ± 13.6 nmol·$mg_{protein}^{-1}$*min^{-1} (Barata et al. 2001). The differences might therefore be due to variation in the protein composition for different clones used. Values obtained for other crustaceans are for example 50.8 ± 1.2 nmol·$mg_{protein}^{-1}$*min^{-1} for *G. pulex* (Xuereb et al. 2007).

Relative contribution of different processes to the measured AChE activity

In Figure S-3.3 the activity towards hydrolysis of the substrate ATCh (in % of control) after incubation with increasing inhibitor concentrations is shown (data points at 10.2 nM for diazoxon and 0.42 µM for eserine sulfate and iso-OMPA were excluded due to erroneous measurement). The horizontal line through the mean of the remaining activity for the three highest inhibitor concentrations represents the maximum inhibition of enzyme activity which can be achieved with the respective inhibitor. Maximum inhibition levels are summarized in Figure S-3.4. For diazoxon, eserine sulfate and iso-OMPA the plateau values are 18, 23 and 94 % of control activity, respectively. Diazoxon and eserine sulfate showed an immediate decrease of activity with increasing inhibitor amount in the low concentration range and a similar maximal inhibition for high concentrations of both compounds is reached (approx. 80% reduction of activity). Iso-OMPA only marginally affects the measured activity (6 % reduction). Since eserine sulfate inhibits all cholinesterases and iso-OMPA only pseudocholinesterases but not AChE the difference between the plateau activities of

these two inhibitors (approx. 70%) can be assigned to AChE. The observed activity towards ATCh is therefore mainly caused by AChE.

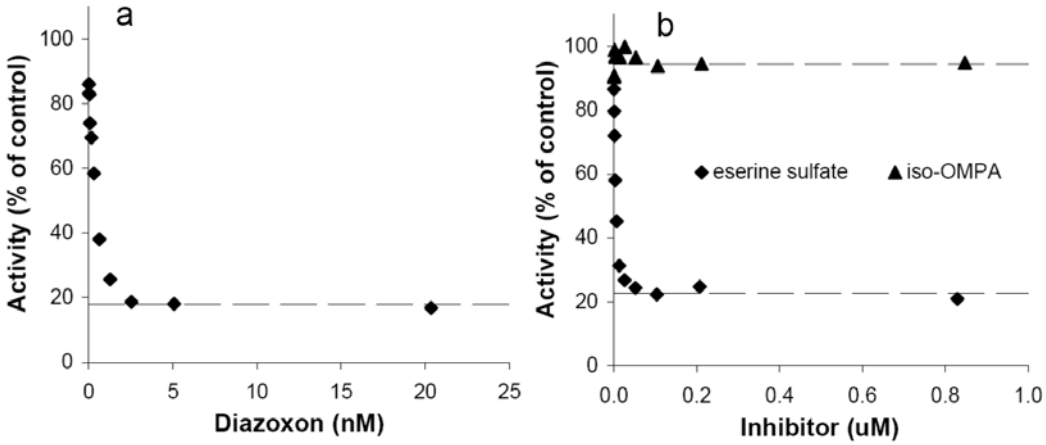

Figure S-3.3. *ChE activity after incubation of Daphnia magna S10 extract with increasing (a) diazoxon, (b) eserine sulfate and iso-OMPA concentrations*

Inhibitor	Diazoxon	Eserine sulfate	Iso-OMPA
Structure	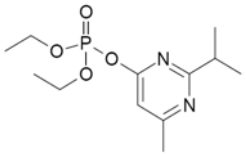	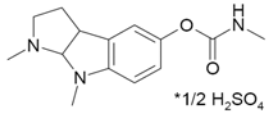	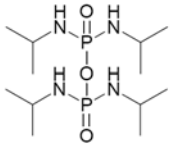
Inhibition of	all ChEs	all ChEs	pseudo-ChEs, not AChE
Maximal inh bition (% of control)	82	77	6

Figure S-3.4. *Maximal inhibition levels (in % of control) of ChE activity in S10 extract from D. magna incubated with diazoxon, eserine sulfate and iso-OMPA*.

These results agree with literature where for different aquatic organisms activity towards ATCh was also mainly caused by AChE (Habig et al. 1988; Barata et al. 2001; Xuereb et al. 2007). This is confirmed by the finding that in isolated neural tissue of the blue crab and of channel catfish primarily true AChE was found (Habig et al. 1988). But also whole body homogenates of *G. pulex* were reported to possess only AChE and no other ChE (Xuereb et al. 2007). In contrast Diamantino et al. (Diamantino et al. 2003) found that cholinesterases present in *D. magna* showed characteristics of AChE as well as of pseudo-ChEs.

The residual activity for high eserine sulfate concentrations is presumably composed of several processes others than ChE hydrolysis (e.g. non enzymatic hydrolysis of ATCh, reaction of DTNB with thiol groups present in S10 extract, enzymatic degradation of formed product). Maximum inhibition levels achieved with eserine sulfate and crustacean species in other studies were < 10 % (Habig et al. 1988; Barata et al. 2001; Monteiro et al. 2005). K_m and v_{max} reported in our study might slightly deviate from the true values since in this experiment no correction with an eserine control was availble.

Iso-OMPA concentrations used in our experiments (up to 0.8 µM) were low compared to other studies with iso-OMPA and aquatic species (up to 8 mM (Diamantino et al. 2003; Monteiro et al. 2005)). Since iso-OMPA is an organophosphate and is expected to inhibit pseudo-ChEs in an irreversible reaction (with respect to a very slow reactivation of phosphorylated ChE) (Hernandez and Rathinavelu 2006) the same concentration range as used for eserine sulfate was assumed to be sufficient. Eserine sulfate belongs to the class of carbamates, which are in general regarded as reversible inhibitors of ChEs due to a relatively fast reactivation of carbamoylated ChE (Hernandez and Rathinavelu 2006). Aldridge et al. compared the inhibitory potency of iso-OMPA and the organophosphate paraoxon for horse ChE. Concentrations needed to cause 50 % inhibition of pseudo-ChE in case of iso-OMPA and true ChE (AChE) in case of paraoxon (after an incubation time of 30 min at 37 °C) were in the same order of magnitude and in the µM range (Aldridge 1953a). For the organophosphate diazoxon we achieved already complete inhibition of ChE activity for 40 times lower concentrations than applied for eserine sulfate and iso-OMPA. This further supports the concentration range applied for iso-OMPA in our experiments. Since no further inhibition could be observed in case of diazoxon and eserine sulfate after an incubation period of 45 min this time was considered to be adequate also for iso-OMPA.

Determination of AChE amount in D. magna

Repetition of the inhibition experiment with diazoxon (see previous section) with higher resolution of the low concentration range revealed an initial linear decrease of AChE activity with increasing diazoxon concentration (see Figure S-3.5).

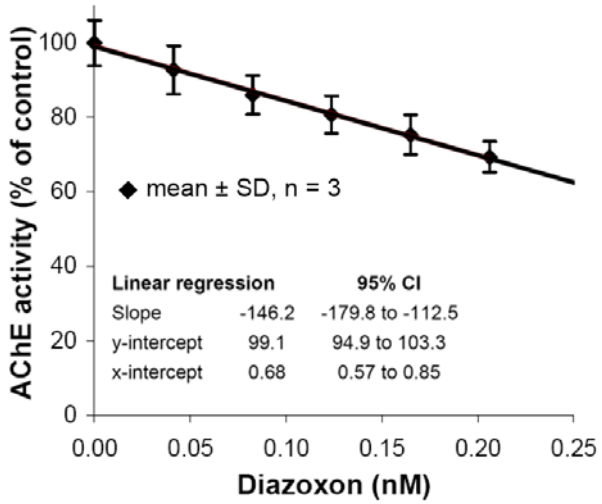

Figure S-3.5. *AChE activity measured after incubation of D. magna S10 extract with increasing diazoxon concentrations. Diamonds correspond to mean values ± standard deviation of three replicate experiments and the best fit results with 95% confidence intervals obtained by linear regression (each replicate was used as single data point in regression).*

Elucidation of AChE inhibition mechanism, determination of inhibition parameters

Reaction progress curves, plots λ and v_z vs. the inhibitor concentration and the respective best fit curves for mechanism I(2) are shown in Figure S-3.6.

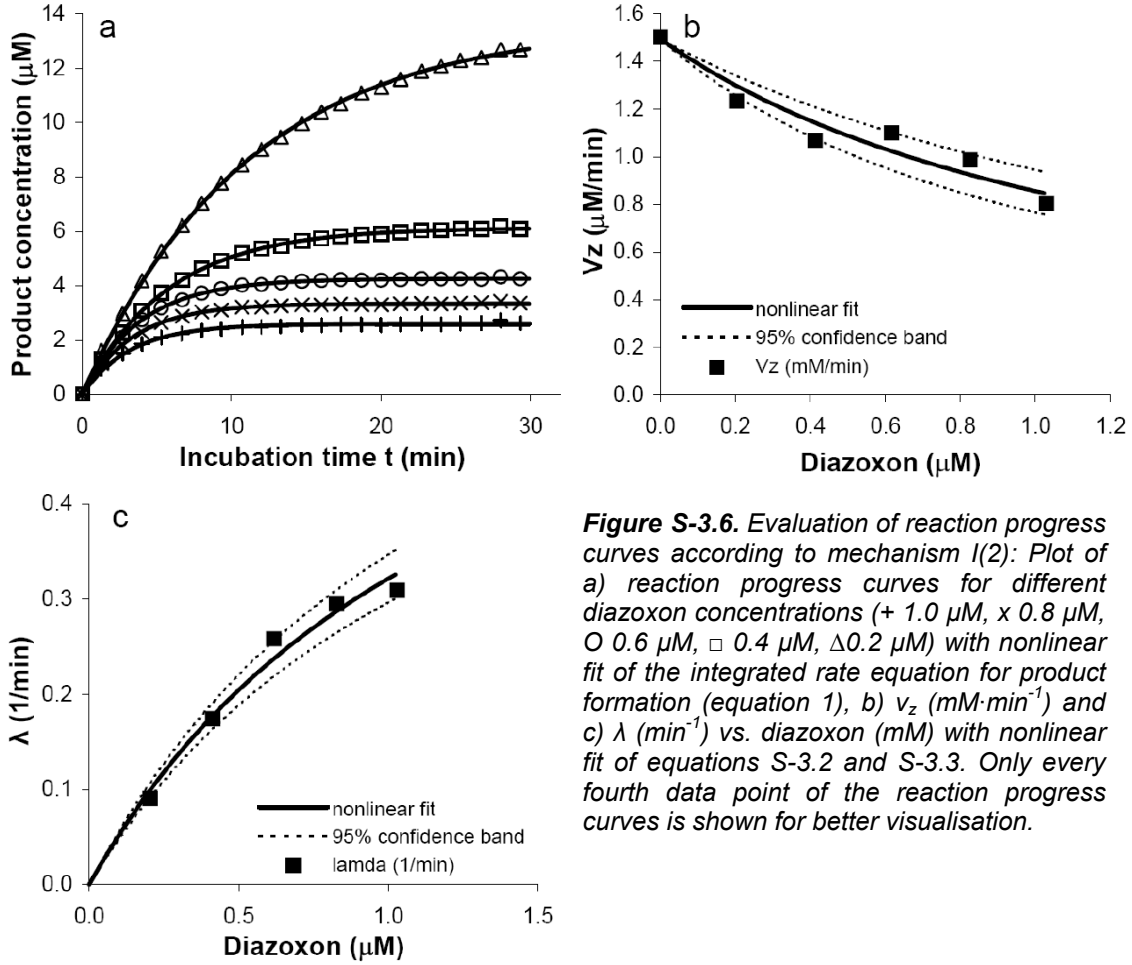

Figure S-3.6. *Evaluation of reaction progress curves according to mechanism I(2): Plot of a) reaction progress curves for different diazoxon concentrations (+ 1.0 µM, x 0.8 µM, O 0.6 µM, □ 0.4 µM, Δ0.2 µM) with nonlinear fit of the integrated rate equation for product formation (equation 1), b) v_z (mM·min^{-1}) and c) λ (min^{-1}) vs. diazoxon (mM) with nonlinear fit of equations S-3.2 and S-3.3. Only every fourth data point of the reaction progress curves is shown for better visualisation.*

For diisopropyl fluorophosphate, which is often used as reference substance in inhibition studies, and AChE from electric eel irreversible inhibition in one step, I(1), was assigned as underlying mechanism (Baici et al. 2009). If for *D. magna* and diazoxon really another mechanism than the assumed I(2) is present was decided by comparison of the experimental data and best fit results for the different mechanisms as depicted in Figure S-3.1: All mechanisms fit the reaction progress curves well ($r^2 > 0.995$, see Figure S-3.6 a for I(2)). λ shows a hyperbolical dependency on the inhibitor concentration. v_z is clearly dependent on the inhibitor concentration and decreases (hyperbolically) with increasing inhibitor concentration (see Figure S-3.6 b and c for mechanism I(2)). Other way round, if v_z is kept fixed during nonlinear fit of the reaction progress curves this gives poor fit. This is a strong indication of an inhibiton in two steps, e.g. via mechanism I(2), I(2,r) and R(2). The slopes of the progress curves in steady state (regression line through data in the range 20 -30 min) are significantly non-zero ($p < 0.0001$, except for diazoxon 0.6 µM, $p = 0.026$). This might be an indication for mechanism I(1,r) and I(2,r) (spontaneous reactivation) or mechanism R(1) and R(2) (reversible formation of EI_r and/ or EI). A y-intercept > 0 of the

nonlinear regression curve through λ vs. I for R(2) and I(2,r) is not vsisible. For mechanism R(2) the best fit value of k_2 is 0.76 min^{-1} (95% CI: 0.66 to 0.85) and of k_{-2} $1.0 \cdot 10^{-7}$ min^{-1} (95% CI: 0.0 to 0.033, with constraint $k_{-2} > 0$) (values derived from fit of λ vs. I, no reasonable fit could be achieved for v_z vs. I). The back reaction can be regarded as negligible. The inhibition is therefore irreversible and R(2) degenerates to irreversible inhibition in two steps I(2). The fit of λ vs. inhibitor concentration according to mechanism I(2,r) gives 0.76 min^{-1} (95% CI: 0.66 to 0.85) for k_2, 6.87 nM (95% CI: 5.23 to 8.51) for K_i and $1.0 \cdot 10^{-7}$ min^{-1} (95% CI: 0.0 to 0.033, with constraint $k_3 > 0$) for k_3. This value is negligible small and I(2,r) degenerates to I(2). Since mechanism I(2) describes the experimental data well in all requirements diazoxon inhibits AChE in *D. magna* indeed irreversibly in two steps (mechanism I(2)).

In vivo exposure experiments

In the preexperiment all daphnids in exposure medium with a diazinon concentration of 13.1 and 26.3 nM were immobilized already after an exposure period of approx. one day. For the 5.3 nM concentrations this state was not reached until two days of exposure. In general as soon as an animal was immobilized the intensity of this effect underwent a continuous change with proceeding exposure: Shortly before immobilization occurred exposed animals tended to swim slightly more hectically compared to controls. The actual incidence of immobilization was clearly noticeable as an intense and fast convulsive movement of the second antennae, which disabled the daphnids to conduct normal locomotion. With ongoing exposure duration the frequency and intensity of this movement decreased until no movement at all was observable anymore with the naked eye, especially for high diazinon concentrations and longer exposure times. Daphnids at the final stage of immobilization were checked under the microscope. In some daphnids indeed no heartbeat and no other movement was detectable. But the major part (> 50%) was still alive since heartbeat and a movement of the filtering apparatus and the second antennae could still be observed, even after three days of exposure to 26.3 nM diazinon.

During the exposure phase of the actual exposure experiments I and II immobilized daphnids were mainly still in the early stage of immobilization. Not yet affected animals showed no difference compared to controls during the whole experiments (exposure + elimination), except a possibly slightly more hectic locomotion. Especially for longer exposure times daphnids seemed partly to perform uncoordinated and hectic movements. During the depuration phase of experiment I daphnids showed similar behavior as in controls apart from 0 - 5 % immobilization.

Measured diazinon concentrations, pH values and oxygen content of the experiments are listed in Table S-3.4. Diazinon concentrations remained stable during the exposure phase (loss ≤ 2% of initial concentration). The diazinon concentrations measured during the depuration phase were negligible (≤ 0.2% of diazinon concentration of the exposure medium). The oxygen content ranged from 8 to 6 mg/L (recommended by OECD ≥ 3 mg/L (OECD 2004)), the pH was in the range of 6.9 - 9.2 (recommended by

OECD pH = 6-9 (OECD 2004)). Measured protein content, AChE activity and % immobilization during the in vivo experiments are listed in Tables S-3.5, S-3.6 and S-3.7.

Table S-3.4. *Measured diazinon concentrations, pH-values and oxygen content during the in vivo exposure experiments. Measurements were performed in duplicate. Low measured diazinon concentrations marked with an asterix were probably due to erroneous sample work up and were not used for further evaluations.*

	Diazinon		**pH**		**Oxygen content**	
	nM				$mg \cdot L^{-1}$	
Experiment I	beginning	end	beginning	end	beginning	end
Exposure phase	9.17	9.03	9	n.d.	7.1	n.d.
	7.95*	7.45*	8.9	n.d.	7.2	n.d.
Depuration phase	0.001	0.001	n.d.	7.2	n.d.	7.2
	< LOQ	< LOQ	n.d.	6.9	n.d.	6.2
Solvent control	n.d.	n.d.	9.2	7.1	6.8	7.4
	n.d.	n.d.	9.2	7.1	7.1	6.5
Experiment II	beginning	end	beginning	end	beginning	end
Exposure phase	9.25	9.13	7.9	n.d.	7.3	n.d.
	9.18	9.12	7.9	n.d.	7.7	n.d.
Depuration phase	0.01	0.02	n.d.	7.7	n.d.	7.1
	0.01	0.01	n.d.	7.5	n.d.	6.6
Solvent control	n.d.	n.d.	7.8	7.4	7.7	6.9
	n.d.	n.d.	7.8	7.7	7.8	6.7

Table S-3.5. *Experimental data of in vivo exposure to diazinon (experiment I).*

Sample name	**Sampling time**	**Number of daphnids**	**Protein content**	**AChE activity**			**Immobili-zation**	**Survival**
	h		$\mu g_{protein} \cdot daphnid^{-1}$	$nM \cdot min^{-1}$	$nmol/(mg_{protein} \cdot min)^{-1}$	% of control	%	%
D-0/A	0	20	41.6	1.15E+03	3.22	98.8	0.0	100.0
D-0/A	0	20	50.8	1.17E+03	2.71	101.2	0.0	100.0
C-1/A	6.4	20	44.4	7.87E+02	2.08		0.0	100.0
C-1/B	6.4	20	43.4	8.90E+02	2.4		0.0	100.0
D-1/A	6.3	20	45.9	7.96E+02	2.03	94.9	0.0	100.0
D-1/B	6.3	20	45.3	7.53E+02	1.95	89.8	0.0	100.0
C-2/A	12.1	20	44.8	7.48E+02	1.95		0.0	100.0
C-2/B	12.1	20	42.9	7.90E+02	2.15		0.0	100.0
D-2/A	11.9	20	47.2	6.16E+02	1.53	80.1	0.0	100.0
D-2/B	11.9	20	45.6	6.01E+02	1.54	78.1	5.0	95.0
C-3/A	18.2	20	43.3	8.86E+02	2.4		0.0	100.0
C-3/B	18.2	20	44.3	9.25E+02	2.44		0.0	100.0
D-3/A	18.1	20	40.6	4.35E+02	1.25	48.1	10.0	90.0
D-3/B	18.1	20	42.9	5.44E+02	1.48	60.0	0.0	100.0
C-4/A	24.4	20	43.4	8.73E+02	2.35		0.0	100.0
C-4/B	24.4	20	47.2	9.48E+02	2.47		0.0	100.0
D-4/A	24.2	20	42.8	1.78E+02	0.49	19.6	0.0	100.0
D-4/B	24.2	21	45.3	2.71E+02	0.7	28.4	23.8	76.2
Del-4/A	24.5	20	46.9	6.69E+02	1.67	73.5	5.0	95.0
Del-4/B	24.5	20	41.4	6.72E+02	1.9	73.8	0.0	100.0
C-5/A	30.3	20	39.3	7.92E+02	2.36		0.0	100.0
C-5/B	30.3	20	41.9	8.17E+02	2.28		0.0	100.0
D-5/A	30.2	20	40.1	6.34E+01	0.19	7.9	65.0	35.0
D-5/B	30.2	20	40.4	8.85E+01	0.26	11.0	80.0	20.0
Del-5/A	30	20	42.4	4.99E+02	1.38	62.0	10.0	90.0
Del-5/B	30	19	36.5	7.27E+02	2.21	95.1	0.0	100.0
C-6/A	36.9	20	39.2	7.86E+02	2.34		0.0	100.0
C-6/B	36.9	20	39.5	9.39E+02	2.78		0.0	100.0
D-6/A	37	20	34.8	3.30E+01	0.11	3.8	100.0	0.0
D-6/B	37	20	35.7	6.28E+01	0.21	7.3	100.0	0.0
Del-6/A	36.9	20	40.9	7.36E+02	2.1	85.3	0.0	100.0
Del-6/B	36.9	20	42.2	6.80E+02	1.89	78.9	0.0	100.0
C-7/A	48.8	21	42.2	1.11E+03	3.23		0.0	100.0
C-7/B	48.8	20	39.5	1.00E+03	2.97		0.0	100.0
Del-7/A	48.8	20	31.6	7.34E+02	2.72	71.2	0.0	100.0
Del-7/B	48.8	20	33.1	8.94E+02	3.16	86.7	0.0	100.0
C-8/A	61.3	20	42.3	1.27E+03	3.51		0.0	100.0
C-8/B	61.3	20	44.7	1.40E+03	3.66		0.0	100.0
Del-8/A	61.4	20	38.6	1.18E+03	3.57	88.4	5.0	95.0
Del-8/B	61.4	20	37.6	1.24E+03	3.85	92.9	0.0	100.0

Table S-3.6. *Experimental data of in vivo exposure to diazinon (experiment II).*

Sample name	**Sampling** time h	**Number** of daphnids	**protein content** µg(protein)·daphnid^{-1}	**AChE activity** nM·min^{-1}	nmol/(mg(protein)·min)$^{-1}$	**AChE activity** % of control
D-0/A	0.0	20	37.7	1.43E+03	3.39	104.6
D-0/B	0.0	20	38.6	1.43E+03	3.09	95.4
C-1/A	21.4	20	39.2	6.63E+02	4.20	
C-1/B	21.4	20	38.9	5.63E+02	4.24	
D-1/A	21.2	20	40.7	1.45E+03	1.87	44.4
D-1/B	21.2	19	32.5	1.37E+03	1.89	44.7
C-2/A	21.2	20	39.4	4.99E+02	4.23	
C-2/B	21.2	20	40.3	4.57E+02	3.91	
Del-2/A	31.3	20	38.6	1.39E+03	1.49	36.5
Del-2/B	31.3	20	35.9	1.30E+03	1.46	35.9
C-3/A	44.4	20	36.5	5.50E+02	4.37	
C-3/B	44.4	20	39.7	4.63E+02	3.75	
Del-3/A	44.2	20	36.7	1.29E+03	1.72	42.4
Del-3/B	44.2	20	31.6	1.40E+03	1.69	41.5
C-4/A	55.1	20	32.9	6.53E+02	4.51	
C-4/B	55.1	20	36.6	6.89E+02	4.40	
Del-4/A	54.8	20	29.5	1.41E+03	2.54	57.1
Del-4/B	54.8	20	34.0	1.38E+03	2.32	52.2
C-5/A	68.8	20	34.2	6.50E+02	4.74	
C-5/B	68.8	20	34.2	6.26E+02	4.62	
Del-5/A	68.4	20	32.2	1.31E+03	2.32	49.6
Del-5/B	68.4	20	30.0	1.32E+03	2.40	51.2
C-6/A	79.4	20	30.1	6.40E+02	4.99	
C-6/B	79.4	19	31.2	5.05E+02	4.87	
Del-6/A	79.2	20	26.0	1.11E+03	2.83	57.4
Del-6/B	79.2	20	24.9	1.04E+03	2.33	47.3

Table S-3.7. *Time course of immobilisation during after in vivo exposure to diazinon and subsequent transfer into clean medium (0.008 % acetone (experiment II).*

Sampling time (h)	**0**	**21.2**	**31.3**	**44.2**	**54.8**	**68.4**	**79.2**
Sample name	**Immobilisation (%)**						
D-1/A	0	20					
D-1/B	0	32					
Del-2/A	0	25	50				
Del-2/B	0	20	55				
Del-3/A	0	5	40	35			
Del-3/B	0	10	70	70			
Del-4/A	0	40	55	55	60		
Del-4/B	0	30	50	50	45		
Del-5/A	0	35	75	70	70	70	
Del-5/B	0	35	60	65	65	65	
Del-6/A	0	30	70	70	70	70	70
Del-6/B	0	20	85	85	85	85	85

Chapter 4

Toxicokinetic Model Describing Bioconcentration and Biotransformation of Diazinon in *Daphnia magna*

Kretschmann, A.; Ashauer, R.; Preuss, T. G.; Spaak, P.; Escher, B. I.; Hollender, J.
Toxicokinetic model describing bioconcentration and biotransformation of diazinon in *Daphnia magna*.
Environmental Science & Technology, **submitted**.

Introduction

Toxicity of a compound towards an organism can in general be described as a function of exposure concentration, exposure duration, and toxicokinetic (TK) and toxicodynamic (TD) processes (Rozman and Doull 2000). TK processes describe the time course of the pathway of a toxicant from the surrounding environment to the target site inside the organism and consist of uptake, partitioning to target and non-target sites, excretion and biotransformation. TD processes link the internal concentration of a toxicant with the toxic effect observed on organism level by describing the time dependent build up and recovery of injury on molecular, organ and organism level (Rozman and Doull 2000; Escher and Hermens 2004; Ashauer et al. 2007a). Only the fraction of a pollutant that reaches the target site is toxicologically active (Escher and Hermens 2004).

The toxic potency of a chemical is commonly assessed via external effect concentrations, e.g. its LC_{50} value. What reflects the toxic potential in a more accurate way is the concentration inside the organism (Escher and Hermens 2004). Quantitative Structure Activity Relationships (QSARs) have been developed for the estimation of the internal concentration of lipophilic chemicals in aquatic organisms via their octanol-water partitioning coefficient (K_{ow}) (Hawker and Connell 1986; Geyer et al. 1991). A drawback of these QSARs is that they are valid only under steady state conditions and do not account for biotransformation. Tools that can predict the time course of the internal concentration of a chemical as function of absorption, distribution, excretion, and especially metabolism, are TK models (Reinert et al. 2002). Often simple one compartment first-order kinetic TK models are applied to describe bioconcentration in aquatic organisms, which do not explicitly account for biotransformation processes (de Bruijn and Hermens 1991).

For phosphorothionate insecticides like diazinon, chlorpyrifos and parathion, it is crucial to consider biotransformation processes in order to accurately assess their toxicity. These compounds are metabolically activated by cytochrome P450 monooxygenases (P450) to their respective oxon-analogues in an oxidative desulfuration (Forsyth and Chambers 1989). In contrast to the thioesters the oxons are very potent inhibitors of acetylcholinesterase (AChE) (Forsyth and Chambers 1989). In addition to activation, phosphorothionates and their oxons can also be metabolically detoxified by several other biotransformation reactions. These reactions include: Oxidative dearylation of the thio-compound catalyzed by P450 (Fabrizi et al. 1999), hydrolysis of the oxon-analog by A-esterases (Keizer et al. 1995; Poet et al. 2003) and dealkylation and dearylation of both the thio-compound and the oxon analog catalyzed by glutathione-S-transferase (GST) (Keizer et al. 1995; Fujioka and Casida 2007). Phenol derivates formed during hydrolysis can further be conjugated with endogeneous substrates like sulfate, glucose or glucuronide (Johnston and Corbett 1986). For different aquatic organisms a multitude of phopshorothionate metabolites could be detected *in vivo* (Takimoto et al. 1987a) but the extent of the different biotransformation processes was highly species and compound dependent (Chambers et al. 1994; Keizer et al. 1995).

This study focuses on the development of a process-based TK model for *Daphnia magna* and the phosphorothionate insecticide diazinon, which explicitly includes biotransformation processes and accounts

for the formation of active and inactive metabolites *in vivo* on a time-resolved basis. In order to identify relevant TK processes and to determine the respective kinetic parameters *D. magna* was exposed to diazinon (with or without inhibtion of P450) as well as to its metabolites diazoxon and 2-isopropyl-6-methyl-4-pyrimidinol (pyrimidinol) *in vivo*. After different exposure times internal concentrations of the parent compound and its metabolites were quantified with LC-MS/MS. Since diazinon with a $\log K_{ow}$ of 3.81 (Bowman and Sans 1983) is likely to accumulate mainly in the lipid phase of *D. magna*, the time course of the lipid content during the exposure experiments and its influence on TK parameter was elucidated.

Theory

TK phase of diazinon in D. magna

The following TK processes were incorporated into the TK model and are depicted in Figure 4.1:

A. Unchanged diazinon is taken up by passive diffusion.

B. Diazinon is eliminated via passive diffusion. Other elimination processes like dealkylation/ dearylation catalyzed by GST, which are not separately considered, are included in this pathway.

C. Diazinon is activated to the oxon analog diazoxon by oxidative desulfuration catalyzed by P450.

D. Diazinon is detoxified under formation of pyrimidinol via oxidative dearylation catalyzed by P450.

E. Diazoxon is eliminated by irreversible binding to the target site AChE. Since AChE in *D. magna* was found to be very sensitive towards diazoxon (see chapter 3), this reaction is assumed to be very fast, so that other elimination processes of diazoxon can be considered as negligible.

F. Pyrimidinol itself can be eliminated by passive diffusion or by conjugation e.g. with sulfate or glucose. Both processes are lumped together in the model.

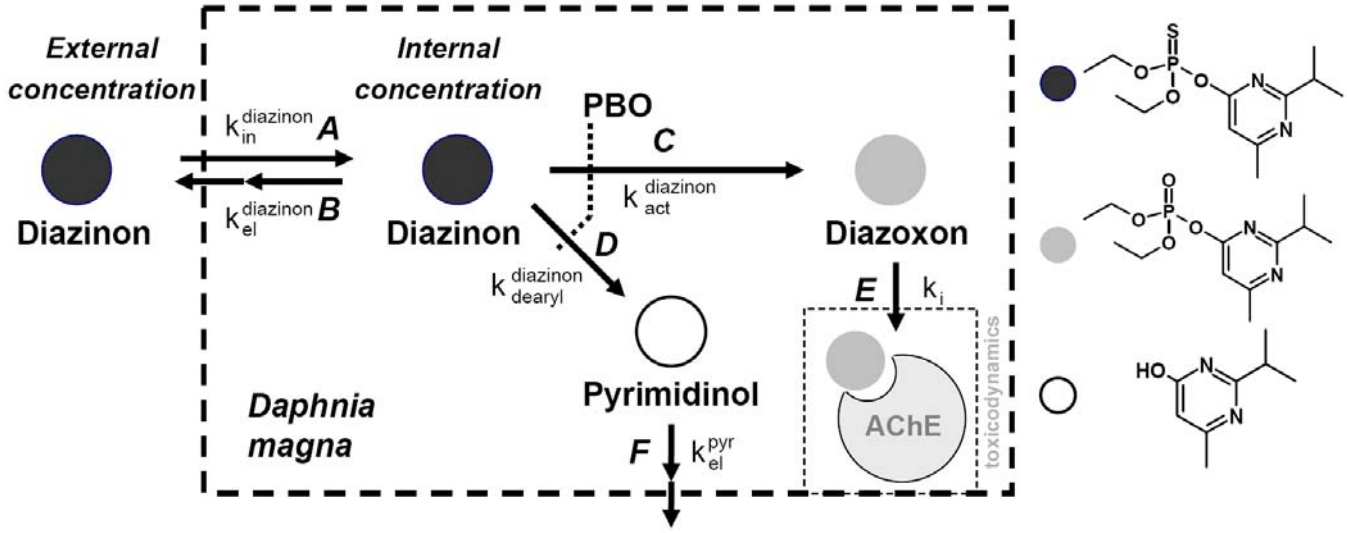

Figure 4.1. *Incorporated toxicokinetic processes of diazinon in D. magna into the TK model (PBO: Piperonyl butoxide as inhibitor of cytochrome P450)*

The interaction of diazoxon with the target site AChE (process E) is actually a TD process. Nevertheless, this pathway has to be considered within the TK phase since it reduces the internal concentration of diazoxon. The formation of pyrimidinol during AChE inhibition in step E is neglected.

If the organism is regarded as a single homogenous compartment and first-order kinetics are assumed for uptake and elimination of a chemical into and out of the organism, respectively, the time course of the internal concentration can be described by a one-compartment first-order kinetics model (Hawker and Connell 1986).

The time course of diazinon and its metabolites diazoxon and pyrimidinol in *D. magna* can therefore be described as:

Diazinon: $$\frac{dc_{int}^{diazinon}(t)}{dt} = k_{in}^{diazinon} \cdot c_{ext}^{diazinon}(t) - k_{el,tot}^{diazinon} \cdot c_{int}^{diazinon}(t) \quad (4.1)$$

with $$k_{el,tot}^{diazinon} = k_{act}^{diazinon} + k_{dearyl}^{diazinon} + k_{el}^{diazinon} \quad (4.2)$$

Diazoxon: $$\frac{dc_{int}^{diazoxon}(t)}{dt} = k_{act}^{diazinon} \cdot c_{int}^{diazinon}(t) - k_i \cdot c_{int}^{diazoxon}(t) \cdot c_{int}^{AChE}(t) \quad (4.3)$$

Pyrimidinol: $$\frac{dc_{int}^{pyr}(t)}{dt} = k_{dearyl}^{diazinon} \cdot c_{int}^{diazinon}(t) - k_{el}^{pyr} \cdot c_{int}^{pyr}(t) \quad (4.4)$$

$c_{ext}^{diazinon}$ (M) is the diazinon concentration in the exposure water, c_{int} ($mol \cdot g_{ww}^{-1}$) is the internal concentration of the respective compound. $k_{in}^{diazinon}$ ($L \cdot g_{ww}^{-1} \cdot h^{-1}$) is the uptake rate constant of diazinon. $k_{el,tot}^{diazinon}$ (h^{-1}) is the cumulative rate constant summarizing all possible elimination processes of diazinon as mentioned above. $k_{dearyl}^{diazinon}$ (h^{-1}) and $k_{act}^{diazinon}$ (h^{-1}) describe the dearylation and activation of diazinon catalyzed by P450, $k_{el}^{diazinon}$ (h^{-1}) the remaining elimination processes. The second term on the right side of equation 4.3 describes the inhibition of AChE (irreversible inhibition in one step; mechanism applies if low internal diazoxon concentrations are assumed, see chapter 3). k_i ($g_{ww} \cdot mol^{-1}\ h^{-1}$) is the second order inhibition rate constant. c_{int}^{AChE} ($mol \cdot g_{ww}$) is the concentration of non-occupied AChE in the organism. k_{el}^{pyr} (h^{-1}) is the elimination rate constant of pyrimidinol.

If the activation and dearylation process of diazinon is inhibited by a specific P450 inhibitor e.g. piperonyl butoxide (PBO), equation 4.2 reduces to:

$$k_{el,tot,inh}^{diazinon} = k_{el,tot}^{diazinon} - (k_{act}^{diazinon} + k_{dearyl}^{diazinon}) = k_{el}^{diazinon} \quad (4.5)$$

In this case $k_{in}^{diazinon}$ is termed $k_{in,inh}^{diazinon}$.

The time required to reach effective steady state ($c_{int} = 0.99 \cdot c_{int}^{ss}$ at t_{ss}) and the time to eliminate 99% of the chemical in the organism (t_{el}) after transfer into toxicant free medium are given by equation 4.6:

$$t_{ss} = t_{el} = \ln 100 / k_{el,tot} \quad (4.6)$$

Material and methods

Chemicals

A list with the chemicals and prepared stock solutions used in the experiments can be found in the supporting information (SI). Reported diazinon, diazoxon and pyrimidinol concentrations are measured, PBO concentrations are nominal. For experiments *D. magna* STRAUS 1820 (clone 5) with an age of 5 - 6 d or 7 - 8 d were used.

In vivo exposure experiments

In *in vivo* experiments *D. magna* was exposed to diazinon, pyrimidinol and diazoxon. Analysis of the uptake and elimination of the respective compound during exposure and after transfer into toxicant free medium, respectively, was performed in separate experiments (experiments I to VII, details see Table 4.1). Diazinon experiments were performed with or without the presence of the P450 inhibitor PBO. Exposure concentrations were chosen in order to have high internal concentrations for analysis but that animals still show no effect (immobilization). EC_{50}(48 h) values for immobilization determined in a preexperiment for 7 - 10 d old daphnids were 5.6 nM for diazinon and 10.1 nM for diazoxon. PBO concentrations were chosen according to Ankley et al. (Ankley et al. 1991). An uptake study with diazinon without PBO was performed twice (experiment IV and V). In experiment III (uptake of diazinon in presence of PBO) an approx. 14x higher diazinon concentration (66.8 nM) was applied compared to the other experiments in order to properly assess the relevance of pyrimidinol formation in case of inhibited P450. No effect was expected due to inhibited diazoxon formation. In experiment II daphnids were transfered in diazinon free medium containing PBO after exposure to diazinon and PBO.

During the uptake and elimination experiments daphnids were sampled after different exposure times out of exposure or toxicant free medium, respectively. Two replicates per treatment and two for each control (pure medium, solvent and solvent + PBO controls) were used. At each sampling time 20 daphnids were sampled in duplicate. No immobilization or mortality was observed in the controls. Mortality/ immobilization was only observed in diazinon treatments at the end of experiments III (7.5 % of daphnids), IV (5%) and V (5%).

Measured oxygen content and pH during the experiments were between 5 - 8 $mg \cdot L^{-1}$ and 7.2 - 8.4, respectively. Compound concentrations in the medium were measured in duplicate at the beginning and the end of the experiments. Compound concentrations remained stable during the exposure phase (loss ≤ 5 % of initial concentration).

Chemical analysis

Prior to compound analysis daphnid samples were homogenized in MeOH using a FastPrep® FP120 Bio 101 (Savant Instruments, Inc., NY, USA). Homogenates were filtered and extracts subsequently diluted with H2O (maximal MeOH content 5 %) For details see SI.

Diazinon and its metabolites diazoxon and pyrimidinol in extracts of *D. magna* and in the exposure medium were analyzed with online-solid phase extraction-HPLC-ESI-MS/MS using a TSQ Quantum Ultra mass spectrometer from Thermo Fisher Scientific (SPE material: ENV+ from International Sorbent Technology Ltd, particle size: 40 - 70 µm; HPLC column: Atlantis T3 column 3.0 x 150 mm, C_{18}, particle size 3 µm, pore size 100Å from Waters). A linear gradient with MeOH and water (2 mM ammonium acetate, NH_4Ac) was applied (total flow 400 $\mu L \cdot min^{-1}$). The limit of detection (LOD) and the limit of quantification (LOQ) in daphnid matrix determined as a signal-to-noise ratio of 3:1 and 10:1 were 0.3 and 1 for diazinon, 0.2 and 1 for diazoxon and 11 and 48 pg absolute for pyrimidinol, respectively. For quantification of diazinon and diazoxon and of pyrimidinol diazinon-diethyl-d10 and pyrimidinol-$^{13}C_4$ served as internal standards, respectively. Data were evaluated with Xcalibur (Thermo Scientific, U.S.) in the Qual and Quan Browser. Measured internal concentrations are refered to the wet weight of the animals at the beginning of the experiment. Measured internal diazinon concentrations used for further evaluations were all ≥ LOQ, pyrimidinol and diazoxon data were all ≥ LOD. Diazoxon data were partly below the calibration range.

Characterization of D. magna

The time course of length, wet weight, dry weight and total lipid content of *D. magna* under culturing conditions (as described in SI) was followed over a period of 3 d. In another experiment the time course of total lipid and wet weight under exposure conditions without feeding was determined. The age of the animals at the beginning of each experiment was 5 - 6 d.

Lipids were extracted according to the method developed by Smedes (Smedes 1999) applying a mixture of cyclohexane, isopropanol (i-PrOH) and water. In case of animals fed during the experiment extracted lipids were determined gravimetrically. For measurement of the relative lipid amount in animals not fed the sulphophosphovanilline method developed by Zöllner et al. (Zöllner and Kirsch 1962) adapted to 96 well plate was used as it has higher sensitivity than the gravimetric method.

Data evaluation and TK parameter estimation

Model equations and TK parameter were fitted to the internal concentrations of the respective experiments as listed in Table 4.1.

The fit of the TK model was performed for internal concentrations normalized to the wet weight and lipid content of *D. magna* at the beginning of the experiments as well as to the lipid content at the respective sampling time point. External concentrations measured at the beginning and the end of the exposure phase were included into the fit. Compound amounts detected in the depuration medium were ≤ 3 % of the exposure concentration and therefore set to 0.

For linear and nonlinear regression and statistical tests the program GraphPad Prism version 4.03 for Windows (GraphPad Software, San Diego California USA, www.graphpad.com) was used. Parameter estimation of the rate constants was performed using ModelMaker version 4.0 (Cherwell Scientific Ltd,

Oxford UK, www.modelkinetix.com). Differential equations were solved with the Runge-Kutta method. Best-fit values were obtained by least-square optimization using the Levenberg-Marquardt method.

Results and discussion

Parameterization of the TK model

Figure 4.2 shows the measured internal concentrations of diazinon, diazoxon, and pyrimidinol during the exposure and subsequent elimination phase of a) pyrimidinol, b) diazinon in presence of PBO and c) diazinon in absence of PBO and the corresponding best fit curves. Experimental details and best fit values are summarized in Table 4.1. In a first step k_{el}^{pyr} and $k_{el}^{diazinon}$ were determined via fit of equation 4.4 and 4.1 to the internal pyrimidinol and diazinon concentrations measured during the elimination phase of experiments I and II (exposure to pyrimidinol and diazinon + PBO, see Figure 4.2 a and b), respectively (for details of the fit procedure see SI). Values for k_{el}^{pyr} and $k_{el}^{diazinon}$ were kept fixed in further fit procedures. In a next step, the uptake rate constant with inhibited P450 $k_{in,inh}^{diazinon}$ was obtained by fit of equation 4.1 to data from experiment III (see Figure 4.2 b). In a last step equations 4.1, 4.3 and 4.4 were fitted simultaneously to internal diazinon, diazoxon, and pyrimidinol concentrations obtained within experiments IV, V and VI (exposure to diazinon without PBO, see Figure 4.2 c). Here, TD parameters (fixed) and equations necessary to describe the time course of diazoxon and AChE in equation 4.3 were taken from chapter 3. The activation rate constant $k_{act}^{diazinon}$ was calculated applying equation 4.2. Besides measured internal concentrations, diazoxon calculated via the time course of AChE measured in a previous experiment (see chapter 3) during *in vivo* exposure to diazinon ($c_{ext}^{diazinon}$ = 9.1 nM) was included in the fit (see below).

Table 4.1.: *Experimental details of separately performed in vivo uptake (up) and depuration (dep) studies with D. magna and diazinon with and without inhibition of cytochrome P450 by piperonyl butoxide (PBO), diazoxon and pyrimidinol as well as best fit results of the TK model fitted to measured internal concentrations. Numbers in brackets indicate used PBO concentrations. Equations 4.1, 4.3, 4.4 were fitted simultaneously to data from experiments IV, V, VI.*

Experiment	Age of daphnids [d]	Exposure			Model fit		
			Concentration [nM] (PBO: [µM])	Duration [h] (PBO: [h])	Equations used	Fitted TK parameters	Best fit results
I	5 -6	Pyrimidinol - Dep	231.7	16.7	4	k_{el}^{pyr}	0.78 ± 0.01 h^{-1}
II	5 -6	Diazinon (PBO) - Dep	4.8 (1.5)	19.1	1, 5	$k_{el}^{diazinon}$	0.08 ± 0.02 h^{-1}
III	7 - 8	Diazinon (PBO) - Up	66.8 (3.0)	61.5 (3.3*)	1, 5	$k_{in,inh}^{diazinon}$	4.08 ± 0.11 $ml \cdot g_{ww}^{-1} \cdot h^{-1}$
IV	7 - 8	Diazinon - Up	4.2	20.8	1, 3, 4	$k_{in}^{diazinon}$	4.63 ± 0.14 $mL \cdot g_{ww}^{-1} \cdot h^{-1}$
V	5 -6	Diazinon - Up	4.8	20.8		$k_{el,tot}^{diazinon}$	0.26 ± 0.01 h^{-1}
VI	5 -6	Diazinon - Dep	4.5	18.5		$k_{dearyl}^{diazinon}$	0.16 ± 0.02 h^{-1}
						k_{act}^{diaz}	0.02 h^{-1}
VII	7 - 8	Diazoxon - Up	10.3	17.8		---**	

* Daphnids were preexposed to 3.0 µM PBO for 3.3 h **No model fit available since internal diazoxon concentrations were too low for clear identification and quantification.

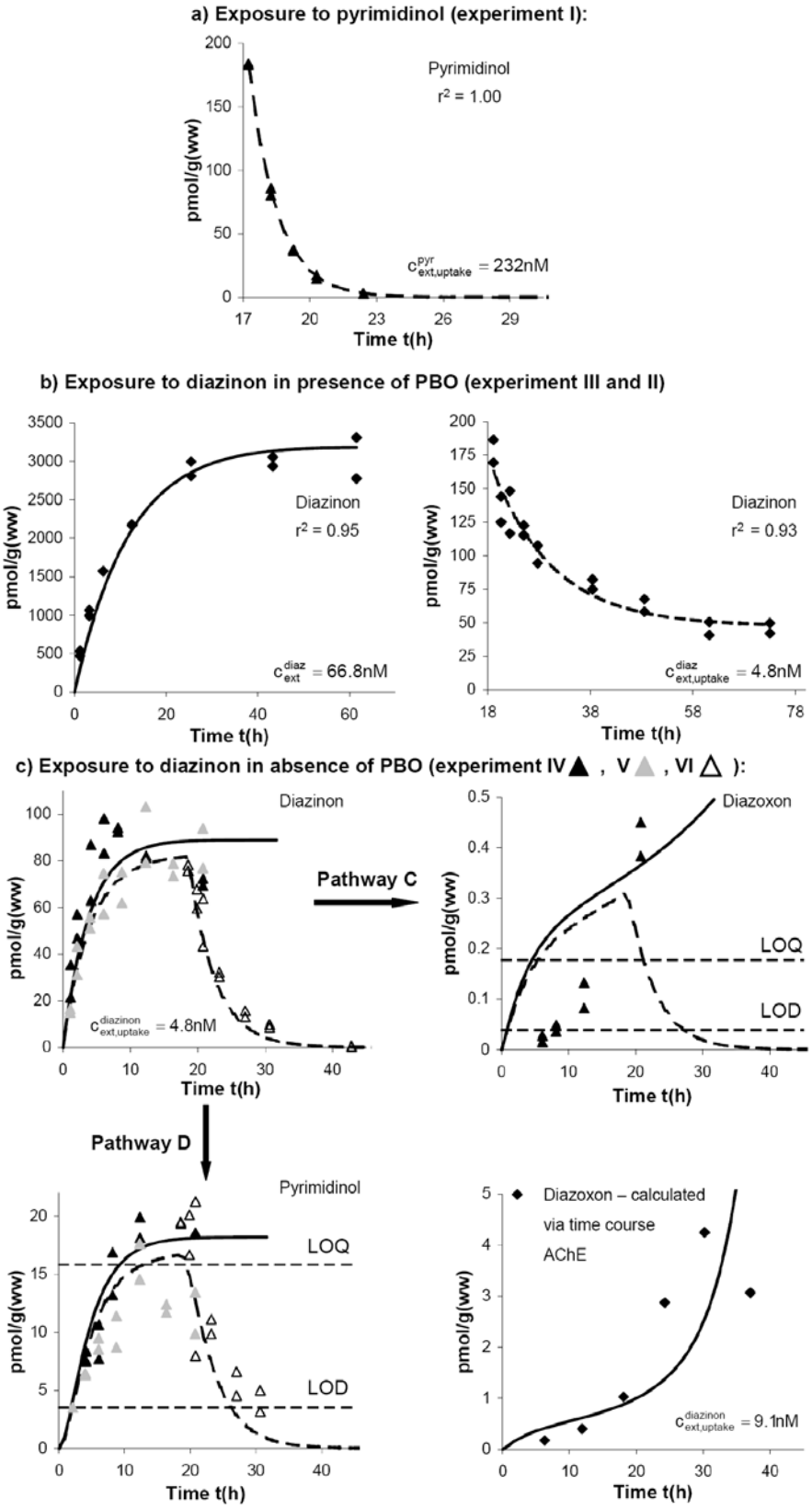

Figure 4.2. *Internal concentration of a) pyrimidinol during the depuration phase after exposure to pyrimidinol (experiment I), b) diazinon during the exposure and depuration phase of diazinon in the presence of piperonyl butoxide (PBO) (experiment II and III), c) diazinon, diazoxon and pyrimidinol during the exposure and depuration phase of diazinon (experiment IV, V and VI). Discret diazoxon values in the lower right figure were calculated via the acetylcholinesterase (AChE) activity measured during in vivo exposure to diazinon (as described in chapter 3) and included in the fit. Solid and dashed lines indicate the best fit of the TK model to the internal concentrations during the exposure and depuration phase, respectively (equations see Table 4.1). Arrows indicate the TK pathway according to Figure 4.1.*

Internal diazinon concentration

The time course of the internal diazinon concentration during uptake and elimination of diazinon in the absence of PBO is well described with first-order kinetics (overall fit: r^2 = 0.93). The best fit values for $k_{in}^{diazinon}$ and $k_{el,tot}^{diazinon}$ (pathway A and B+C+D, respectively, in Figure 4.1) amount to 4.63 ± 0.14 $mL \cdot g_{ww}^{-1} \cdot h^{-1}$ and 0.26 ± 0.01 h^{-1}, respectively. Steady state during exposure and complete elimination after transfer into clean medium, respectively, was reached after approx. 18 h (equation 4.6). The kinetic BCF = k_{in}/k_{el} was 17.8 $mL \cdot g_{ww}^{-1}$ in the absence of PBO and 51.0 $mL \cdot g_{ww}^{-1}$ in the presence of the inhibitor. The elimination rate constant of diazinon with inhibited P450 is reduced by approximately 70 %. This indicates that diazinon is biotransformed to a high degree in *D. magna* and that reactions catalyzed by P450 are the major biotransformation processes. This is consistent with a reduced BCF attributed to metabolic degradation observed for several organophosphates (OPs) in fish (de Bruijn and Hermens 1991).

When calculated via a QSAR according to (Geyer et al. 1991) applying a $logK_{ow}$ of diazinon of 3.81 (Bowman and Sans 1983) a BCF value of 137.6 $mL \cdot g_{ww}^{-1}$ is obtained. In comparison to the experimental BCF, this high value confirms the high susceptibility of diazinon to biotransformation since this relationship is only valid for chemicals that are not metabolized (Hawker and Connell 1986).

Internal pyrimidinol concentration

During exposure to diazinon the internal concentration of pyrimidinol reached approximately 20 % of the parent compound in steady state (determined via the best fit curves of experiment IV and V). The time course was linearly dependent on diazinon. The first-order rate constant for the formation of pyrimidinol via oxidative dearylation of diazinon $k_{dearyl}^{diazinon}$ (pathway D in Figure 4.1) was 0.16 ± 0.01 h^{-1}. This dearylation is therefore the major elimination process of diazinon (62 % of total elimination). k_{el}^{pyr} (0.78 ± 0.01 h^{-1}) determined after direct exposure to pyrimidinol is fast compared to diazinon, presumably due to its better water solubility and/ or fast biotransformation. A possible reaction could be the conjugation with sulfate as it was reported for *D. magna* exposed to pyrene (Ikenaka et al. 2006).

Similar to our findings, fish exposed to diazinon *in vivo* also exhibited lower internal pyrimidinol than diazinon levels but the ratio of the internal concentrations differed between different fish species (Keizer et al. 1991). In contrary to our study, the freshwater shrimp *Gammarus pulex* exhibited internal pyrimidinol concentrations four times higher than diazinon (Ashauer et al. 2010).

Internal diazoxon concentration

The toxic metabolite diazoxon could only be detected in very low concentrations near the LOD and LOQ during exposure to diazinon. It amounted to approx. 0.5 % of the internal diazinon concentration after 21 h of exposure in experiment IV. In experiment II and III as well as when directly exposed to diazoxon in experiment VII, the internal diazoxon concentrations were too low for a clear identification and

quantification. According to our TK model, the activation of diazinon to diazoxon ($k_{act}^{diazinon}$ = 0.02 h^{-1}, calculated via equation 4.2) contributes only 8 % to the total elimination of diazinon. In combination with a very reactive AChE in *D. magna* (as shown *in vitro* in previous TD experiments, see chapter 3), this may explain the very low diazoxon concentrations found. As for pyrimidinol, the amount of the toxic metabolite diazoxon present during *in vivo* exposure to diazinon seems to be strongly species dependent: For *G. pulex* the steady state concentration was approx. 20% compared to diazinon (Ashauer et al. 2010), in fish no diazoxon could be detected (Keizer et al. 1991).

In contrast to pyrimidinol, the time course of diazoxon was not linearly dependent on diazinon: The amount of diazoxon increased exponentially with increasing velocity but this conclusion is subject to high uncertainty due to the very low levels found in the organism. Preexperiments showed that these low levels are robust, i.e. they are unlikely to be formed due to non-physiological factors during the HPLC-measurement or due to contamination. For verification, measured diazoxon data were compared with the internal diazoxon concentration calculated via the time course of AChE activity during *in vivo* exposure to 9.1 nM diazinon (see Figure 4.2 c, experiments and calculations are described in chapter 3). The calculated diazoxon concentration exhibits an analog time course and is in the same order of magnitude (considering an approximately two fold higher external diazinon concentration as in experiment IV) and therefore supports our data.

The TK model is able to explain the data satisfactorily only for the higher calculated diazoxon concentrations. In our model we assume elimination of diazoxon solely via a fast reaction with AChE. The increase of diazoxon can therefore be explained by a depletion of non-occupied target sites with ongoing exposure. The misfit, especially for the low measured diazoxon concentrations, indicates that a further factor might play a role, which might be induction of P450. This factor is more pronounced for low diazoxon concentrations where AChE is saturated slowly. Expression of P450 genes was reported for example for *D. pulex* after exposure to environmental inducers (David et al. 2003). Since we have no data about the time course of P450 in *D. magna* during our exposure experiments, induction of P450 is not considered in our model.

Discussion of model assumptions

When P450 was inhibited by PBO, the internal amounts of diazoxon and pyrimidinol were too low for clear identification and quantification (≤ LOQ) or showed no clear time pattern despite the fact that the external diazinon concentration was approximately 14x higher (66.8 nM) during the uptake phase in experiment III. Furthermore, no toxic effect (immobilization) could be observed even after 60 h of exposure and even though an LC_{50} (48 h) value for diazinon of approximately 5.6 nM. These findings clearly indicate the inhibition of the activation step and the inhibition of pyrimidinol formation and confirm the model assumption that diazinon is activated to diazoxon and detoxified under formation of pyrimidinol, both catalyzed by P450 (pathways C and D in Figure 4.1). Furthermore, hydrolysis of diazinon by A-esterases (not inhibited by

PBO) to pyrimidinol was negligible. That activation of diazinon to diazoxon (oxidative desulfuration) and detoxification to pyrimidinol (oxidative dearylation) are catalyzed both by P450, as assumed in our model, was reported by Fabrizi et al. *in vitro* for cell preparations from rat liver (Fabrizi et al. 1999). Diazoxon and pyrimidinol were detected as products of an oxidative diazinon metabolism not only for mammals but also for fish (Keizer et al. 1995). Here, monooxygenase activities with respect to diazoxon and pyrimidinol formation were highly species dependent (Keizer et al. 1995). In general for phosphorothionates, the ratio of oxidative dearylation and desulfuration is dependent on the different P450 isozymes involved (Fabrizi et al. 1999; Mutch and Williams 2006) and differs also between different compounds (Mutch and Williams 2006). Since different isozymes were identified in the *Daphnia* species (Baldwin and Leblanc 1994) the presence of both oxidative desulfuration and oxidative dearylation in *D. magna* is a reasonable assumption supported (albeit not proven) by experimental evidence.

The model assumption that formation of pyrimidinol during inhibition of AChE by diazoxon is negligible, is justified since internal concentrations of diazoxon found in *D. magna* during exposure to diazinon were small compared to the parent compound. Furthermore, hydrolysis of diazoxon to pyrimidinol by A-esterases was regarded as negligible assuming a very fast reaction with AChE. This detoxification process indeed might rather play a minor role in *D. magna* as is supported by the fact that pyrimidinol was present only in very low amounts (< LOQ) and without a clear increase with time when directly exposed to diazoxon (10 nM, data not shown). Also for different fish species in *in vitro* experiments only a very low or no A-esterase activity at all towards diazinon was reported (Keizer et al. 1995).

Influence of lipid content on the bioaccumulation of diazinon

When *D. magna* was cultured with constant food supply, the lipid content increased linearly to the wet weight and amounted to 1.7 ± 0.1 % of the wet weight. If daphnids were kept under exposure conditions (no feeding) the lipid content was declining according to an exponential decay. The best fit value for the first order depletion rate constant was 0.013 h^{-1} (95 % CI: 0.012 to 0.015, r^2 = 0.94). After 24 h and 48 h approximately 70 % and 50 %, respectively, of the initial total lipid was left in the animals. In contrast to total lipid, the wet weight increased with time. Details are given in the SI.

As a moderately hydrophobic chemical, diazinon will accumulate in the lipids of *D. magna.* Therefore dilution of internal concentrations by growth of the organism was not incorporated into the TK model. The influence of the lipid depletion on the TK parameter was estimated by fitting the TK model to internal diazinon concentrations normalized to the lipid content at the beginning of the experiment as well as at the respective sampling time point (in units $nmol \cdot g_{lipid}^{-1}$) (Figure 4.3 a). When equation 4.1 was fitted simultaneously to experiments IV, V and VI the rate constants for uptake of diazinon $k_{in}^{diazinon}$ with and without correction by the lipid time course were almost identical. The elimination rate constant $k_{el,tot}^{diazinon}$ was lower by approx. 20 % if the decline in lipid content was considered. If the two uptake experiments were regarded separately during the fit (IV + VI and V + VI, respectively) without correction by the time course of

lipid content, the observed differences between the rate constants were larger compared to the simultaneous fit with and without correction via the lipid time course (best fit results see SI). It can therefore be concluded that for short exposure times the depletion in lipid content has only a minor relevance compared to inter-experimental variability. For this reason experimental data were not corrected via the lipid time course. Furthermore the lipid phase might not be the primary storage compartment for the less hydrophobic metabolites, which are of major interest in our study.

For longer exposure times the influence of the lipid content in *D. magna* is more significant. Figure 4.3 b compares the internal concentrations during exposure to diazinon with inhibited P450 (experiment III) with and without correction by the lipid time course. In the first case, diazinon is continuosly increasing and higher by 75 % and 122 % after 43 and 62 h, respectively, compared to the non-corrected data. This is in agreement with findings for fish with varying lipid content (Van den Heuvel et al. 1991). Our results suggests that in case of longer exposure times the lipid content in *D. magna* has a more significant influence on bioaccumulation rate constants of diazinon and it is therefore recommended to account for the variability in lipid content over the course of the experiment if *Daphnia* are fasted for more than 24h. That a change in lipid content might indeed have a significant influence on the toxicokinetics was for example shown for the amphipod *Pontoporeia hoyi*: Here, the elimination rate constant of polycyclic aromatic hydrocarbons was inversely proportional to the lipid content (Landrum 1988).

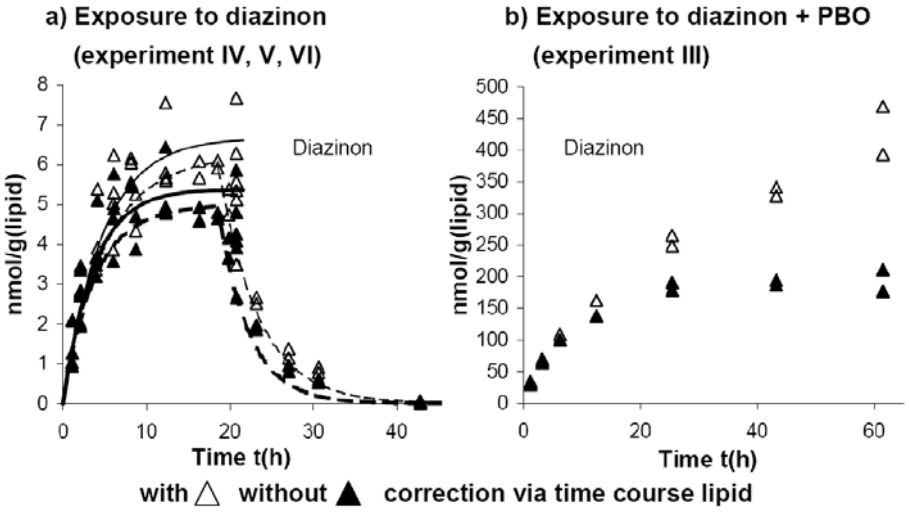

Figure 4.3.: *Internal concentrations of diazinon during the exposure and depuration phase of diazinon (a) without (experiment IV, V and VI, best fit of equation 4.1) and (b) with (experiment III) inhibition of cytochrome P450 monooxygenase with piperonyl butoxide (PBO). Internal concentrations shown with filled triangles are refered to the lipid content at the beginning of the respective experiment. Data shown with hollow triangles are corrected via the time course of lipid content during the experiment (Daphnia not fed). Solid lines indicate the best fit curves of the uptake phase, dashed lines the ones of the depuration phase of diazinon.*

Implications for risk assessement

TK pathways involved in the toxicity of phosphorothionate insecticides are manifold and highly species dependent. The presented TK model is able to combine the complex TK pattern of phosphorothionates and particularly includes detailed information about biotransformation processes. This model enables the time-dependent prediction of active metabolites inside the organism, which triggers the toxic effect. Such an approach is of great importance for the estimation and prediction of the toxic potency of xenobiotics where biotransformation has a strong influence on the toxic effect. This is a significant advance to conventional tools where i.e. the bioaccumulation potential of chemicals is estimated via their K_{ow} applying QSARs. These tools can not account for complex TK patterns as it is the case for phosphorothionate insecticides.

Supporting information for chapter 4

Additional information on Theory

Bioconcentration of xenobiotics in aquatic organisms

The term bioconcentration (also bioaccumulation) describes the accumulation of a xenobiotic in an organism solely via nondietary routes. The bioconcentration factor (BCF) describes the extent of bioconcentration. For aquatic organisms the BCF is defined as the ratio of the concentration in the organism cint and in the surrounding water cext under steady state conditions (Schwarzenbach et al. 2003):

$$BCF = \frac{c_{int}^{ss}}{c_{ext}} \qquad \text{(S-4.1)}$$

The internal concentration is defined as the amount of chemical per wet weight of the organism ($mol \cdot g_{ww}^{-1}$). The external concentration has the units $mol \cdot L^{-1}$, the BCF $L \cdot g_{ww}^{-1}$. With the rate constants for uptake and elimination of a chemical into and out of an organism (first-order kinetics) the BCF can be expressed as the kinetic BCF (Spacie 1983):

$$BCF = \frac{k_{in}}{k_{el}} \qquad \text{(S-4.2)}$$

k_{in} ($L \cdot g_{ww}^{-1} \cdot h^{-1}$) is the uptake rate constant and k_{el} (h^{-1}) the elimination rate constant.

Additional information on Material and methods

Used chemicals

Diazinon (CAS 333-41-5, 99.5 % purity) and standard solutions of diazoxon and diazinon (both 100 µg mL^{-1} acetonitrile) were obtained from Ultra Scientific Analytical Solutions (N. Kingstown RI, USA). Diazoxon (CAS 962-58-3, 99.5 % purity) was obtained from Wako Pure Chemical Industries, Ltd. (Osaka, Japan). 2-Isopropyl-6-methyl-4-pyrimidinol (pyrimidinol, CAS 2814-20-2, 99.5 % purity) and isotope labeled diazinon-diethyl-d_{10} (98 %, CAS 100155-47-3, 100 µg/ml acetone) were obtained from Dr. Ehrenstorfer GmbH (Augsburg, Germany). Stock solution of 2-Isopropyl-6-methyl-4-pyrimidinol-methyl-4,5,6-$^{13}C_4$ (pyrimidinol-$^{13}C_4$, 2814-20-2, 100 µg ml^{-1} acetonitrile) was purchased from Cambridge Isotope Laborities (Andover, MA, USA). Piperonylbutoxide (PBO, CAS 51-03-6, 98.2 % purity), triolein (CAS 122-32-7, 99 % purity), vanillin (CAS 148-53-8, 99 % purity), H_3PO_4 (85 % wt. in H_2O, CAS 7664-38-2) and H_2SO_4 (CAS 7664-93-9, 95 - 98 % purity) were purchased from Sigma-Aldrich (Buchs, Switzerland).

For preparation of the M4 medium according to (OECD 2004) only chemicals of analytical grade were used (Sigma-Aldrich, Buchs, Switzerland). All solvents used were of analytical grade (Acros Organics, New Jersey, USA; Merck, Darmstadt, Germany; Sigma Aldrich, Buchs, Switzerland). For preparation of solutions and M4 medium ultrapure water from a Milli-Q® system (Millipore AG, Zug, Switzerland) was taken.

Solutions for in vivo experiments

Stock solutions of diazinon, pyrimidinol, diazoxon and PBO were prepared by weighing of the respective compound and solvent. Concentrations were calculated with a density of 0.792 g cm^{-3} for MeOH and 0.791 g cm^{-3} for acetone. Dilutions were obtained by dissolving an appropriate volume of stock solution in acetone (see Table S-4.1).

Table S-4.1. *Stock solutions and dilutions used for preparation of exposure medium for the in vivo exposure experiments.*

Compound	Stock solution	Dilution 1	Dilution 2	Dilution 3
	mg mL^{-1} (mM), solvent	µg mL^{-1} (µM), solvent	µg mL^{-1} (µM), solvent	µg mL^{-1} (µM), solvent
Diazinon	6.85 (22.5), methanol	99.4 (326), acetone	39.8 (131), acetone	19.9 (65.3), acetone
Diazoxon	0.99 (3.43), acetone	9.89 (34.3), acetone		
Pyrimidinol	0.92 (6.04), acetone			
Piperonyl butoxide	10.2 (30.2), acetone			
	10.0 (29.4), acetone			

Exposure medium for uptake and elimination studies with diazinon without PBO (experiments IV, V and VI, Table 4.1) was prepared by adding M4 medium and 80 µL of diazinon dilution 3 per liter medium into a glass flask. In case of uptake and depuration studies with diazinon and inhibition of cytochrome P450 monooxygenase (P450) (experiment II and III) 200 µL of diazinon dilution 1 and 95 µL of the 10.2 mg mL^{-1} PBO stock solution and 40 µl of the diazinon dilution 2 and 50 µL of the 10.0 mg mL^{-1} PBO stock solution were spiked per liter M4 medium, respectively. Preexposure medium and depuration medium containing PBO were prepared by disolving the same volume of PBO solution as applied in the respective experiment. In exposure experiments to diazoxon (experiment VII) and pyrimidinol (experiment I) 250 µL of the diazoxon dilution 1 and 40 µL of the pyrimidinol stock solution were applied per liter M4 medium, respectively.

Culturing of D. magna

For information about the culturing of mothers and also determination of the wet weight (ww) the reader is refered to the SI of chapter 3.

For experiments Neonates ≤ 24h were separated from the 3rd and 4th week of the main culture. If not otherwise stated these were raised for 5 or 7 days under the same conditions as the main culture apart from one beaker containing 40 animals fed with 0.025 mg(particulated organic carbon)·$daphnid^{-1}$·d^{-1}. After 5 or 7 days daphnids were transferred into clean M4 medium for approx. 1 - 3 h prior to experiments. The wet weight (ww) was determined and daphnids checked for ovaries, eggs or males under the microscope.

In case of *in vivo* exposure experiments daphnids were directly transfered into the exposure medium. Prior to further analysis daphnids were sieved, washed with water, snap frozen in liquid nitrogen and stored at -80°C.

In vivo exposure to diazinon, pyrimidinol and diazoxon

Exposure and depuration medium were prepared as described above. The acetone content in the medium ranged from 0.004 to 0.03 % v/v. For each experiment solvent and solvent + PBO controls containing the same amount of acetone (and PBO) as the exposure medium were applied. Experiments were performed at 20 ± 1 °C in the dark without feeding as approved in the OECD Guidline 202 (OECD 2004).

At the beginning of the uptake experiments 20 daphnids were transferred in 250 mL Schott bottles containing 200 mL of exposure medium. Preexposure to PBO (experiment III) was conducted by placing 170 daphnids in 500 mL preexposure medium in 500 mL Schott bottles. Prior to the elimination phase of diazinon and pyrimidinol daphnids were exposed in groups of 80 per 800 mL exposure medium in 1L Schott bottles. Exposed animals were subsequently transfered into clean M4 medium or M4 medium containing PBO. During the experiments daphnids were sampled after different exposure times out of exposure or elimination medium. In the uptake and elimination experiments control samples were taken out of clean M4 medium or PBO preexposure medium at exposure time t = 0 and out of control or solvent (+PBO) controls at the end of the experiment, respectively. Two replicates per treatment and two for each control were used. At each sampling time daphnids were processed as described above for experimental daphnids. Compound concentrations in the exposure medium were measured in duplicate at the beginning and the end of the experiments. 100 µL of a mixture of diazinon-d_{10} and pyrimidinol-$^{13}C_4$ (internal standard IS, 5 or 10 ng·mL^{-1}) in methanol (MeOH) were added to 1 mL medium and the sample stored at -20°C till further analysis.

At the beginning of the experiments in daphnids no eggs and ovaries were visible under the microscope apart from experiment II where 75 % of the daphnids possessed ovaries.

Work up of daphnid samples

Prior to compound analysis *D. magna* were homogenized using a FastPrep® FP120 Bio 101 (Savant Instruments, Inc., NY, USA). 20 Daphnids, which were stored at -80 °C, were put together with 200 mg zirconia/ silica beads (Ø 0.5 mm, BioSpec Products, Bartlesville, OK, USA), 300 - 500 µL MeOH and 100 µl of internal standard (IS) in 2 mL screw cap plastic vials . Samples were treated 2x 15 - 30 s at a level of 5.5 - 6.5 m·s^{-1} with ice cooling before, in between and after the homogenization process. In a final step the homogenate was filtered through regenerated cellulose (0.45 µm) and plastic vials and filter washed with 400 - 500 µL MeOH. Extracts of daphnids exposed to diazoxon were prepared applying the same procedure but using a glass micro mortar (Carl Roth GmbH + Co. KG, Karlsruhe, Germany). Medium samples were thawed, filtered as described above and vials and filters were washed with 500 - 900 µL

methanol. Filtrates were filled up to 20 mL with water prior to chemical analyis. Maximal MeOH concentrations in the final solutions were ≤ 5 %.

The recovery of the work up method used for exposed *D. magna* was determined according to the scheme shown in Table S-4.2. An analyte solution in methanol containing 100 ng·mL^{-1} pyrimidinol and 10 ng·mL^{-1} diazinon and diazoxon were spiked to sample 1 and 2 prior to homogenization and to the final solutions at the end of the procedure, respectively. IS (5 ng·mL^{-1}) in MeOH was added at the end of the procedure to each sample in the measurement vials. Each sample was performed in triplicate. In case of pyrimidinol and diazinon the evaluation was done via the ratio peak area of analyte to internal standard. Since diazinon-d_{10} is not an ideal standard for diazoxon, here the peak area was used. Recoveries of the actual work up method for pyrimidinol, diazoxon and diazinon were 89 ± 4 %, 81 ± 4 % and 85 ± 7 % (FastPrep for 2x 15 s at level 5.5 m·s^{-1}) and 85 ± 0 %, 94 ± 7 %, and 87 ± 1 % (FastPrep for 2x 20 s at level 6.5 m·s^{-1}), respectively.

Online-SPE HPLC-ESI-MS/MS method

Compounds were analyzed with online-SPE HPLC-ESI-MS/MS. Optimized scan parameters of the target compounds and the respective internal standards are listed in Table S-4.4. The following ESI parameters were used (positive mode): Spray voltage: 3800 V. Sheath gas pressure: 50 bar. Auxiliary gas pressure: 10 bar. Transfer capillary temperature: 350 °C. The collision gas pressure was 1.5 mTorr. The MS was run in the selected reaction monitoring (SRM) mode.

The online-SPE method is based on the method developed by Stoob et al. (for a detailed method description the reader is refered to (Stoob et al. 2005)) and was modified to our needs as described below. The online-SPE procedure consists of three steps: Loading of the sample, enrichment of the sample and elution of the sample. The sequence of steps and actions during the procedure can be seen in Table S-4.5. If not otherwise stated the following parameters were applied: For separation of compounds by HPLC a linear gradient was run from 15 % MeOH and 85 % H_2O (2 mM ammonium acetate NH_4Ac, pH = 6.2 -6.5) to 90 % MeOH and 10 % H_2O (2 mM NH_4Ac) (total flow 400 µL·min^{-1}, see Table S-4.3). The sample was injected from 20 mL glass vials. Prior to injection 80 µL of 0.5 M NH_4Ac were spiked to the samples. Samples were loaded via the load pump (H_2O, 2 mM NH_4Ac, pH = 6.2 - 6.5).

For quantification of diazinon, diazoxon and pyrimidinol present in exposure medium or in daphnid samples calibration curves were prepared in water and daphnid matrix, respectively. Analyte and internal standard solutions prepared in MeOH were spiked to 20 mL glass vials and filled up with H_2O. In case of daphnid matrix daphnids were homogenized in MeOH with FastPrep and the filtrated extract spiked to the vials. If necessary, measured data were corrected via control samples only containing internal standards without analytes.

Table S-4.2. *Validation procedure of the work up method used for daphnid samples obtained from the in vivo exposure experiments (IS: internal standard solution)*

Procedure	Sample 1	Sample 2
Addition to FastPrep vials	400 µL methanol	500 µL methanol
	20 daphnids	20 daphnids
	200 mg Zr/Si beads	200 mg Zr/Si beads
	100 µL analyte solution	
Homogenization with FastPrep	2x 15 s, 5.5 m s^{-1} or 2x 20 s, 6.5 m s^{-1}	2x 15 s, 5.5 m s^{-1} or 2x 20 s, 6.5 m s^{-1}
Filtration in measurement vials	reg. cellulose 0.45 µm	reg. cellulose 0.45 µm
Washing filter + FastPrep vials	500 µL methanol	500 µL methanol
Addition to measurement vials	100 µL IS	100 µL IS
	100 µL methanol	100 µL analyte solution
	18.8 mL water	18.8 mL water

Table S-4.3. *Gradient used for separation of target compounds*

Time	min		0	8	21	25	25.5	28
Elution pump	MeOH	µL min^{-1}	60	60	360	360	60	60
Precolumn addition pump	H_20 (2mM NH_4Ac)	µL min^{-1}	340	340	40	40	340	340

Table S-4.4. *MS/MS scan parameters for target compounds measured in positive mode (ESI+). Shown are the masses of the precursor ion and its fragments (quantifier and qualifier). CE: Collision energy; PW Q1,3: Peak width (FWHM) Quadrupole 1,3.*

Analyte	Precursor ion	Quantifier	CE	Qualifier	CE	Scan Width	Scan time	PW Q1	PW Q3	Tube lens	Skimmer offset
	m/z	m/z	V	m/z	V	m/z	s			V	V
Diazinon	305.00	169.10	17	153.12	17	0.60	0.05	0.7	0.7	124	14
Diazoxon	289.20	153.11	17	84.11	32	0.60	0.05	0.7	0.7	109	16
Pyrimidinol	153.15	84.09	11	70.22	14	0.60	0.40	0.7	0.7	80	16
Pyrimidinol-$^{13}C_4$	157.15	88.14	14	70.17	17	0.60	0.05	0.7	0.7	111	16
Diazinon-diethyl-d_{10}	315.10	170.10	17	154.12	17	0.60	0.05	0.7	0.7	129	14

Table S-4.5. *Sequence of different steps during one run of the online-SPE procedure (Table adapted from (Stoob et al. 2005) with modifications)*

SPE-step		Time	Valve 1	Valve 2	Dispenser	Load pump	
		min			Action	Action	Solvent
III	SPE-Elution sample n	0		Switch			
		0 - 1				Wash sample loop	AcCN
		1 - 10			Buffer addition	Wash sample loop	H_2O (2mM NH_4Ac)
I	Loading sample n + 1	10	Switch	Switch	Charge dispenser		
		10 - 13			and sample loop	Wash SPE cartridge	AcCN
		13 - 19			with sample n + 1	Conditioning SPE cartridge	H_2O (2mM NH_4Ac)
II	Enrichment sample n + 1	19	Switch				
		19 - 29.5			Wash diluter system	Extract sample n + 1	

Development and validation of an online-SPE method

1) Test of different SPE sorbents:

In order to find a suitable sorbent for extraction of diazinon and its metabolites elution profiles were recorded for different materials and the respective peak areas compared. For this purpose the eluat from the SPE cartrige was directly injected into the MS without seperation by LC. Tested materials were: Strata-X from Phenomenex (particle size: 33 µm), Oasis HLB from Waters (particle size: 60 µm), ENV+ from International Sorbent Technology Ltd (particle size: 40 - 70 µm). The dimensions of the extraction cartridge were 20x2.1 mm. MeOH was used as eluent with a flow rate of 40 $\mu L \cdot min^{-1}$. Elution profiles for samples prepared in water spiked with daphnid extract (analyte concentration 10 ng absolute, MeOH content 5 % v/v) are shown in Figure S-4.1. Extraction efficiencies for diazinon and diazoxon were similar for HLB, Strata-X and ENV+. In contrast, elution of the polar pyrimidinol from ENV+ exhibited a at least three times higher peak area compared to HLB and Strata-X.

Breakthrough of substances was analyzed by arranging two SPE cartridges of the same sorbent material in series (in flow direction of the load pump: HLB1, HLB2 and ENV+1, ENV+2, respectively). After the enrichment step elution was performed with each catridge separately. Here, analog samples as above but without daphnid matrix were extracted. Both HLB and ENV+ retained diazinon and diazoxon completely already on the first cartridge. In contrast pyrimidinol was found in similar amounts on the first and the second cartridge (see Figure S-4.2). In order to improve the extraction efficiency of pyrimidinol Oasis HLB with smaller particle size (15 µm) and a bigger cartridge (20x4 mm) filled with conventional Oasis HLB (60 µm) were tested. This lead to no significant improvement. A major drawback of the big cartridge were high MeOH flow rates (80 $\mu L \cdot min^{-1}$) necessary for an efficient eluation.

The influence of the MeOH content of the sample (1.5 to 10 %) on the extraction efficiency is shown in Figure S-4.3. Diazinon and diazoxon are relatively independent on the solvent content. In contrast the detected amount of pyrimidinol is strongly decreasing with increasing % of MeOH. Approx. 35 % less are enriched at 5 % MeOH in comparison to 1.5 %. Therefore the observed breakthrough of the relatively polar metabolite pyrimidinol is probably due to a reduced absorbtion caused by MeOH present in the samples.

However, a MeOH content lower than 5 % was not applicable in samples with daphnid matrix since precipitation in the measurement vials occured. For further measurements ENV+ was chosen as sorbent. As eluent flow rate 60 $\mu L \cdot min^{-1}$ was regarded as appropriate (total flow 400 $\mu L \cdot min^{-1}$) resulting in sharp elution profiles and still providing a good trapping and focusing on the HPLC column.

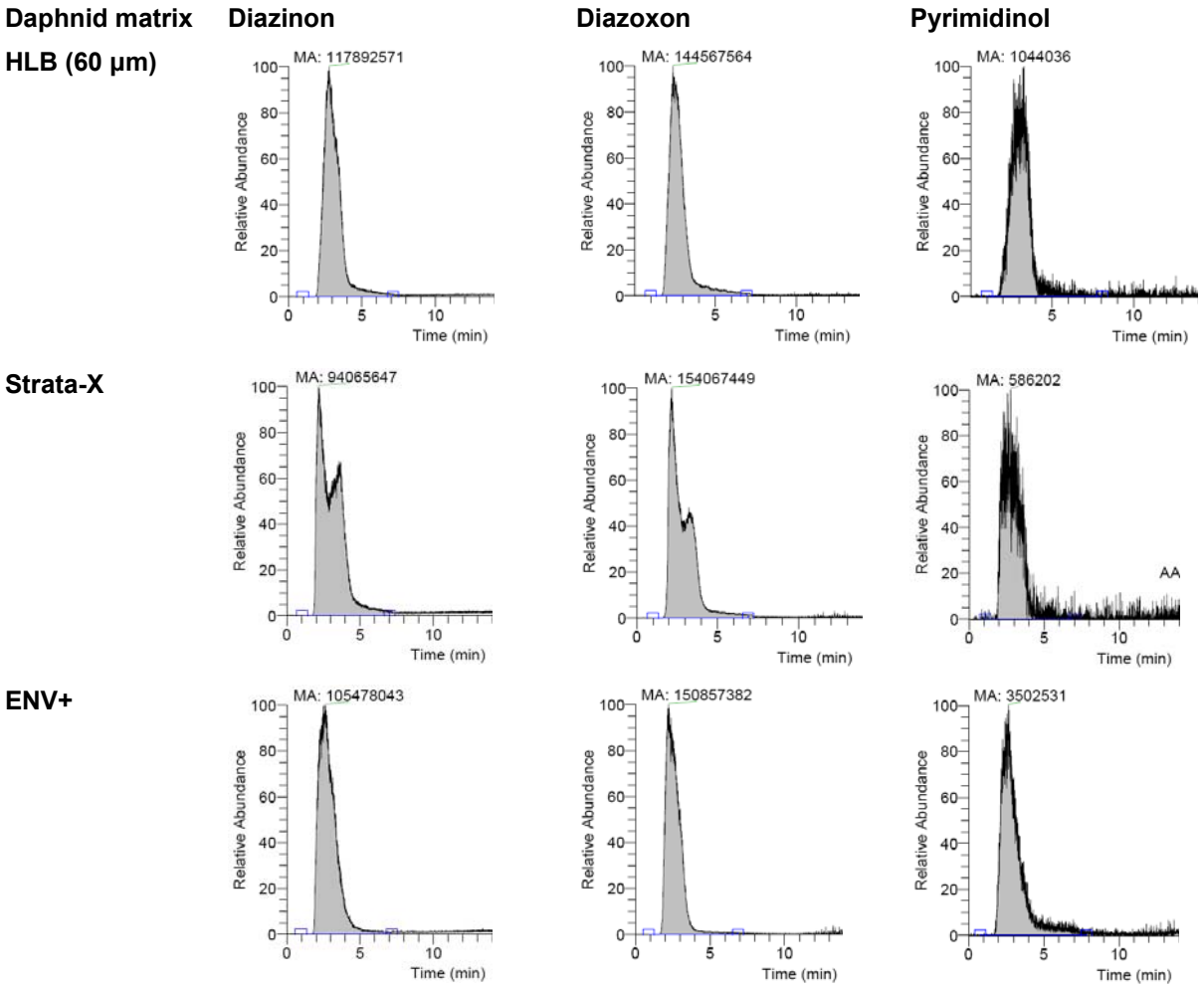

Figure S-4.1. *Elution profiles for different SPE materials. Samples (5 % v/v MeOH) with daphnid matrix containing 10 ng of each analyte. Measurements were performed without buffer. Elution with MeOH (40 µL·min^{-1}). The peak areas of the respective compounds are shown.*

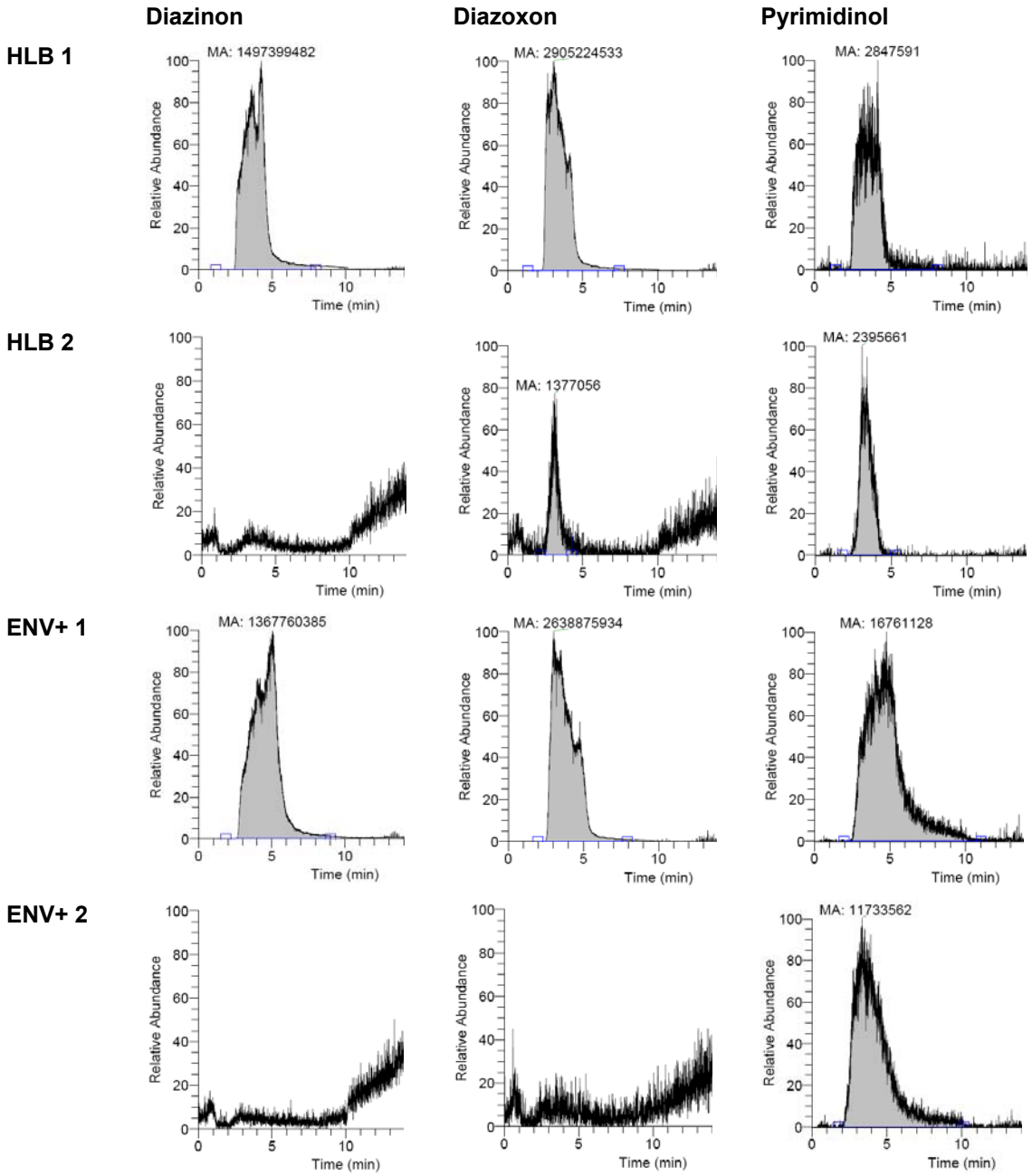

Figure S-4.2. *Breakthrough of analytes extracted with HLB and ENV+. Samples (5 % v/v MeOH) prepared in water containing 10 ng of analyte. Elution with MeOH (40 µL·min^{-1}). Measurements were performed without buffer. The peak area of the respective quantifier products are shown.*

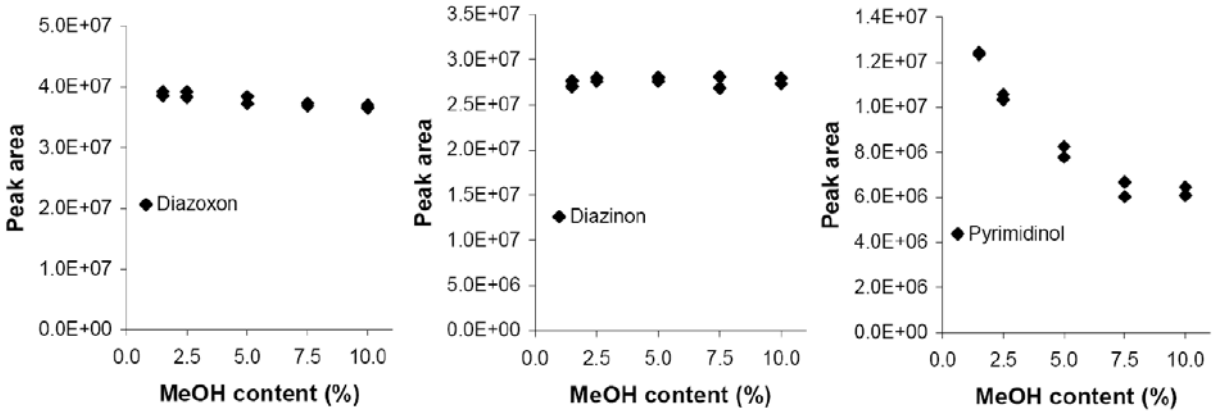

Figure S-4.3. *Influence of MeOH content (% v/v) in the samples on the analyte amount detected with online-SPE HPLC-MS/MS. SPE material: ENV+. Concentration in samples: 1 ng pyrimidinol, 0.1 ng diazinon, 0.1 ng diazoxon. Samples were prepared without daphnid matrix and were measured in duplicate.*

2) Validation of the online SPE method

The recovery of the online-SPE method with ENV+ as sorbent was determined for diazinon, diazoxon and pyrimidinol in daphnid matrix. For this purpose two separate experiments were performed (experiment I and II): In experiment I samples containing only daphnid matrix in water were loaded on the SPE material and the eluate collected directly after the cartridge for 11.5 min after beginning of elution. Subsequently analytes and internal standard were added. This procedure was repeated but this time analytes were spiked before enrichment of the sample (see Figure S-4.4).

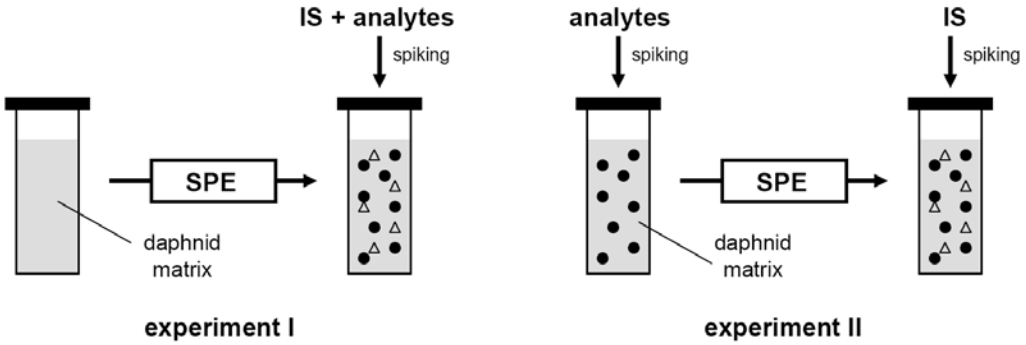

Figure S-4.4. *Schematic illustration of the online-SPE validation experiment. Experiment I: Analytes and internal standard spiked after elution from the SPE cartridge. Experiment II: Analytes and internal standard spiked before enrichment and after elution, respectively.*

In Table S-4.6 the amount of daphnid extract, analyte and internal standard solution added to 20 mL vials before and after the elution are listed. Samples were filled up to 20 mL with water (2 mM NH_4Ac). In all samples the final MeOH content was 5 % v/v. These two experiments were performed with five equidistant compound concentrations (ng absolute) in the range 2.0 to 10.0 ng for pyrimidinol and 0.2 to 1.0 ng for diazion and diazoxon. Two analyte mixtures in MeOH containing 100 and 20 $ng \cdot mL^{-1}$ pyrimidinol and 10 and 2 $ng \cdot mL^{-1}$ diazinon and diazoxon, respectively, were spiked to the samples. Daphnid extract was prepared by homogenizing 40 daphnids in 400 µL MeOH with 300 mg Zr/Si beads (FastPrep® FP120 Cell

Disrupter, 45 s, 6.5 m/s). After addition of 400 µL methanol the homogenate was filtrated with reg. cellulose. Recovery was determined via the slopes of the linear regression line through the plot measured response ratio (RR) vs. nominal compound concentration (see Figure S-4.5). For diazoxon this evaluation was additionally done via solely the peak area. Measured RR or peak area of experiment II were corrected with the amount of sample not injected (approx. 900 µl, injection volume 19 ml). Recoveries determined were 80 %, 77 % (81 %) and 52 % for diazinon, diazoxon (evaluation solely via the peak area of diazoxon without internal standard) and pyrimidinol, respectively. In comparison recoveries determined with Oasis HLB (particle size 60 µm) were approx. 70 - 80 % for diazinon and diazoxon, but only approx. 10 % for pyrimidinol (data not shown here). The MeOH content in the vials prior to enrichment was 5 % v/v.

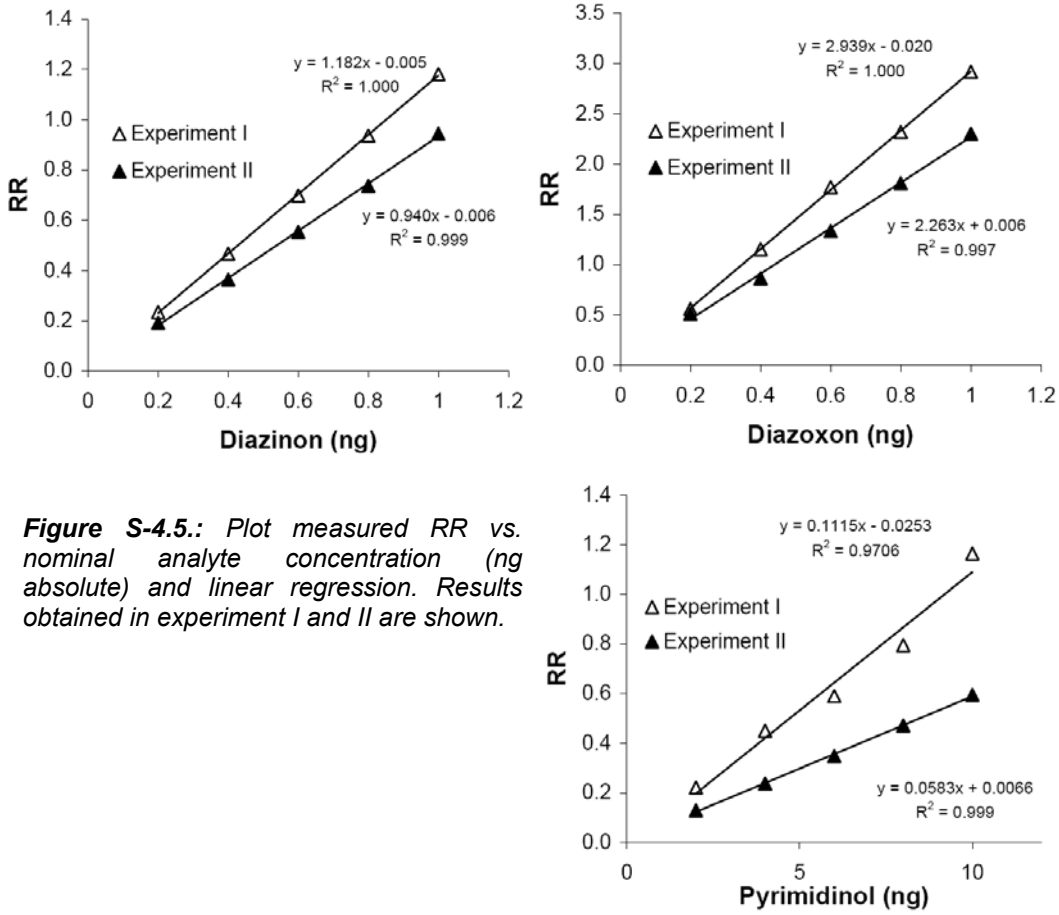

Figure S-4.5.: *Plot measured RR vs. nominal analyte concentration (ng absolute) and linear regression. Results obtained in experiment I and II are shown.*

Table S-4.6. *Amounts of analyte solution, IS, daphnid extract etc. spiked to 20 mL vials during the SPE validation experiments I and II. Nominal sample concentrations are expressed as ng absolute .*

Experiment I:		**Sample concentrations:**	**10.0 + 1.0 ng**	**8.0 + 0.8 ng**	**6.0 + 0.6 ng**	**4.0 + 0.4 ng**	**2.0 + 0.2 ng**
Spiking	Before enrichment	MeOH (µL)	600	600	600	600	600
		Daphnid extract (µL)	400	400	400	400	400
		H2O (2 mM NH4Ac) (ml)	19.0	19.0	19.0	19.0	19.0
	After elution	Collected eluate (µL)	≈900	≈900	≈900	≈900	≈900
		Analyte mix1 (100+10 ng/mL) (µl)	100	80	60		
		Analyte mix2 (20+2 ng/ml) (µL)				200	100
		MeOH (µL)	100	120	140		100
		IS (10 ng/mL) (µL)	100	100	100	100	100
		H2O (2 mM NH4Ac) (mL)	19.0	19.0	19.0	19.0	19.0

Experiment II:		**Sample concentrations:**	**10.0 + 1.0 ng**	**8.0 + 0.8 ng**	**6.0 + 0.6 ng**	**4.0 + 0.4 ng**	**2.0 + 0.2 ng**
Spiking	Before enrichment	Analyte mix1 (100+10 ng/mL) (µL)	100	80	60		
		Analyte mix2 (20+2 ng/mL) (µL)				200	100
		MeOH (µL)	500	520	540	400	500
		Daphnid extract (µL)	400	400	400	400	400
		H2O (2 mM NH4Ac) (mL)	19.0	19.0	19.0	19.0	19.0
	After elution	Collected eluate (µL)	≈900	≈900	≈900	≈900	≈900
		MeOH (µL)	200	200	200	200	200
		IS (10 ng/mL) (µL)	100	100	100	100	100
		H2O (2 mM NH4Ac) (mL)	19.0	19.0	19.0	19.0	19.0

Limit of detection (LOD) and limit of quantification (LOQ)

LOD and LOQ of the target compounds were determined applying the online-SPE HPLC-ESI-MS/MS method. The LOD and the LOQ were defined as the amount of analyte (ng absolute) to which a peak intensity three and ten times higher than the background noise corresponds, respectively. Furthermore ion supression caused by the daphnid matrix was considered. For this purpose samples with and without daphnid matrix containing diazinon, diazoxon and pyrimidinol in the range 0.001 - 0.075 and 0.001 - 0.050 ng absolute, respectively, were measured. For each sample daphnid extract was prepared by homogenizing 20 daphnids in MeOH with the FastPrep. IS (1ng·mL^{-1}) and analytes solutions in MeOH were spiked and samples filled up to 20 mL with water. The final MeOH content was 5 % v/v. The intensity of the background noise was determined as the (vertical) difference between the upper and lower limit of the background scatter. The peak intensity was calculated as the difference between the total peak height and the height of the lower background limit at the respective retention time (see example in Figure S-4.6).

The LOD and LOQ (in ng absolute) were calculated via the linear relationship between peak intensity and the nominal analyte concentration (linear regression line forced through the background height for x = 0 ng). Prior to calculations peak intensities were corrected via intensities found in controls consisting of

analyte free samples. Units were transformed into pmoL g_{ww}^{-1} assuming a number of 20 daphnids per sample and a wet weight of 1 mg per daphnid. The effect of the daphnid matrix on the peak intensity was estimated via the ratio of the slopes of the best fit lines through peak area vs. analyte concentration (see Figure S-4.7). This ratio equals the factor by which the peak intensity is reduced due to the matrix effect. Results are shown in Table S-4.7.

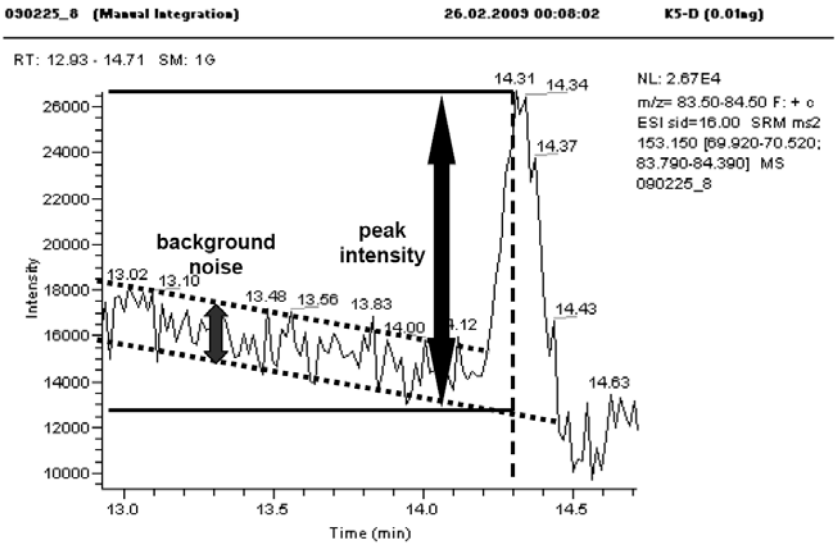

Figure S-4.6 *Chromatogram of pyrimidinol (fragment with m/z = 84). Illustration of background noise and peak intensity.*

Table S-4.7 *LOD and LOQ in pg absolute determined with and without daphnid matrix. Matrix effect describes the loss of peakintensity in % caused by the daphnid matrix.*

	Without daphnid matrix:		**With daphnid matrix:**				**Matrix effect (%)**
	LOD	LOQ	LOD		LOQ		
	pg	pg	pg	pmol·g_{ww}^{-1}	pg	pmol·g_{ww}^{-1}	
Diazinon	0.27	0.95	0.34	0.06	1.19	0.20	22
Diazoxon	0.20	0.89	0.22	0.04	1.00	0.18	14
Pyrimidinol	9.05	40.74	10.70	3.51	48.14	15.82	51

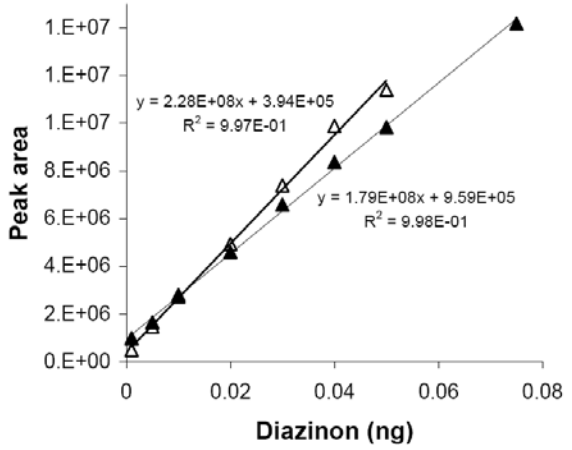

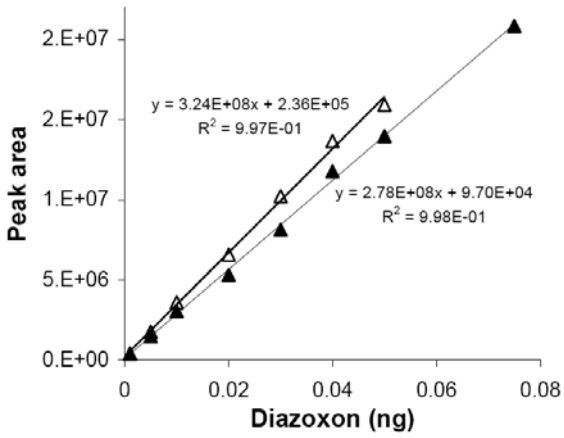

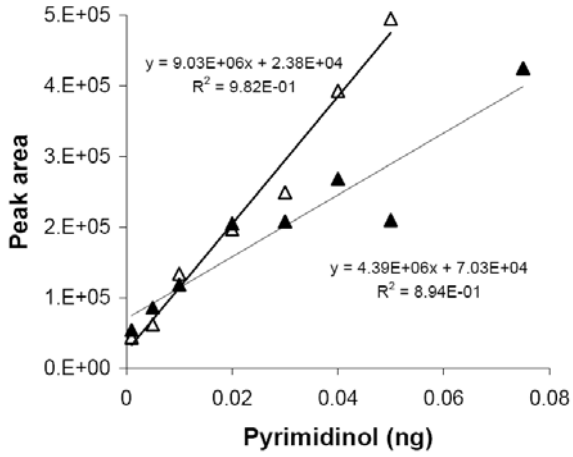

Figure S-4.7. *Estimation of the daphnid matrix effect. Plot peak area vs. nominal analyte concentration (ng absolute) and best fit line for samples without daphnid matrix (∆) and with daphnid matrix (▲).*

Additional Information on Results and discussion

Parameterization of the TK model

k_{el}^{pyr} and $k_{el}^{diazinon}$ were determined via fit of equation 4.4 and 4.1 to the internal pyrimidinol and diazinon concentration measured during the depuration phase of experiment I and II (exposure to pyrimidinol and diazinon + PBO, see Figure 4.2 a and b), respectively. Here, the integrated form $c_{int}(t) = c_{int}(0) \cdot e^{-k_{el} \cdot t} + c_{int}(\infty)$ of the respective equations was applied with $c_{int}(0)$ (the internal concentration at time point of transfer into toxicant free medium), $c_{int}(\infty)$ (residual internal concentration for $t \rightarrow \infty$) and k_{el} as fit parameters. In case of pyrimidinol $c_{int}(\infty)$ was set to zero (best fit value for $c_{int}(\infty)$: 183.8 ± 1.1 pmol·g_{ww}^{-1}). In case of diazinon + PBO internal diazinon concentrations did not eliminate to 0 and a certain amount seemed to remain in daphnids (best fit values for $c_{int}(0)$ and $c_{int}(\infty)$ are 115.6 ± 8.1 pmol·g_{ww}^{-1} and 47.5 ± 6.9 pmol·g_{ww}^{-1}, respectively). A possible explanation for this could be accumulation of diazinon into ovaries and eggs formed during the experiment (75 % of daphnids with ovaries at the beginning of experiment II). In ovaries and eggs no biotransformation and therefore slow elimination can be assumed. However, in a preexperiment with diazinon + PBO internal concentrations approximated 0 during the depuration phase although 40 - 60 % of the daphnids possessed eggs at the end of the experiment.

Discussion of model assumptions

Even when *Daphnia* were directly exposed to diazoxon (experiment VII), it could hardly be detected (≈ LOD). One possible explanation could be a lower accumulation than diazinon due to a lower octanol-water partition coefficient and/ or a fast elimination via binding to sites like AChE. In the latter case pyrimidinol formed during this reaction should be detectable in corresponding amounts. In addition diazoxon would possess a very low LC_{50} value. In contrast, diazoxon exhibited LC_{50} (48 h) values in the same order of magnitude as diazinon (10.1 nM for 7 - 10 d old daphnids). Therefore an additional elimination step without production of pyrimidinol must be involved in diazoxon elimination e.g. conjugation with glutathione. Indeed in *D. magna* multiple isoforms of glutathione-S-tranferase could be identified (Leblanc and Cochrane 1987).

Characterization of D. magna - Influence of lipid content on the bioaccumulation of diazinon

1) Time course of body length, wet weight, dry weight and lipid content under culturing conditions:

D. magna were cultured for 8 d under the same conditions as animals used for experiments. After 5, 6, 7, 8 d length, wet weight, dry weight and lipid content were measured. In addition the number of daphnids possessing ovaries and eggs was determined. As body length the distance between the forehead and the beginning of the tail spine was taken (see Figure S-4.8). The wet weight was determined as described in SI of chapter 3. Weighing daphnids dried over a period of 24 h in the oven at 60 °C provided the dry weight. For lipid determination (n = 3) 80 daphnids per replicate were sieved, washed with water, snap-frozen in liquid nitrogen and stored at -80°C till further analysis.

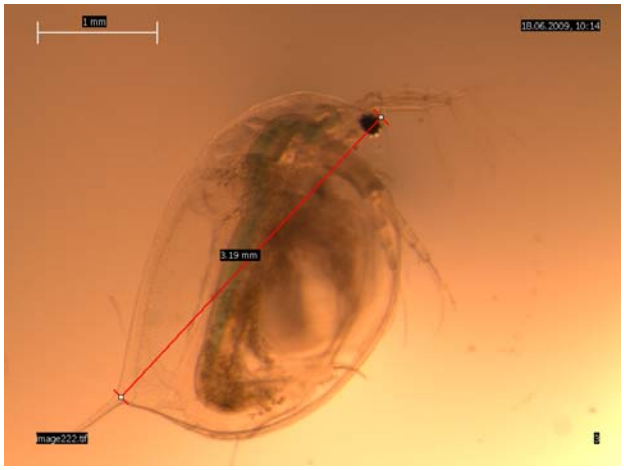

Figure S-4.8. *Body length of D. magna. The length is defined as the distance between the forehead and the beginning of the tail spine.*

Lipids were extracted from daphnid homogenates according to the method developed by Smedes (Smedes 1999). Here, extraction of lipids was done with a mixture of H_2O, i-PrOH and cyclohexane at the ratio of 11:8:10. This ratio is crucial for a complete removal also of polar lipids from the aqueous phase without extracting non-lipids. The extraction was performed twice (Smedes 1999). The working procedure applied for *D. magna* is shown in Figure S-4.9. In order to achieve the correct solvent ratio also the water content of the daphnid sample was considered with the assumption of a dry weight of 10 % of the wet weight. Phase separation was achieved by centrifugation. In our case three phases formed: An aqueous phase on the bottom, an upper organic phase (orange color) and a layer in between composed of a white precipitate. The organic phases were separated and collected. After evaporation of the solvents and drying of the extract in the oven the remaining lipid was weighted. A certain amount was also weighted in solvent controls (n = 3), which were processed the same way but without daphnids, probably due to extractable components present in the used screw cap plastic vials. Data were corrected by the solvent controls. For future application of the gravimetrical lipid determination 2 mL Eppendorf tubes are recommended, where this problem did not occur.

The plot measured parameters against the average age of the animals is shown in Figure S-4.10. Dry weight, wet weight, and lipid content are increasing in a linear way with increasing age. r^2 values of the linear regression lines are 0.98, 0.96 and 0.95, respectively. The dry weight was always approx. 10 % of the wet weight. Lipids amount approx. 1.5 to 1.8 % of the wet weight. The body length is increasing from 5.5 to 6.5 d, but then stays more or less constant. Lipid content and wet weight exhibit a linear relationship. The equation of the best fit line is given by:

$$\text{Lipid}(\mu g \cdot \text{daphnid}^{-1}) = 19.7 \cdot \text{mg}_{ww} \cdot \text{daphnid}^{-1} - 3.6 \qquad \text{(S-4.3)}$$

(r^2 = 0.95, fit through replicates as single data points, as x values mean values of the wet weight were applied). A compilation of results can be found in Table S-4.8.

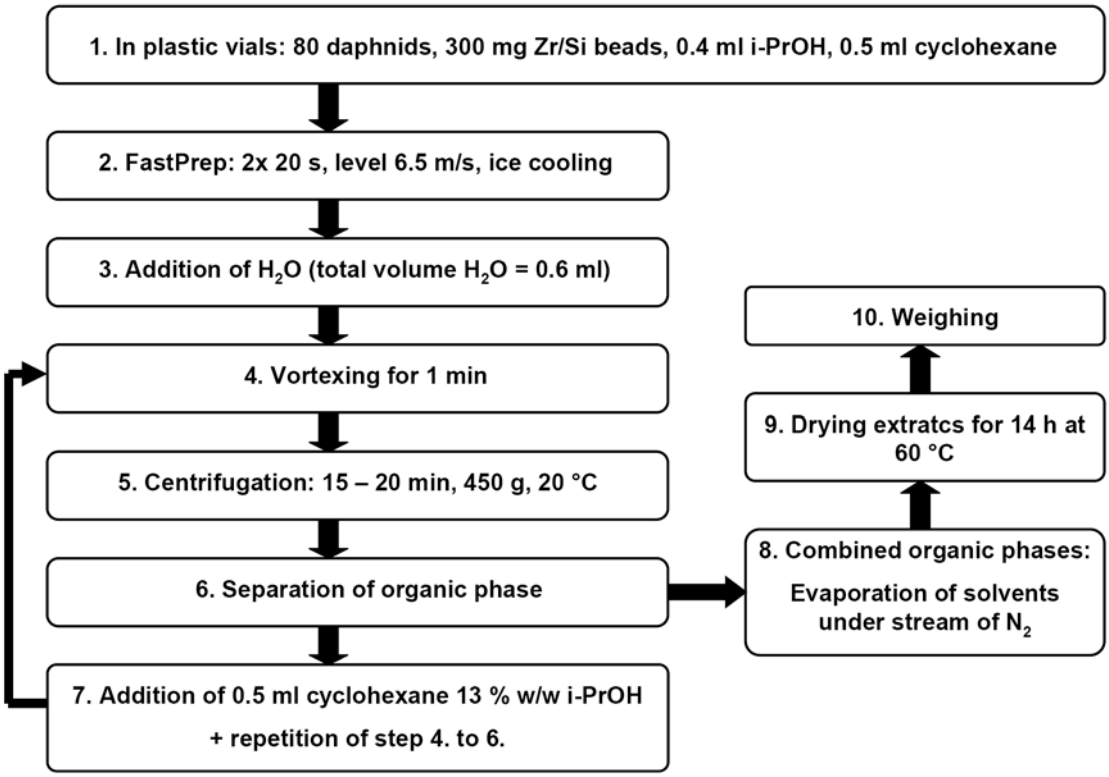

Figure S-4.9 *Working procedure for the determination of the absolute amount of total lipids in D. magna. The extraction is based on the method developed by Smedes (Smedes 1999).*

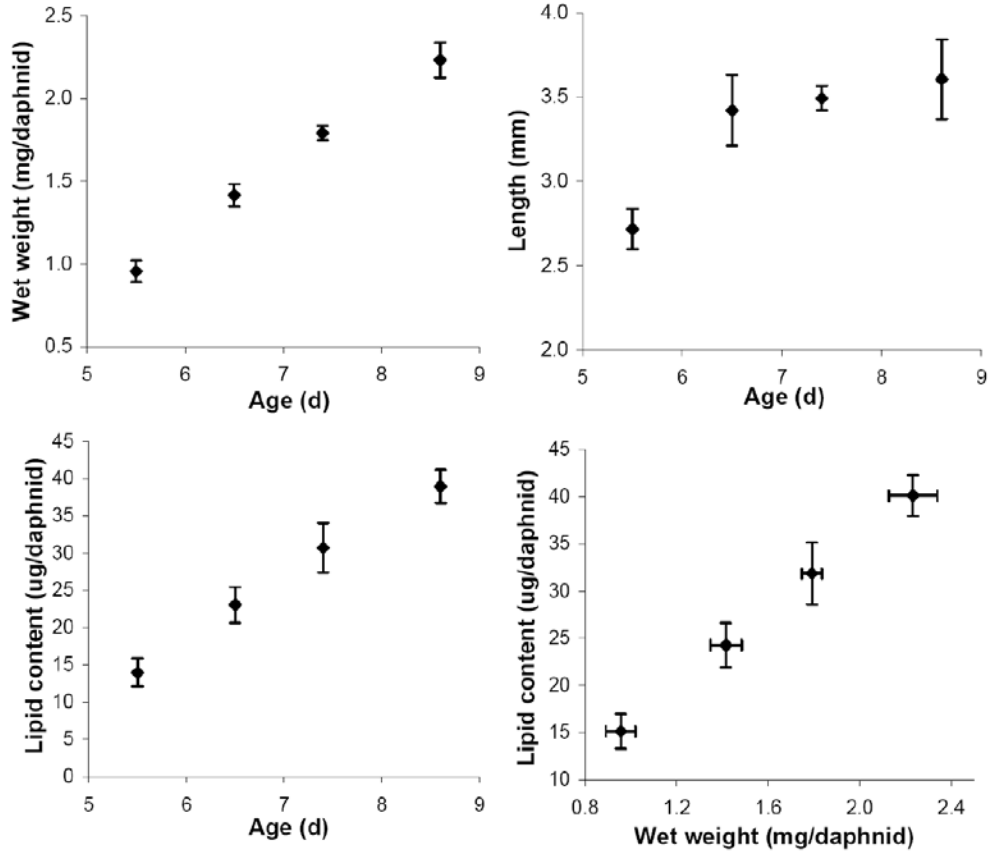

Figure S-4.10. *Body length (n = 5), wet weight (n = 4) and lipid content (n = 3) vs. the average age of experimental animals and lipid content vs. wet weight. D. magna were kept under culturing conditions. All data are presented as mean values ± SD.*

2) Time course of lipid content and wet weight under exposure conditions

The lipid content in *D. magna* under exposure conditions was measured with the Sulphophosphovanilline (SPV) method as described in (Zöllner and Kirsch 1962) and adapted to 96 well plates. The SPV method is applicable for the sensitive detection of predominantly unsaturated lipids in the µg range (recommended 10 - 120 µg). Within the SPV method lipids are treated with concentrated sulfuric acid. The addition of an phosphoric acid-vanilline reagent (vanilline 0.6 % w/w in H_2O:H_3PO_4 85 % w/w. in H_2O = 1:4) results in a purple solution whose extinction is measured photometrically. The formed color is stable for a period of 30 to 50 min (Zöllner and Kirsch 1962). The working procedure is shown in Figure S-4.11.

Prior to detection lipids present in *D. magna* were extracted with the method described above with minor changes: Homogenization of 10 daphnids with FastPrep and centrifugation were performed 2x 15s at level 5.5 $m \cdot s^{-1}$ and at 1000 g for 10 min, respectively. 2 mL Eppendorf tubes were used for homogenization since the originally used srew cap plastic vials caused high extinction values also in the solvent controls.

Since also other organic compounds, e.g. solvents like i-PrOH, give a color reaction (Zöllner and Kirsch 1962), the drying time neccesary to completely evaporate the solvents from the lipid extracts was determined in a preexperiment. 100 µL of a 1$mg \cdot mL^{-1}$ triolein solution in cyclohexane were mixed with 900

µL cyclohexane containing 13 % w/w i-PrOH. Prior to the SPV approach solvents were evaporated under a stream of N_2 and samples put in the oven for 2, 6 and 12 h at 60 °C. Solvent controls consisted of 1 mL cyclohexane (13 % w/w i-PrOH) and were dried for 12 h. Each sample was performed in duplicate. The extinction was stable already after 2 h in the oven. For further experiments drying for 6 h at 60 °C was therefore regarded as appropriate.

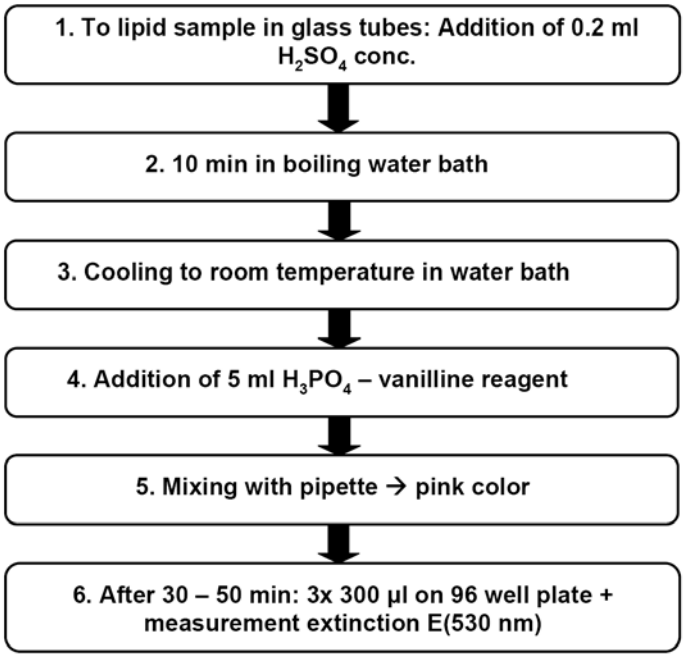

Figure S-4.11. *Lipid determination according to the SPV method as described in (Zöllner and Kirsch 1962) and adapted to 96 well plate.*

With triolein as standard a recovery of the extraction step of about 97 % was determined. A pretest of the whole method with 10 daphnids (age: 5 - 6 d) yielded an exctinction of about 1.1. This value was regarded as still beeing within the acceptable linear range of the method.

In the actual experiment animals were treated the same way as described for exposure experiments with diazinon (no feeding) but without the toxicant. Briefly, 20 daphnids were placed in 200 mL M4 medium in 250 mL Schott bottles. After different „exposure“ times 4x 10 daphnids out of 2 bottles were frozen for lipid determination. In addition the wet weigth and the number of animals possessing overies and/ or eggs was determined. The experiment lasted for approx. 92 h. The results are listed in Table S-4.9. The time course of the lipid content and the wet weight is shown in Figure S-4.12. Lipid data are corrected by controls without daphnids.

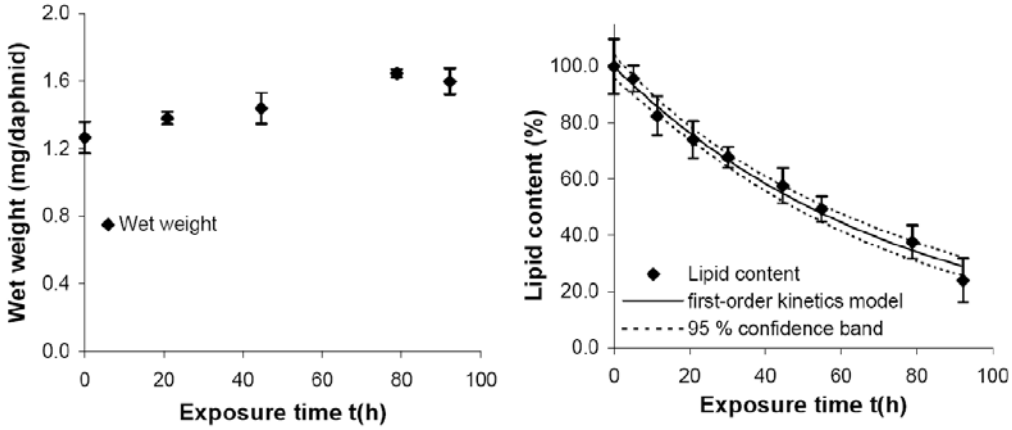

Figure S-4.12. *Time course of wet weight and lipid content of Daphnia magna kept in M4 medium under exposure conditions (no feeding). Shown are mean values ± SD (lipid content: n = 4, wet weight: n = 3 -5). Lipid content is expressed in % of the mean value at t = 0. Solid line is the best fit line of equation S4 obtained by nonlinear regression.*

In contrast to the wet weight, which is increasing with time, the lipid content is declining. At the end of the experiment only 24 % of the initial lipid amount is left. The decline of the lipid content under exposure conditions can be described by a first-oder elimination process:

$$\text{Lipid}_t = \text{Lipid}_0 \cdot e^{-k_{el} \cdot t} \qquad \text{(S-4.4)}$$

Lipid_t and lipid_0 (in µg·daphnid^{-1} or %) are the lipid content at time t and at t = 0, respectively. k_{el} (h^{-1}) is the first order elimination rate constant. Equation S-4.4 was fitted to the data via nonlinear regression. The best fit value for k_{el} is 0.013 h^{-1} (95 % CI: 0.012 to 0.015).

Here the relative amount of lipid was measured. Quantification would in principle be possible via external calibration e.g. with triolein as standard. But same amounts of different lipids give different color intensities with the SPV method. Since triolein causes a relatively high intensity and since in organisms several types of lipids are present this would lead to an overestimation of the actual lipid content (Zöllner and Kirsch 1962). Lipid_0 in µg·daphnid^{-1} can be calculated via the wet weight with equation S-4.3 and subsequently the absolute amount at exposure time t with equation S-4.4.

3) Influence of lipid content on the bioaccumulation of diazinon

In Table S-4.10 the best fit results for TK parameters of equation 4.1 fitted to internal diazinon concentrations measured during exposure and depuration experiments with diazinon without inhibition of P450 (experiments IV, V and VI) are shown. Compared are results of the simultaneous fit to data of experiments IV, V and VI with and without correction via the time course of lipid content in *D. magna* and separate fit of experiments IV + VI and V + VI without correction via the time course of lipid content.

Table S-4.8 *Body length, wet weight, dry weight and lipid content for D. magna kept under culturing conditions (with feeding). The number of animals possessing eggs and ovaries in % is given as the mean value of two to three replicates with 20 daphnids each.*

Age	**Body length**			**Wet weight**			**Dry weight**			**Lipid**			**Animals with**	
(d)	**(mm)**			**(mg·daphnid^{-1})**			**(mg·daphnid^{-1})**			**(µg(lipid)·daphnid^{-1})**				
	mean	± SD	n	mean	± SD	n	mean	± SD	n	mean	± SD	n	ovaries (%)	eggs (%)
5.0 - 6.0	2.72	0.12	5	0.956	0.065	4	0.093	0.004	4	14.0	1.9	3	0	0
6.0 - 7.0	3.42	0.21	5	1.416	0.068	3	0.143	0.007	3	23.1	2.4	3	20-23	0
6.9 - 7.9	3.49	0.07	5	1.791	0.043	4	0.188	0.004	4	30.7	3.3	3	87	0
8.1 - 9.0	3.61	0.24	7	2.232	0.106	4	0.230	0.007	4	39.0	2.2	3	73	23

Table S-4.9 *Wet weight and relative lipid content of D. magna kept under exposure conditions without feeding. Data are presented as mean values ± SD. n is the number of replicate measurements. The number of animals possessing eggs and ovaries in % is given as the mean value of two replicates with 20 daphnids each.*

Exposure time	**Lipid content (%)**			**Wet weight (mg·daphnid^{-1})**			**Animals with**	
h	mean	± SD	n	mean	± SD	n	ovaries (%)	eggs (%)
0	100.0	9.8	4	1.266	0.092	5	7.5 - 10.0	0.0
5.1	95.7	4.6	4					
11.4	82.4	7.0	4					
20.9	74.1	6.5	4	1.386	0.028	3	12.5	0.0
30.1	67.7	3.7	4					
44.6	57.7	6.3	4	1.421	0.104	3	7.5	0.0
54.8	49.4	4.5	4					
78.8	37.6	5.9	3	1.646	0.021	4	0.0	17.5
92.2	24.0	7.9	4	1.598	0.076	4	0.0	17.5

Table S-4.10. *Best fit results for TK parameters of equation 4.1 fitted to internal concentrations measured during exposure and depuration experiments with diazinon (without inhibition of P450, experiments IV, V and VI) with and without correction of data via the time course of lipid content in D. magna.*

Correction via time course lipid	no						yes	
Experiments included in fit	IV + VI		V + VI		IV + V + VI		IV + V + VI	
Parameters	$k_{in}^{diazinon}$	$k_{el,tot}^{diazinon}$	$k_{in}^{diazinon}$	$k_{el,tot}^{diazinon}$	$k_{in}^{diazinon}$	$k_{el,tot}^{diazinon}$	$k_{in}^{diazinon}$	$k_{el,tot}^{diazinon}$
	$L \cdot g_{lipid}^{-1} \cdot h^{-1}$	h^{-1}	$L \cdot g_{lipid}^{-1} \cdot h^{-1}$	h^{-1}	$L \cdot g_{lipid}^{-1} \cdot h^{-1}$	h^{-1}	$L \cdot g_{lipid}^{-1} \cdot h^{-1}$	h^{-1}
Best fit results	0.31 ± 0.03	0.28 ± 0.03	0.25 ± 0.02	0.21 ± 0.02	0.30 ± 0.02	0.27 ± 0.03	0.28 ± 0.02	0.21 ± 0.02

Chapter 5

Mechanistic effect model for diazinon in *Daphnia magna*

Kretschmann, A.; Ashauer, R.; Escher, B. I.; Hollender, J.
Mechanistic Effect Model for Diazinon in *Daphnia magna*
to be submitted

Introduction

Organophosphates (OPs) are a large group of insecticides used worldwide e.g. to control pest insects in agriculture (Chambers 1992). These compounds reach non-target environmental compartments like surface waters due to runoff from agricultural fields after rain events, where they occur in fluctuating concentrations (Holmes and de Vlaming 2003; Pedersen et al. 2006; Wittmer et al. 2010) and where they may pose a threat to aquatic organisms. Characteristic of toxicity of OP compounds is a large variation in species sensitivity e.g. observed for aquatic organisms (Vaal et al. 1997b) and a pronounced time-dependency of toxic effects like a decrease of LC_{50} values with increasing exposure times, even after steady state between the exposure concentration and the concentration inside an organism has been reached (Legierse et al. 1999).

Time dependent and species selective OP toxicity are influenced by a multitude of species and compound specific properties and processes like uptake, distribution, biotransformation and elimination (toxicokinetics, TK) as well as the interaction with the target site and recovery of the organism from damage (toxicodynamics, TD) (Wallace and Kemp 1991; Keizer et al. 1995; Legierse et al. 1999; Ashauer et al. 2010; Rubach et al. 2010b). Inside an organism OP compounds, belonging to the class of phosphorothionate insecticides, can be biotransformed by various processes, including metabolic activation to their respective oxon analogues or detoxification of the parent compound and the oxon by several oxidative and hydrolytic reactions (Chambers and Carr 1995; Keizer et al. 1995). Acute toxic effects of OP compounds are in general related to inhibition of the enzyme acetylcholinesterase (AChE) (Chambers 1992; Maxwell et al. 2006), although for some OPs toxic effects might also be related to secondary modes of action (Printes and Callaghan 2004; Pope et al. 2005).

Previous studies analyzed in detail TK and TD related processes of OP compounds in aquatic organisms with *in vivo* and *in vitro* experiments including uptake and elimination kinetics (de Bruijn and Hermens 1991; Rubach et al. 2010b), biotransformation (Johnston and Corbett 1986; Takimoto et al. 1987a; Keizer et al. 1995; Nuutinen et al. 2003) and the interaction with the target site AChE (Johnson and Wallace 1987; Kemp and Wallace 1990). Also the effect on organism level (e.g. immobilization, mortality), e.g. after different exposure scenarios to OP insecticides, is well studied (Naddy and Klaine 2001; Andersen et al. 2006; Ashauer et al. 2007a). The combination of all these processes creates the species and compound specific time course and severity of a toxic effect and should therefore be seen in relation to each other. Approaches in current risk assessment that estimate the toxic potency of chemicals solely via external concentrations (e.g. LC_{50} values) can not deal with such a complex mechanistic background and are not able to explain time and species dependent toxicity (Jager et al. 2006).

In fact, a systematic and mechanistic link of TKs and TDs is necessary to extrapolate toxic effects between different species and also time varying exposure scenarios. Approaches, which enable such a link of TK and TD processes on a time resolved basis are TKTD models (Ashauer and Escher 2010). Examples are the threshold damage assessment model (TDM) (Ashauer et al. 2007a; Ashauer et al. 2010), the

critical target occupation model (CTO) (Legierse et al. 1999) and the DEBtox receptor kinetics model (Jager and Kooijman 2005). The TDM was developed to deal with a broad range of chemicals, whereas the latter two models were designed especially for receptor-mediated toxicity by OPs. Within the TDM the internal damage is not further specified. Within the other two models the interaction with the target site (AChE) and the corresponding kinetic parameters were not further verified e.g. with mechanistic *in vitro* studies or via measurement of the internal effect (AChE activity). Biotransformation processes were based on assumptions or were not considered in these two models since they were not verified and quantified via measured metabolite concentrations.

In the following a mechanistic TKTD model for the prediction of acute toxic effects of the phosphorothionate insecticide diazinon in *Daphnia magna* is presented. This model combines detailed information on the toxicokinetics, including all relevant biotransformation processes, and the toxicodynamics, i.e. the interaction of the toxic metabolite diazoxon with the target site AChE. Data and TK and TD sub-models were obtained and developed in previous studies (see chapter 3 and 4). In contrast to the previously published TKTD models biotransformation pathways are verified and quantified explicitely via internal metabolite concentrations measured *in vivo*. The underlying mechanism of AChE inhibition and the respective kinetics elucidated *in vitro* were implemented into the model. The internal concentration of the toxic metabolite was explicitely linked to the external effect (immobilization/ mortality) via the molecular effect (AChE activity) measured *in vivo*. Such a comprehensive link of TK with TD processes will provide a coherent picture of toxic mechanism from initial exposure to the final effect, which is required to understand phenomena like species selective and time dependent toxicity of OP insecticides in aquatic organisms.

Theory

Figure 5.1 and Table 5.1 give an overview of all TK and TD processes that were included in the comprehensive TKTD model of diazinon in *D. magna.* The proposed model treats *D. magna* as a single homogenous compartment. The model equations and definitions of the kinetic rate constants are listed in Table 5.2. A detailed analysis of the separate TK and TD part can be found in chapter 3 and chapter 4, respectively.

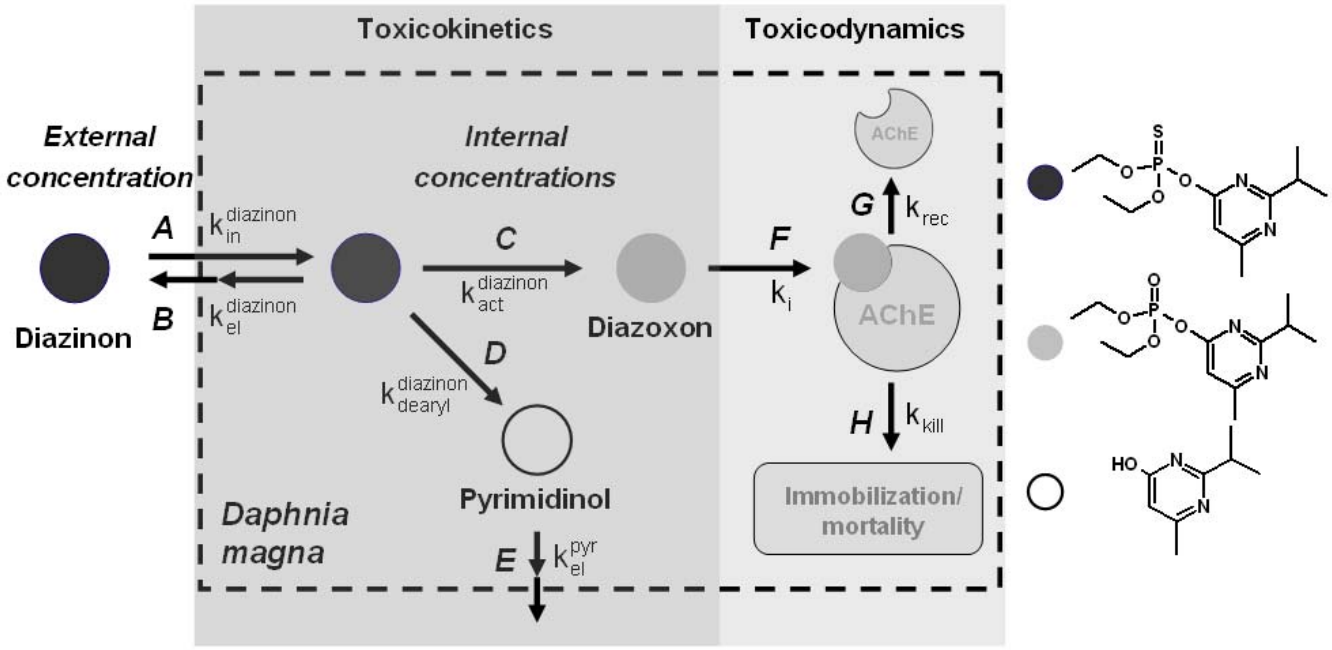

Figure 5.1. *Toxicokinetic (TK) and toxicodynamic (TD) phase of diazinon in D. magna. Shown are the different TK and TD pathways and the respective kinetic rate constants of the TKTD model.*

The TK phase consists of the pathways A to E in Figure 5.1. Equation 5.1 describes the time-course of the internal diazinon concentration with the assumption of first-order kinetics. Diazinon is taken up by passive diffusion. It is eliminated by activation to its toxic metabolite diazoxon and detoxification by dearylation under formation of pyrimidinol, both catalyzed by P450 (pathways C and D, respectively), as well as by passive diffusion and/ or other, not further elucidated elimination processes (pathway B). Hereby, the total elimination rate constant $k_{el,tot}^{diazinon}$ lumps together all possible elimination processes (pathways A, B, C, see equation 5.2). The time course of diazoxon, as described in equation 5.3, is dominated by the activation step C and the reaction with the target site AChE (step F). Based on a very sensitive AChE towards diazoxon in *D. magna* (see chapter 3) this inhibition reaction (2nd order kinetics) was assumed to be very fast and other elimination processes of diazoxon were therefore considered as negligible. The metabolite pyrimidinol was assumed to be exclusively formed from diazinon via pathway D and eliminated e.g. via passive diffusion and/ or conjugation processes (first-order kinetics, equation 5.4).

The formation of pyrimidinol during AChE inhibition was neglected because amounts of diazoxon present in the organism during *in vivo* exposure to diazinon were found to be small compared to the parent compound.

The TD part (pathways F to H) is based on the structure of two hazard models, the threshold damage assessment model (TDM) (Ashauer et al. 2007a) and the dynamic energy budget toxicity (DEBtox) model for receptor kinetics (Jager and Kooijman 2005). The TD phase consists of the effect on molecular scale (inhibition and recovery of AChE activity, pathway F and H) and the link to the effect on organism scale (immobilization, mortality, pathway H). With the assumption of low internal diazoxon concentrations *in vivo*, AChE inhibition was proven to be irreversibly in one step following second-order kinetics (see chapter 3 and equation 5.5). Recovery of AChE activity occurs through *de novo* synthesis and/ or spontaneous reactivation of inhibited AChE, here regarded as a first-order kinetics process (equation 5.5). A previous experiment showed that daphnids are not able to recover from immobilization by diazinon and that immobilization leads inevitably to death (see chapter 3). Therefore, immobilization was set equal to mortality. In the proposed model the occurence of an effect on organism scale is a stochastic process and is linked to the effect on molecular scale via the hazard rate h (equation 5.6, with k_{kill} as the killing rate constant). The cumulative hazard H is linked to the probability of surviving until a given time t in equation 5.7. We assume that the probability of dying (hazard rate h) only increases above zero when the amount of active AChE falls below a certain threshold value $c_{int,threshold}^{AChE}$ (see equation 5.6). Growth dilution of internal concentrations was neglected in our model since during our exposure experiments (where *Daphnia* were not fed) concomitantly with an increase in wet weight, a decrease in lipid and a more or less stable protein content was observed. A more mechanistic link of AChE activity with immobilization/ mortality via the neurotransmitter acetylcholine (ACh) instead of the hazard rate could not be applied since no experimental data on ACh accumulation were available.

Table 5.1. *Toxicokinetic (TK) and toxicodynamic (TD) processes implemented in the TKTD model according to Figure 5.1*

TK + TD processes of diazinon in *Daphnia magna*						
Phase	Pathway	Description	Rate constant	Unit	Best fit values	± SD
TK	A	Uptake of diazinon by passive diffusion	$k_{in}^{diazinon}$	$mL \cdot g_{ww}^{-1} \cdot h^{-1}$	4.80	0.09
	B	Elimination of diazinon by passive diffusion and other processes like dealkylation/ dearylation catalyzed by glutathione-S-transferase (GST)	$k_{el}^{diazinon}$	h^{-1}	0.083*	0.018
	C	Activation of diazinon to its oxon analog diazoxon by oxidative desulfuration catalyzed by cytochrome P450 monooxygenase (P450)	$k_{act}^{diazinon}$	h^{-1}	0.016**	
	D	Detoxification of diazinon under formation of 2-isopropyl-4-methyl-6-pyrimidinol (pyrimidinol) in an oxidative dearylation catalyzed by P450	$k_{dearyl}^{diazinon}$	h^{-1}	0.173	0.001
	E	Elimination of pyrimidinol by passive diffusion or by conjugation e.g. with sulfate or glucose.	k_{el}^{pyr}	h^{-1}	0.78*	0.01
	B+C+D	Sum of all elimination processes of diazinon	$k_{el,tot}^{diazinon}$	h^{-1}	0.272	0.001
TD	F	Effect on molecular level: Irreversible inhibition of the target site AChE by diazoxon	k_i	$g_{ww} \cdot pmol^{-1}\ h^{-1}$	0.080*	
	G	Recovery from AChE inhibition by spontaneous reactivation of the enzyme-inhibitor complex and/ or by *de novo* synthesis of AChE	k_{rec}	h^{-1}	0.017	0.003
	H	Effect on organism level: Immobilization, mortality	k_{kill}	$g_{ww} \cdot pmol^{-1}\ h^{-1}$	0.012	0.004
			*parameters determined in previous experiments and kept fixed **calculated according to equation 2 from total elimination and $k_{el}^{diazinon}$ and $k_{dearyl}^{diazinon}$.			

Table 5.2. *Equations used in the TKTD model*

Model equations				List of parameters in addition to Table 1			
Phase	Time course	Equations		Parameters	Description	Unit	Best fit values ± SD
TK	Diazinon	$\frac{dc_{int}^{diazinon}(t)}{dt} = k_{in}^{diazinon} \cdot c_{ext}^{diazinon}(t) - k_{el,tot}^{diazinon} \cdot c_{int}^{diazinon}(t)$	(5.1)	$c_{ext}^{diazinon}$	External concentration of diazinon in the medium	pmol·L^{-1}	
		with $k_{el,tot}^{diazinon} = k_{act}^{diazinon} + k_{dearyl}^{diazinon} + k_{el}^{diazinon}$	(5.2)	$c_{int}^{diazinon}$, $c_{int}^{diazoxon}$, $c_{int}^{pyrimidinol}$	Internal concentrations of diazinon, diazoxon, pyrimidinol in the organism	pmol·g_{ww}^{-1}	
	Diazoxon	$\frac{dc_{int}^{diazoxon}(t)}{dt} = k_{act}^{diazinon} \cdot c_{int}^{diazinon}(t) - k_i \cdot c_{int}^{diazoxon}(t) \cdot c_{int}^{AChE}(t)$	(5.3)	c_{int}^{AChE}	Internal concentration of active AChE in the organism	pmol·g_{ww}^{-1}	
	Pyrimidinol	$\frac{dc_{int}^{pyr}(t)}{dt} = k_{dearyl}^{diazinon} \cdot c_{int}^{diazinon}(t) - k_{el}^{pyr} \cdot c_{int}^{pyr}(t)$	(5.4)	$c_{int,threshold}^{AChE}$	Threshold concentration of active AChE for immobilization	pmol·g_{ww}^{-1}	29.0 ± 2.3
TD	AChE	$\frac{dc_{int}^{AChE}(t)}{dt} = -k_i \cdot c_{int}^{diazoxon} \cdot c_{int}^{AChE}(t) + k_{rec} \cdot \left[c_{int}^{AChE}(0) - c_{int}^{AChE}(t)\right]$	(5.5)	h(t)	Hazard rate	h^{-1}	
	Hazard	$h(t) = \frac{dH(t)}{dt} = k_{kill} \cdot \max\left[c_{int,threshold}^{AChE} - c_{int}^{AChE}(t), 0\right]$	(5.6)	H(t)	Cumulative hazard	---	
	Survival	$S(t) = \exp\left[-H(t)\right]$	(5.7)	S(t)	Survival probability	-	

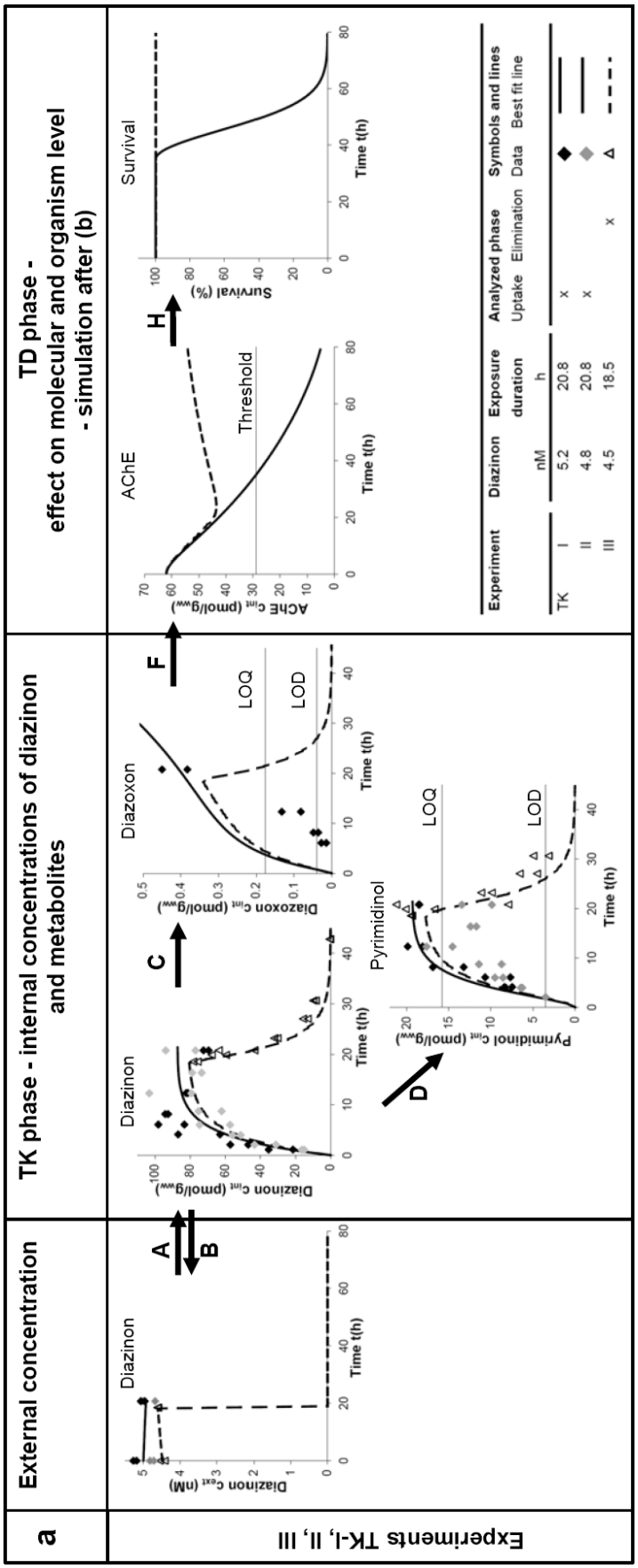
a
Experiments TK-I, II, III
External concentration
TK phase - internal concentrations of diazinon and metabolites
TD phase - effect on molecular and organism level - simulation after (b)
Diazinon
A
B
C
D
F
H
Diazoxon
Pyrimidinol
LOQ
LOD
Threshold
AChE
Survival
Time t(h)
Experiment
Diazinon
Exposure duration
Analyzed phase
Symbols and lines
Uptake
Elimination
Data
Best fit line
TK
I
II
III
nM
h
5.2
4.8
4.5
20.8
20.8
18.5

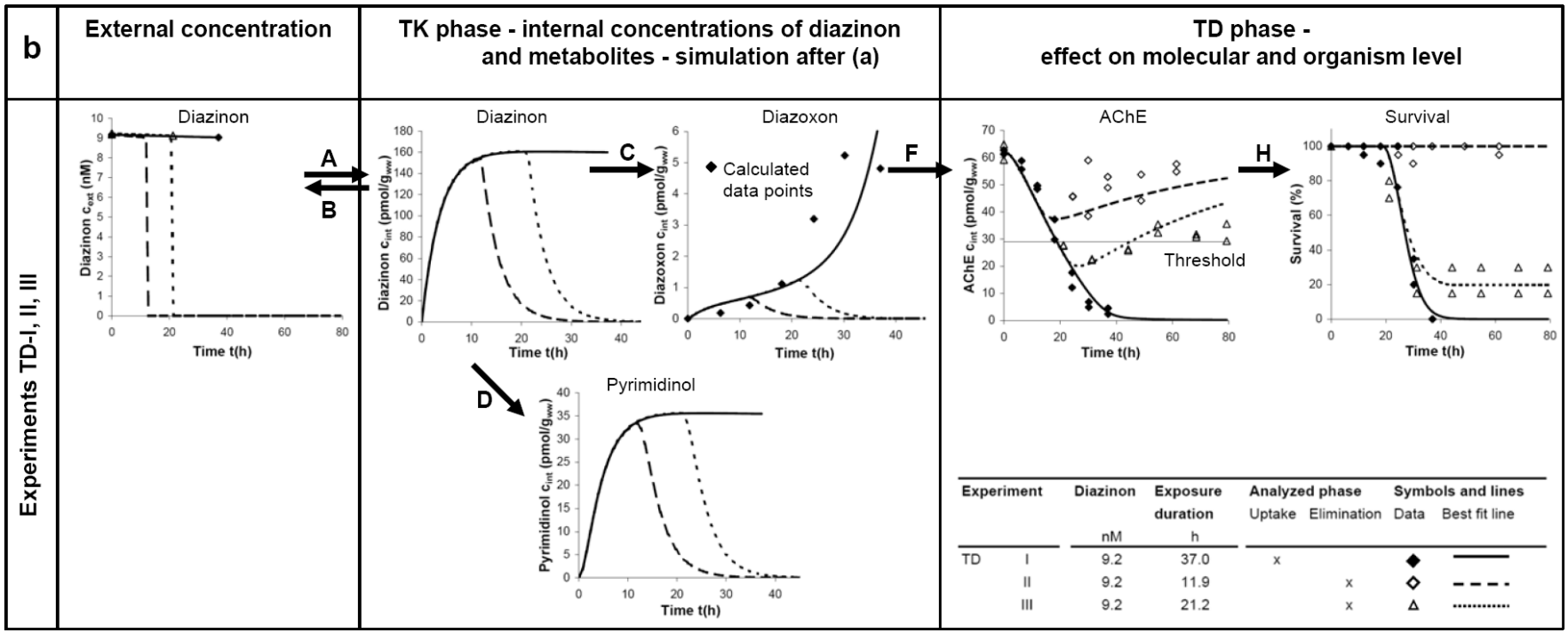

Figure 5.2. *Fit of the TKTD model (equations 5.1 - 5.7) to a) internal concentrations of diazinon and metabolites measured during the TK experiments as well as b) AChE activity and survival measured in the TD experiments. All equations were fitted simultaneously to the measured data shown in (a) and (b). Letters and arrows indicate the TK and TD pathways according to Figure 5.1. Internal diazoxon concentrations shown in (b) were calculated after the fit via the measured AChE activity in experiment TD-I and the best fit values obtained in (b).*

Material and methods

Experimental data

Experimental data were taken from previous studies (see chapter 3 and 4). Briefly, in *in vivo* experiments *D. magna* (age at beginning of experiment: 5 - 6 or 7 - 8 d) were exposed to diazinon and subsequently transferred into toxicant free medium (exposure and elimination phase). For the TK experiments, concentrations of diazinon and its metabolites in extracts of *D. magna* were measured after different exposure and elimination times (TK-I, TK-II and TK-III, mean exposure concentration 4.8 nM diazinon). In the TD experiments, the AChE activity was measured and the number of immobilized animals recorded (TD-I, TD-II and TD-III, mean exposure concentration 9.2 nM diazinon). In experiments TD-I and TD-II immobilization was recorded from the same sample as used for AChE activity measurement at the respective sampling time. In experiment TD-III immobilization was continuously recorded using one duplicate sample, which was used for AChE measurement in the end of the experiment, in order to show potential recovery from immobilization of one consistent sample. All measurements were performed in duplicate. Each sampling point consisted of 20 daphnids. An overview of exposure concentrations and exposure times is given in Figure 5.2 a and b. The inhibition rate constant k_i and the underlying kinetic inhibition mechanism of diazoxon and AChE from *D. magna* (pathway F in Figure 5.1) were determined *in vitro*. Enzyme activity was normalized with respect to control activity at the respective sampling time. The internal concentrations of the chemicals were normalized to the wet weight of the organism at the beginning of the experiments ($mol \cdot g_{ww}^{-1}$).

Parameter estimation

Contrary to our previous studies in chapter 3 and 4, where TK and TD model parts were parameterized separately, we here estimate model parameters for TK and TD simultaneously. Equations 5.1 to 5.7 (Table 5.2) were implemented into ModelMaker version 4.0 (Cherwell Scientific Ltd, Oxford UK, www.modelkinetix.com) and fitted simultaneously to the measured internal concentrations of diazinon, its metabolites and AChE as well as the survival data (% immobilization is translated into % survival as daphnids immobilization was irreversible in our study). Prior to modeling, the measured AChE activity (% of control) was converted into absolute amounts of active enzyme ($mol \cdot g_{ww}^{-1}$) by multiplying with the absolute AChE amount per gram wet weight at the beginning of the exposure experiment. An absolute AChE amount of 62 $pmol \cdot g_{ww}^{-1}$ was determined via the measured protein content of daphnids of experiment TD-I applying an AChE content of 0.02 % of total protein (see chapter 3). This AChE amount was used as approximation for all exposure experiments (TK and TD). The concentrations measured in duplicate in the medium at the beginning and the end of the exposure phases were used as external concentrations (model input). Uptake experiments TK-I and TK-II were treated as one experiment and modeled together. Compound amounts detected in the depuration medium were in general below the quantification limit and therefore set to 0. The parameters $k_{el}^{diazinon}$, k_{el}^{pyr} and k_i (pathway B, E and F in Figure 5.1, respectively)

were determined in chapter 3 and 4 and kept fixed. The parameters $k_{in}^{diazinon}$, $k_{dearyl}^{diazinon}$, $k_{el,tot}^{diazinon}$, k_{rec} and k_{kill} describing the pathways A, D, B+C+D, G and H, respectively, as well as $c_{int,threshold}^{AChE}$ were kept variable. Best-fit values for these parameters obtained in our previous studies via a separate fit of the TK and the TD model part (see chapter 3 and 4) were applied as initial values. $k_{act}^{diazinon}$ (pathway C) was calculated via equation 5.2. Differential equations were solved with the Runge-Kutta method. Best-fit values were obtained by least-square optimization using the Levenberg-Marquardt method.

Results and discussion

The fit of the TKTD model (equations 5.1 to 5.7) to the internal concentrations obtained in experiments TK -I, II and III and effect data obtained in experiments TD-I, II and III is shown in Figure 5.2 a and b, respectively (overall fit r^2 = 0.95). From the left to the right experimental data and model simulations are arranged from external concentrations to the final effect via internal concentrations of diazinon and metabolites and the effect on molecular level (pathways A to H in Figure 5.1). Best-fit values of the estimated parameters are listed in Table 5.1 and Table 5.2. As TK and TD experiments were performed at two different exposure concentrations, in the TK experiments (panel a) the TD effect was simulated with best fit values obtained with data from the TD experiments, while in the TD experiments (panel b) the TK phase was simulated using best fit values obtained with data from the TK experiments. The internal diazoxon concentration during the experiment TD-I in Figure 5.2 b was calculated after the fit via the measured AChE activity applying equation 5.5 and the best-fit value for k_{rec} as described in chapter 3.

TK phase - Internal concentrations of diazinon and metabolites

The best-fit kinetic rate constants show that the major elimination process of diazinon is its oxidative dearylation to pyrimidinol (pathway D in Figure 5.1), whereas the activation to the toxic metabolite diazoxon (pathway C) plays only a minor quantitative role (64 % and 6 % of the total elimination of diazinon, respectively). For high diazinon exposure concentrations (see TD experiments in Figure 5.2 b) the model prediction of the diazoxon time course fits quite well with the calculated diazoxon concentration. With increasing exposure time diazoxon increased inversely to the AChE activity due to an increasing saturation of available target sites. For lower exposure concentrations (see Figure 5.2 a) our model is not able to accurately describe the diazoxon time course. As discussed in chapter 4, this misfit might be explained by induction of certain isozymes of P450, which are responsible for the activation of diazinon. This factor might be especially pronounced for the lower diazoxon concentrations since target sites become saturated more slowly compared to high concentrations.

If the initial AChE amount in *D. magna* is assumed to remain unchanged during inhibition ($c_{int,0}^{AChE}$ = 62 pmol·g_{ww}^{-1}) we obtain a pseudo first-order rate constant for pathway F of $k_i^{`} = k_i \cdot c_{int,0}^{AChE}$ = 5.0 h^{-1}. Applying this rate constant 99 % of diazoxon would be eliminated out of the organism after 0.9 h, whereas for the parent compound 17.1 h ($k_{el,tot}^{diazinon}$ = 0.272 h^{-1}) are needed. This underlines the very fast elimination of the toxic metabolite by its reaction with AChE.

TD phase - Effect on molecular and organism level

The TKTD model can well describe the measured effect data (TD experiments) in dependence of the internal metabolite diazoxon: AChE activity declined with time during exposure to diazinon. As soon as the amount of active AChE fell below the threshold value (best fit value $c_{int,threshold}^{AChE}$ = 29.0 ± 2.3 pmol·g_{ww}^{-1}, 47

% of initial AChE amount) immobilization/ mortality increased with ongoing exposure until all animals were affected. For higher external diazinon concentrations, the same threshold value of active AChE, where observable effects kicked in, was already reached earlier than compared to the model predictions for the low diazinon concentrations. In the TD experiments, all daphnids were immobilized already within 40h, whereas for the TK experiments this state was not reached before 80 h of exposure.

If daphnids were transferred into toxicant free medium AChE activity continued to decline initially until diazoxon was completely eliminated from the organism. After this period recovery of AChE activity set in, e.g., through *de novo* synthesis of AChE. In experiment TD-II (transfer in clean medium after 12 h of exposure) AChE activity started to increase again before the threshold was reached. The model therefore correctly simulates no effect on organism level (see Figure 5.2 b). In the beginning of the elimination phase of experiment TD-III (transfer to clean medium after 21 h of exposure) AChE activity was below the threshold value and the percentage of immobilized animals increased with time. Although AChE activity rose again above the threshold value the number of immobilized animals stayed constant (we never observed recovery of daphnids from immobilization by diazinon, see chapter 3).

According to the TKTD model (equation 5.5 with $c_{int}^{diazoxon}$ = 0 and a best-fit value for k_{rec} of 0.017 ± 0.003 h^{-1}) AChE activity recovers by 99 % within approx. 11 d. It has to be considered that experiments were performed without feeding of animals in order to avoid uptake of diazinon via the food. Feeding would probably increase the speed of recovery to some extent due to higher energy reserves. Recovery is very slow compared to the elimination of diazinon and diazoxon. This means that animals are still affected when diazinon and its toxic metabolite were fully eliminated from the body. TD processes are therefore rate limiting. This finding is important for the interpretation and prediction of toxic effects resulting from time-varying exposure conditions. For example the observation that mortality and immobilization increased when *D. magna* were exposed to repeated pulses of OP compounds although organisms had apparently fully recovered from immobilization after the first pulse (Andersen et al. 2006) could be explained via a slow TD recovery (*de novo* synthesis of AChE) and therefore accumulation of inhibited AChE.

TK and TD in comparison - what determines the toxicity of diazinon towards D. magna?

The LC_{50} (48 h) of diazinon determined in a preexperiment with 7 - 10 d old daphnids was 5.7 nM. LC_{50}(96 h) values reported for diazinon and fish are 2.6 µM (guppy) and 26 µM (zebra fish) (Keizer et al. 1991). Thus *D. magna* is more sensitive to diazinon than fish. Factors decisive for the toxicity of diazinon in *D. magna* are the internal levels of its toxic metabolite diazoxon, ideally its concentration directly at the target site, and/or the sensitivity of the target site AChE towards diazoxon. In panel b of Figure 5.2 the internal diazoxon concentration is equal to the amount of diazoxon, which reacted ultimately with the target site. The highest calculated concentration amounted only to 3 % of the diazinon concentration in steady state. Together with a low activation rate constant ($k_{act}^{diazinon}$ = 0.016 h^{-1} for pathway C in Figure 5.1) the activation step seems not to be responsible for the high toxicity of diazinon. In comparison, the pseudo

first-order rate constant for the inhibition of AChE $k_i^{`} = k_i \cdot c_{int,0}^{AChE} = 5.0\ h^{-1}$ (pathway F) is much higher. Therefore, although activation to diazoxon is a rather slow process, the very reactive target site leads to the very low LC_{50} value of diazinon in *D. magna* and makes this species so sensitive.

For compounds with a specific mode of action, as organophosphates, a very wide species sensitivity distribution of acute effects covering a range of five to six orders of magnitude was observed (Vaal et al. 1997b). In comparison to other species daphnids and other crustaceans were found to be extremely sensitive to OP compounds (Vaal et al. 1997a; Rubach et al. 2010c). For phosphorothionate insecticides these large differences in species sensitivity were attributed to strong interspecies variation in TK as well as TD processes: Differences in acute toxicity of diazinon in four fish species (guppy, zebra fish, trout and carp) could be explained by an interplay of target site (AChE) sensitivity and activation and detoxification activities, which were analyzed *in vitro* (Keizer et al. 1995). For example, the most resistant species carp possessed the most sensitive target site AChE, but also the highest activity of A-esterase, which catalyzes the hydrolysis of the oxon, besides a very low activation of diazinon to diazoxon. In comparison, the high sensitivity of trout, although exhibiting a low activation rate, could be explained by a very sensitive AChE and a lack of A-esterase activity (Keizer et al. 1995). Differences in OP toxicity were even observed in different clones of *D. magna*. These were related to differences in biotransformation rather than differences in AChE sensitivity (Barata et al. 2001; Damasio et al. 2007). In conclusion, both processes, TK as well as TD, have to be considered in order to accurately describe species selective toxicity to phosphorothionate insecticides.

Stochastic or deterministic death?

The CTO (Legierse et al. 1999), TDM (Ashauer et al. 2007a), the DEBtox receptor kinetics (Jager and Kooijman 2005) as well as the proposed TKTD model are based on two fundamentally different assumptions applied in ecotoxicological survival modeling (Ashauer and Brown 2008): The CTO model assumes that death is deterministic and occurs instantly after a certain threshold of occupied target sites is exceeded. That threshold is assumed to be distributed between the individual organisms (individual tolerance distribution). The latter approaches assume that all organisms possess equal properties and that death is a chance process (stochastic concept) (Newman and McCloskey 2000; Ashauer and Brown 2008). Experiments performed to test if the sensitivity distribution of a population is best explained by either the individual tolerance distribution concept or the stochastic concept showed that neither solely applies but rather both contribute (Newman and McCloskey 2000; Zhao and Newman 2007). At least in our case (hazard modeling based on the stochastic concept) the assumption of an invariant AChE threshold is reasonable for the daphnids in our experiments, which consisted of a single clone of approximately the same age.

If we assume that the threshold values for AChE activity is distributed but an effect occurs instantaneously after exceeding the threshold, this distribution would be very narrow. Therefore, the

immobilization over time curve is expected to be steep: All animals are immobilized within a short time interval. According to our hazard model this would mean that the hazard rate (the probability of being immobilized) increases very rapidly with increasing occupation of active AChE once the threshold is passed. This condition is given for a high killing rate constant k_{kill}.

The actual reason why immobilization arises is accumulation of the neurotransmitter ACh as soon as AChE is inhibited to a certain percentage leading to overstimulation of ACh receptors (Boelsterli 2007). If we assume that ACh accumulation is a relatively slow process a possible interpretation of the increasing probability of immobilization might be an accelerated accumulation ACh with increasing AChE inhibition. Here, k_{kill} would resemble an accumulation rate constant. But since all animals are assumed to be equal within the stochastic concept all animals would reach a hypothetical critical ACh value at the same time. That all animals are immobilized at the same time was not observed in our experiments. The observed behavior can be described in a correct way if ACh accumulation is assumed to be instantaneous and the occurrence of an external effect (immobilization) is assumed to be a chance process as soon as a critical value of ACh is reached.

If the daphnids differed in their properties, different scenarios would lead to an immobilization vs. time curve with a slope different from infinite: 1. The AChE threshold would follow a distribution and ACh accumulation would be instantaneous. Immobilization would occur immediately after exceeding the AChE threshold but this threshold is reached at different time points for each animal. 2. The AChE threshold would be equal for all animals but ACh accumulation is slow and rate-determining and the critical ACh amount or the speed of accumulation would differ.

Since a number of factors play a role in the sequence from AChE inhibition to immobilization, which are represented by the hazard rate, and since no ACh measurement was performed in our experiments the above thoughts are all speculative and no clear distinction between stochastic and deterministic concept is possible.

Comparison to the CTO, TDM and the DEBtox receptor kinetics model

The TKTD model presented here builds up on the DEBtox receptor kinetics model (Jager and Kooijman 2005) but the TK part was extended in order to account for biotransformation processes via implementation of internal metabolites measured *in vivo*. This allows us to predict the time course of the internal active metabolite, which triggers the toxic effect. An analog extension of the TK part of the TDM model was recently presented by Ashauer et al. (Ashauer et al. 2010).

The TD part explicitly implements information on the AChE inhibition mechanism, which was obtained in *in vitro* experiments. Such models containing mechanism based *in vitro* parameters are called “hard link” models (Derendorf and Meibohm 1999). Although it was shown that the TDM, in which the internal damage is not further specified, is an appropriate approach for modeling survival in *Gammarus* after exposure to diazinon (Ashauer et al. 2010) the implementation of specific information about the interaction with the

target site obtained *in vitro* is important e.g. if differences in toxicity between different species need to be explained. The inhibition parameter k_i (composed of an association constant and a phosphorylation rate constant) is a direct descriptor of species sensitivity (Wallace 1992), although not the only species trait of relevance (Rubach et al. 2010a).

A further advantage of this approach is that the TD action of new chemicals can be predicted without the need of time and cost intensive *in vivo* parameterization of the TD part (Derendorf and Meibohm 1999). If $c_{int,threshold}^{AChE}$, k_{kill} and k_{rec} are assumed to be dependent only on the biological species and the mode of action but independent of the chemical, and once these values are determined for one OP compound, then *in vivo* TK and *in vitro* TD studies are sufficient to forecast the time course of AChE activity and survival also for other OP insecticides. Furthermore, Quantitative Structure Activity relationships were set up e.g. for trout, which allow the estimation of inhibition parameters of untested OP compounds via physico-chemical properties (Wallace and Kemp 1991).

The TD parameters of the DEBtox receptor kinetics and CTO model, which are parameterized with *in vivo* survival data, could if desired be replaced by *in vitro* inhibition parameters. A limitation is the requirement of an *a priori* assumption about the inhibition mechanism, as for example pseudo first-order inhibition in case of the CTO model (target site concentration assumed to be constant, no saturation of target sites possible).

Our model as well as the TDM (Ashauer et al. 2007a) and the DEBtox receptor kinetics model (Jager and Kooijman 2005) describe recovery from damage as a dynamic process (first-order kinetics). This allows their application for the prediction of effects after time variable and pulsed exposure. In contrast, the CTO model implements a fixed term, which equates to an incipient LC50 for infinite exposure times, in order to account for repair from damage (e.g. *de novo* synthesis) (Legierse et al. 1999).

Implications for enviromental risk assessment

The approach taken in this study enables the identification of processes, which determine differences in species and compound specific toxicity. This is not only of scientific interest but provides also advantages for risk assessment: Knowing the molecular determinants of species specific toxicity facilitates the development of new pesticides, which are more specific and less dangerous to non-target organisms (Wallace and Kemp 1991). Furthermore process-based TKTD models enable a mechanism based extrapolation of toxic effects to untested compounds using QSARs for the estimation of TK and TD parameter (Ashauer and Escher 2010). This saves animals and time needed for the assessment of new chemicals.

Since the presented model relates the effect on organism level to its trigger, the inhibition of AChE, on a time-resolved basis, it might help to mechanistically explain and simulate effects resulting from time-varying exposure conditions as they do occur in the field. For example subsequent pulses of toxicants might lead to

increased mortality due to an accumulated damage („carry-over toxicity“ (Ashauer et al. 2010)), i.e. an accumulation of inhibited AChE due to a slow recovery of AChE activity.

For a more complete and more mechanistic picture of toxic action in case of AChE inhibition in future work e.g. the neurotransmitter ACh could be implemented in the chain from exposure to the final effect. It is important for risk assessment to mechanistically link the effect of OP compounds on molecular scale (e.g. enzyme inhibition) with long-term effects on individual level and higher levels of biological organization (e.g. populations), as observed for example after pulsed exposure of *D. magna* to paraoxon-methyl (Duquesne 2006). OPs are capable to bind also to other macromolecules than AChE (as reviewed in (Pope et al. 2005)). In the toxicity of some OP compounds towards *D. magna* a secondary mode of action is supposed to be involved (Printes and Callaghan 2004). Therefore, further mechanistic studies are needed to enable a more precise prediction of acute and chronic effects of OP pesticides in aquatic organisms.

The presented TKTD model predicts receptor mediated toxic effects in *D. magna* through time by combining mechanistic information on biotransformation and interaction of the active compound with the target site obtained via *in vivo* and *in vitro* experiments. Such a detailed process-based effect model yields insights into the complex time-dependent interaction of biochemical processes that quantitatively link exposure with toxic effect. It therefore assists in a better understanding of the mechanism of toxicity.

Chapter 6

Conclusions and Outlook

In traditional risk assessment the toxicity of xenobiotics towards aquatic organisms is commonly expressed as a function of the external concentration and the resulting effect on the individual level. For example LC_{50} values are determined for fixed exposure concentrations and durations. Sensitivities of species are ranked according to their LC_{50} values. This approach is not able to mechanistically explain time and species dependent toxicity (Jager et al. 2006). To provide a more accurate and mechanistical interpretation of toxicity the concentration of a chemical (and its active metabolites) inside an organism, ideally its concentration at the target site, the mechanism of interaction with the target site and the target site sensitivity have to be considered (Escher and Hermens 2004).

In this study a mechanistic effect model for the time-resolved description of receptor-mediated toxic effects of the organothiophosphate insecticide diazinon in *Daphnia magna* was developed. The novelty of the approach lies in the consideration of active and inactive metabolites formed inside the organism and the inclusion of measured target site (AChE) activity as link between exposure and the toxic effect. To accurately describe the time course of AChE activity in dependence of the toxic metabolite diazoxon *in vivo* the inhibition mechanism was elucidated with *in vitro* methods (chapter 3). The derived kinetic parameters for inhibition allowed the assessment of compound and species specific affinity and reactivity of the inhibitor enzyme system. Implementation of the confirmed inhibition mechanism into the effect model provided a sound basis for a mechanistic link between the internal concentration of the active metabolite and the target site activity. Measurement of the intrinsic effect (AChE activity, its inhibition and recovery) *in vivo* enabled us to parameterize the TD part of our model in particular the recovery rate k_{rec} and the killing rate k_{kill} directly via the intrinsic effect within single pulse experiments. Using absolute AChE amounts enabled us furthermore to make the link of AChE activity and active metabolite on a quantitative basis and to calcuate the diazoxon concentration directly present at the target site, which provides a direct measure of toxic potency of the parent compound diazinon. The TK part of our model was parameterized via internal concentrations of diazinon and its metabolites measured during *in vivo* exposure to diazinon (Chapter 4). It enabled the prediction of the time course of the parent compound diazinon as well as of the non-active metabolite pyrimidinol and especially the active metabolite diazoxon inside *D. magna*. In a last step of the model development all the TK and TD parameters obtained with *in vivo* and *in vitro* studies were combined in a mechanistic effect model for receptor mediated toxicity in *D. magna* (chapter 5). This provided a coherent picture from initial exposure to the final observed effect via the effect on molecular scale.

The model developed in this work is an advance to previous TKTD models like the TDM (Ashauer et al. 2007a), the CTO (Legierse et al. 1999) and the DEBtox model for receptor kinetics (Jager and Kooijman 2005), because it explicitely specified and verified the kinetics/ mechanism of the interaction with the target site. In comparison our model approach requires in addition to *in vivo* studies on the external effect *in vitro* experiments and *in vivo* measurement of the intrinsic effect (AChE activity) for parameterization of the TD part. But once the model is parameterized for a certain species and parameters like the recovery rate, killing rate and critical threshold value are assumed to be solely species dependent it is in principle

possible to predict effects of other OP compounds solely with *in vivo* TK and *in vitro* TD data. An additional *in vivo* parameterization of the TD part is not needed (Derendorf and Meibohm 1999). For fish quite a large number of *in vitro* inhibiton parameters for different OP insecticides are available in literature (Wang and Murphy 1982; Forsberg and Puu 1984; Johnson and Wallace 1987; Kemp and Wallace 1990; Carr and Chambers 1996) and could be applied in the model. This approach could save time and also number of animals needed for the model development.

The inclusion of the measured intrinsic effect in our model provides a possible alternative to previous approaches, where recovery from OP exposure was determined solely via external effect data (survival, immobilization) obtained from pulsed exposure experiments (Naddy and Klaine 2001; Andersen et al. 2006; Ashauer et al. 2007a). Besides a direct determination of intrinsic recovery inclusion of measured AChE activity might furthermore provide a mechanistic explanation for recovery observed on organism level after pulsed exposure patterns (e.g. that AChE activity reached again levels above the critical threshold for AChE activity or not between two pulses). These benefits of our approach are valid only if AChE inhibition is the sole initial molecular event, wich triggers the effect on organism scale. In comparison the more general TDM model has the advantage that mortality is related to a not further specified internal damage, which includes all processes leading to reduced health and to recovery of the organism.

The combination of the underlying mechanism of interaction with the target site, of kinetic parameters describing the target site sensitivity and the internal concentrations of the parent compound and especially of its active metabolites, as it was done within our model approach, enable a more accurate and mechanistic interpretation of the toxic potency of xenobiotics. As shown in our study a mechanistic link of TK and TD processes (biotransformation, interaction with the target site) helps to reveal processes, which are decisive for species and compound selective toxicity. This is not only of scientific interest but also an advance to traditional risk assessment. A further advantage of process-based TKTD models compared to traditional risk assessment is that they can predict toxic effects resulting from fluctuating exposure scenarios (Ashauer et al. 2007a; Ashauer and Escher 2010; Ashauer et al. 2010). Ashauer et al. recently successfully applied the TDM model to the risk quantification of time varying diazinon concentrations measured in freshwater streams (Ashauer et al. 2010 - submitted). A similar application of the model developed here to predict risk for time-variable exposure scenarios is possible.

Our study should be seen as proof of concept for the implementation of internal metabolites and intrinsic effects in ecotoxicological effect modeling. Further work is needed to proof the benefits of the developed model for risk assessment. Measurement of the time course of internal metabolites, AChE activity and survival should be performed for different aquatic species/ compound combinations under single and multiple pulse exposure scenarios in order to test the model performance under fluctuating exposure conditions and the benefits for the explanation of species selective toxicity. In our study solely acute effects in *D. magna* after exposure to diazinon concentrations in the $\mu g \cdot L^{-1}$ were analysed. Since OP compounds

in surface waters are usually detected in the ng·L^{-1} range (e.g. diazinon > 50 ng·L^{-1} (Wittmer et al. 2010)) future work should also combine this model approach with chronic effects (e.g. reproduction).

To conclude, the developed TKTD model for the organothiophosphate diazinon and *D. magna* presented in this work is a contribution to a more mechanistic understanding of the relationship between external concentration of a chemical in the environment and the resulting toxic effects in (aquatic) organisms. Although mechanistic effect models are hardly applied in current risk assessment (Preuss et al. 2009) they provide clear scientific advances and application potential for regulatory purposes. The further refinement and implementation of such tools in risk assessment is promising considering an increasing number of chemicals entering the environment worldwide.

References

Abel, E. L.; Bammler, T. K.; Eaton, D. L. Biotransformation of methyl parathion by glutathione S-transferases. *Toxicological Sciences* **2004**, *79*, 224-232.

Akkanen, J.; Kukkonen, J. V. K. Biotransformation and bioconcentration of pyrene in *Daphnia magna*. *Aquatic Toxicology* **2003**, *64*, 53-61.

Aldridge, W. N. Some properties of specific cholinesterase with particular reference to the mechanism of inhibition by diethyl p-nitrophenyl thiophosphate (E 605) and analogues. *Biochemical Journal* **1950**, *46*, 451–460.

Aldridge, W. N. The differentiation of true and pseudo-cholinesterase by organophosphorus compounds. *Biochemical Journal* **1953a**, *53*, 62-67.

Aldridge, W. N. Serum esterases. I. Two types of esterase (A and B) hydrolysing p-nitrophenyl acetate, propionate and butyrate, and a method for their determination. *The Biochemical journal* **1953b**, *53*, 110-117.

Andersen, T. H.; Tjornhoj, R.; Wollenberger, L.; Slothuus, T.; Baun, A. Acute and chronic effects of pulse exposure of *Daphnia magna* to dimethoate and pirimicarb. *Environmental Toxicology and Chemistry* **2006**, *25*, 1187-1195.

Ankley, G. T.; Dierkes, J. R.; Jensen, D. A.; Peterson, G. S. Piperonyl butoxide as a tool in aquatic toxicological research with organophosphate insecticides. *Ecotoxicology and Environmental Safety* **1991**, *21*, 266-274.

Ashauer, R.; Boxall, A. B. A.; Brown, C. D. Predicting effects on aquatic organisms from fluctuating or pulsed exposure to pesticides. (vol 25, pg 1899, 2006). *Environmental Toxicology and Chemistry* **2006**, *25*, -.

Ashauer, R.; Boxall, A. B. A.; Brown, C. D. New ecotoxicological model to simulate survival of aquatic invertebrates after exposure to fluctuating and sequential pulses of pesticides. *Environmental Science & Technology* **2007a**, *41*, 1480-1486.

Ashauer, R.; Boxall, A. B. A.; Brown, C. D. Simulating toxicity of carbaryl to *Gammarus pulex* after sequential pulsed exposure. *Environmental Science and Technology* **2007b**, *41*, 5528-5534.

Ashauer, R.; Brown, C. D. Toxicodynamic assumptions in ecotoxicological hazard models. *Environmental Toxicology and Chemistry* **2008**, *27*, 1817-1821.

Ashauer, R.; Escher, B. I. Advantages of toxicokinetic and toxicodynamic modelling in aquatic ecotoxicology and risk assessment. *Journal of Environmental Monitoring* **2010**, *12*, 2056-2061.

Ashauer, R.; Hintermeister, A.; Caravatti, I.; Kretschmann, A.; Escher, B. I. Toxicokinetic and toxicodynamic modeling explains carry-over toxicity from exposure to diazinon by slow organism recovery. *Environmental Science and Technology* **2010**, *44*, 3963-3971.

Ashauer, R.; Wittmer, I.; Stamm, C.; Escher, B. I. Environmental risk assessment of fluctuating diazinon concentrations in an urban and agricultural catchment using toxicokinetic - toxicodynamic modeling. *Environmental Science & Technology* **2010 - submitted**.

Baici, A.; Schenker, P.; Wächter, M.; Rüedi, P. 3-Fluoro-2,4-dioxa-3-phosphadecalins as inhibitors of acetylcholinesterase. A reappraisal of kinetic mechanisms and diagnostic methods. *Chemistry and Biodiversity* **2009**, *6*, 261-282.

Baldwin, W. S.; Leblanc, G. A. Identification of Multiple Steroid Hydroxylases in *Daphnia magna* and Their Modulation by Xenobiotics. *Environmental Toxicology and Chemistry* **1994**, *13*, 1013-1021.

Barata, C.; Baird, D. J.; Soares, A. M. V. M.; Guilhermino, L. Biochemical factors contributing to response variation among resistant and sensitive clones of Daphnia magna straus exposed to ethyl parathion. *Ecotoxicology and Environmental Safety* **2001**, *49*, 155-163.

Barata, C.; Solayan, A.; Porte, C. Role of B-esterases in assessing toxicity of organophosphorus (chlorpyrifos, malathion) and carbamate (carbofuran) pesticides to *Daphnia magna*. *Aquatic Toxicology* **2004**, *66*, 125-139.

Barron, M. G. Bioconcentration. *Environmental Science & Technology* **1990**, *24*, 1612-1618.

Benke, G. M.; Murphy, S. D. Anticholinesterase action of methyl parathion, parathion and azinphosmethyl in mice and fish: Onset and recovery of inhibition. *Bulletin of Environmental Contamination and Toxicology* **1974**, *12*, 117-122.

Bisswanger, H. *Enzyme Kinetics - Principles and Methods*; Wiley-VCH Verlag GmbH & Co. KGaA: Weinheim, Germany, 2008.

Boelsterli, U. *Mechanistic Toxicology: The Molecular Basis of How Chemicals Disrupt Biological Targets*, 2nd, ed.; CRC Press - Taylor & Francis Group, LLC: Boca Rato, 2007.

Boone, J. S.; Chambers, U. E. Time course of inhibition of cholinesterase and aliesterase activities, and nonprotein sulfhydryl levels following exposure to organophosphorus insecticides in mosquitofish (Gambusia affinis). *Fundamental and Applied Toxicology* **1996**, *29*, 202-207.

Bowman, B. T.; Sans, W. W. Determination of octanol-water partitioning coefficients (K(ow)) of 61 organophosphorus and carbamate insecticides and their relationship to respective water solubility (S) values. *Journal of Environmental Science and Health - Part B Pesticides, Food Contaminants, and Agricultural Wastes* **1983**, *18*, 667-683.

Brealey, C. J.; Walker, C. H.; Baldwin, B. C. A-esterase activities in relation to the differential toxicity of pirimiphos-methyl to birds and mammals. *Pesticide Science* **1980**, *11*, 546-554.

Carletti, E.; Li, H.; Li, B.; Ekström, F.; Nicolet, Y.; Loiodice, M.; Gillon, E.; Froment, M. T.; Lockridge, O.; Schopfer, L. M.; Masson, P.; Nachon, F. Aging of cholinesterases phosphylated by tabun proceeds through O-dealkylation. *Journal of the American Chemical Society* **2008**, *130*, 16011-16020.

Carr, R. L.; Chambers, J. E. Kinetic analysis of the in vitro inhibition, aging, and reactivation of brain acetylcholinesterase from rat and channel catfish by paraoxon and chlorpyrifos-oxon. *Toxicology and Applied Pharmacology* **1996**, *139*, 365-373.

Chambers, H. W. Organophosphorus compounds: an overview. In *Organophosphates. Chemistry, Fate, and Effects*; Chambers, J. E., Levi, P. E., Eds.; Academic Press, Inc.: San Diego, California 1992.

Chambers, J. E.; Carr, R. L. Biochemical mechanisms contributing to species differences in insecticidal toxicity. *Toxicology* **1995**, *105*, 291-304.

Chambers, J. E.; Ma, T.; Scott Boone, J.; Chambers, H. W. Role of detoxication pathways in acute toxicity levels of phosphorothionate insecticides in the rat. *Life Sciences* **1994**, *54*, 1357-1364.

Damasio, J.; Guilhermino, L.; Soares, A. M. V. M.; Riva, M. C.; Barata, C. Biochemical mechanisms of resistance in *Daphnia magna* exposed to the insecticide fenitrothion. *Chemosphere* **2007**, *70*, 74-82.

Dauble, D. D.; Klopfer, D. C.; Carlile, D. W.; Jr., R. W. H. Usefulness of the Lipid Index for Bioaccumulation Studies with *Daphnia magna*. *Aquatic Toxicology and Hazard Assessment: Eighth Symposium* **1985**, 350-358.

David, P.; Dauphin-Villemant, C.; Mesneau, A.; Meyran, J. C. Molecular approach to aquatic environmental bioreporting: Differential response to environmental inducers of cytochrome P450 monooxygenase genes in the detritivorous subalpine planktonic Crustacea, Daphnia pulex. *Molecular Ecology* **2003**, *12*, 2473-2481.

de Bruijn, J.; Hermens, J. Uptake and elimination kinetics of organophosphorous pesticides in the guppy (Poecilia reticulata): Correlations with the octanol/water partition coefficient. *Environmental Toxicology and Chemistry* **1991**, *10*, 791-804.

de Wolf, W.; de Bruijn, J. H. M.; Seinen, W.; Hermens, J. L. M. Influence of biotransformation on the relationship between bioconcentration factors and octanol-water partition coefficients. *Environmental Science and Technology* **1992**, *26*, 1197-1201.

Derendorf, H.; Meibohm, B. Modeling of pharmacokinetic/pharmacodynamic (PK/PD) relationships: Concepts and perspectives. *Pharmaceutical Research* **1999**, *16*, 176-185.

Diamantino, T. C.; Almeida, E.; Soares, A. M. V. M.; Guilhermino, L. Characterization of cholinesterases from *Daphnia magna* Straus and their inhibition by zinc. *Bulletin of Environmental Contamination and Toxicology* **2003**, *71*, 219-225.

Dudai, Y.; Silman, I. The molecular weight and subunit structure of acetylcholinesterase preparations from the electric organ of the electric eel. *Biochemical and Biophysical Research Communications* **1974**, *59*, 117-124.

Duquesne, S. Effects of an organophosphate on *Daphnia magna* at suborganismal and organismal levels: Implications for population dynamics. *Ecotoxicology and Environmental Safety* **2006**, *65*, 145-150.

Elliott, J. E.; Wilson, L. K.; Langelier, K. M.; Mineau, P.; Sinclair, P. H. Secondary poisoning of birds of prey by the organophosphorus insecticide, phorate. *Ecotoxicology* **1997**, *6*, 219-231.

Ellman, G. L.; Courtney, K. D.; Andres, V.; Featherstone, R. M. A new and rapid colorimetric determination of acetylcholinesterase activity. *Biochemical Pharmacology* **1961**, *7*, 88-95.

Engels, H.; Neef, J.; Von Wachtendonk, D. Preparation and properties of acetylcholinesterase from the sea mussel *Mytilus edulis*. *Hoppe-Seyler's Zeitschrift fur Physiologische Chemie* **1978**, *359*, 1783-1795.

EPA Pesticides Industry Sales and Usage - 2000 and 2001 Market Estimates. *U.S. Environmental Protection Agency. Pesticide industry sales and usage.* http://www.epa.gov/oppbead1/pestsales **2004**.

EPA Aquatic Life Ambient Water Quality Criteria - Diazinon - Final. *U.S. Environmental Protection Agency.* http://water.epa.gov/scitech/swguidance/waterquality/standards/criteria/aqlife/pollutants/diazinon/index.cfm **2005**.

EPA Diazinon IRED Facts. *U.S. Environmental Protection Agency.* http://www.epa.gov/oppsrrd1/REDs/factsheets/diazinon_ired_fs.htm **2008**.

Escartin, E.; Porte, C. Bioaccumulation, metabolism, and biochemical effects of the organophosphorus pesticide fenitrothion in Procambarus clarkii. *Environmental Toxicology and Chemistry* **1996**, *15*, 915-920.

Escher, B. I.; Hermens, J. L. M. Modes of action in ecotoxicology: Their role in body burdens, species sensitivity, QSARs, and mixture effects. *Environmental Science and Technology* **2002**, *36*, 4201-4217.

Escher, B. I.; Hermens, J. L. M. Internal exposure: Linking bioavailability to effects. *Environmental Science and Technology* **2004**, *38*.

Eto, M. *Organophosphorus pesticides: organic and biological chemistry*; CRC Press, Inc.: Cleveland, Ohio, 1974.

Fabrizi, L.; Gemma, S.; Testai, E.; Vittozzi, L. Identification of the cytochrome P450 isoenzymes involved in the metabolism of diazinon in the rat liver. *Journal of Biochemical and Molecular Toxicology* **1999**, *13*, 53-61.

Fent, K. *Oekotoxikologie - Umweltchemie, Toxikologie, Oekologie*; Georg Thieme Verlag: Stuttgart, 1998.

Forget, J.; Livet, S.; Leboulenger, F. Partial purification and characterization of acetylcholinesterase (AChE) from the estuarine copepod *Eurytemora affinis* (Poppe). *Comparative Biochemistry and Physiology - C Toxicology and Pharmacology* **2002**, *132*, 85-92.

Forsberg, A.; Puu, G. Kinetics for the inhibition of acetylcholinesterase from the electric eel by some organophosphates and carbamates. *European Journal of Biochemistry* **1984**, *140*, 153-156.

Forsyth, C. S.; Chambers, J. E. Activation and degradation of the phosphorothionate insecticides parathion and EPN by rat brain. *Biochemical Pharmacology* **1989**, *38*, 1597-1603.

Fujioka, K.; Casida, J. E. Glutathione S-transferase conjugation of organophosphorus pesticides yields S-phospho-, S-aryl-, and S-alkylglutathione derivatives. *Chemical Research in Toxicology* **2007**, *20*, 1211-1217.

Fukami, J. Metabolism of Several Insecticides by Glutathione S-Transferase. *Pharmacology & Therapeutics* **1980**, *10*, 473-514.

Fukuto, T. R. Mechanism of action of organophosphorus and carbamate insecticides. *Environmental Health Perspectives* **1990**, *87*, 245-254.

Fukuto, T. R.; Metcalf, R. L. Structure and insecticidal activity of some diethyl substituted phenyl phosphates. *Journal of Agricltural and Food Chemistry* **1956**, *4*, 930-935.

Fukuto, T. R.; Metcalf, R. L. The effect of structure on the reactivity of alkylphosphonate esters. *Journal of the American Chemical Society* **1959**, *81*, 372-377.

Fulton, M. H.; Key, P. B. Acetylcholinesterase inhibition in estuarine fish and invertebrates as an indicator of organophosphorus insecticide exposure and effects. *Environmental Toxicology and Chemistry* **2001**, *20*, 37-45.

Gaddum, J. H. Reports on biological standards. III. Methods of biological assay depending on a quantal response. *Med. Research Council Spec. Rept.* **1933**, 1-46.

Gaddum, J. H. Bioassays and mathematics. *Pharmacological reviews* **1953**, *5*, 87-134.

Geyer, H. J.; Scheunert, I.; Bruggemann, R.; Steinberg, C.; Korte, F.; Kettrup, A. Qsar for Organic-Chemical Bioconcentration in Daphnia, Algae, and Mussels. *Science of the Total Environment* **1991**, *109*, 387-394.

Habig, C.; Di Giulio, R. T.; Abou-Donia, M. B. Comparative properties of channel catfish (Ictalurus punctatus) and blue crab (Callinectes sapidus) acetylcholinesterases. *Comparative Biochemistry and Physiology - C Pharmacology Toxicology and Endocrinology* **1988**, *91*, 293-300.

Habig, C.; Giulio, R. T. D. *Biochemical characteristics of cholinesterases in aquatic organisms*; Elsevier: Amsterdam, London, New York, Tokyo, 1991.

Hamers, T.; Molin, K. R. J.; Koeman, J. H.; Murk, A. J. A small-volume bioassay for quantification of the esterase inhibiting potency of mixtures of organophosphate and carbamate insecticides in rainwater: Development and optimization. *Toxicological Sciences* **2000**, *58*, 60-67.

Hawker, D. W.; Connell, D. W. Bioconcentration of Lipophilic Compounds by Some Aquatic Organisms. *Ecotoxicology and Environmental Safety* **1986**, *11*, 184-197.

Hermens, J. L. M. Electrophiles and acute toxicity to fish. *Environmental Health Perspectives* **1990**, *87*, 219-225.

Hernandez, M. M.; Rathinavelu, A. *Basic Pharmacology - Understanding Drug Actions and Reactions*; Taylor & Francis: Boca Raton, 2006.

Hogan, J. W.; Knowles, C. O. Metabolism of diazinon by fish liver microsomes. *Bulletin of Environmental Contamination and Toxicology* **1972**, *8*, 61-64.

Holmes, R. W.; de Vlaming, V. Monitoring of diazinon concentrations and loadings, and identification of geographic origins consequent to stormwater runoff from orchards in the Sacramento River watershed, U.S.A. *Environmental Monitoring and Assessment* **2003**, *87*, 57-79.

Ikenaka, Y.; Eun, H.; Ishizaka, M.; Miyabara, Y. Metabolism of pyrene by aquatic crustacean, *Daphnia magna*. *Aquatic Toxicology* **2006**, *80*, 158-165.

Jager, T.; Heugens, E. H. W.; Kooijman, S. A. L. M. Making sense of ecotoxicological test results: Towards application of process-based models. *Ecotoxicology* **2006**, *15*, 305-314.

Jager, T.; Kooijman, S. A. L. M. Modeling receptor kinetics in the analysis of survival data for organophosphorus pesticides. *Environmental Science & Technology* **2005**, *39*, 8307-8314.

Johnson, J. A.; Wallace, K. B. Species-related differences in the inhibition of brain acetylcholinesterase by paraoxon and malaoxon. *Toxicology and Applied Pharmacology* **1987**, *88*, 234-241.

Johnston, J. J.; Corbett, M. D. The uptake and in vivo metabolism of the organophosphate insecticide fenitrothion by the blue crab, Callinectes sapidus. *Toxicology and Applied Pharmacology* **1986**, *85*, 181-188.

Jusko, W. J.; Ko, H. C. Physiologic indirect response models characterize diverse types of pharmacodynamic effects. *Clinical Pharmacology and Therapeutics* **1994**, *56*, 406-419.

Kappers, W. A.; Edwards, R. J.; Murray, S.; Boobis, A. R. Diazinon is activated by CYP2C19 in human liver. *Toxicology and Applied Pharmacology* **2001**, *177*, 68-76.

Kasai, Y.; Konno, T.; Dauterman, W. C. *Role of Phosphorotriester Hydrolases in the Detoxication of Organophosphorus Insecticides*; Academic Press, Inc.: San Diego, California, 1992.

Keizer, J.; D'Agostino, G.; Vittozzi, L. The importance of biotransformation in the toxicity of xenobiotics to fish. I. Toxicity and bioaccumulation of diazinon in guppy (*Poecilia reticulata*) and zebra fish (*Brachydanio rerio*). *Aquatic Toxicology* **1991**, *21*, 239-254.

Keizer, J.; Dagostino, G.; Nagel, R.; Volpe, T.; Gnemi, P.; Vittozzi, L. Enzymological Differences of Ache and Diazinon Hepatic-Metabolism - Correlation of in-Vitro Data with the Selective Toxicity of Diazinon to Fish Species. *Science of the Total Environment* **1995**, *171*, 213-220.

Kemp, J. R.; Wallace, K. B. Molecular determinants of the species-selective inhibition of brain acetylcholinesterase. *Toxicology and Applied Pharmacology* **1990**, *104*, 246-258.

Kuhn, K.; Streit, B. Detecting sublethal effects of organophosphates by measuring acetylcholinesterase activity in *Gammarus*. *Bulletin of Environmental Contamination and Toxicology* **1994**, *53*, 398-404.

Kukkonen, J.; Oikari, A. Sulfate Conjugation Is the Main Route of Pentachlorophenol Metabolism in *Daphnia magna*. *Comparative Biochemistry and Physiology C-Pharmacology Toxicology & Endocrinology* **1988**, *91*, 465-468.

Landis, W. G.; Yu, M.-H. *Introduction to environmental toxicology: impacts of chemicals upon ecological systems*; CRC Press, Inc.: Boca Raton, 1995.

Landrum, P. F. Toxicokinetics of organic xenobiotics in the amphipod, *Pontoporeia hoyi*: Role of physiological and environmental variables. *Aquatic Toxicology* **1988**, *12*, 245-271.

Larkin, D. J.; Tjeerdema, R. S. Fate and effects of diazinon. *Reviews of Environmental Contamination and Toxicology, Vol 166* **2000**, *166*, 49-82.

Leblanc, G. A.; Cochrane, B. J. Identification of Multiple Glutathione S-Transferases from Daphnia-Magna. *Comparative Biochemistry and Physiology B-Biochemistry & Molecular Biology* **1987**, *88*, 39-45.

Legierse, K. C. H. M.; Verhaar, H. J. M.; Vaes, W. H. J.; De Bruijn, J. H. M.; Hermens, J. L. M. Analysis of the time-dependent acute aquatic toxicity of organophosphorus pesticides: The critical target occupation model. *Environmental Science & Technology* **1999**, *33*, 917-925.

Levi, P. E.; Hollingworth, R. M.; Hodgson, E. Differences in oxidative dearylation and desulfuration of fenitrothion by cytochrome P-450 isozymes and in the subsequent inhibition of monooxygenase activity. *Pesticide Biochemistry and Physiology* **1988**, *32*, 224-231.

Li, W. F.; Furlong, C. E.; Costa, L. G. Paraoxonase protects against chlorpyrifos toxicity in mice. *Toxicology Letters* **1995**, *76*, 219-226.

Lowry, O. H.; Rosebrough, N. J.; Farr, A. L.; Randall, R. J. Protein measurement with the Folin phenol reagent. *The Journal of Biological Chemistry* **1951**, *193*, 265-275.

Mackay, D.; Fraser, A. Bioaccumulation of persistent organic chemicals: mechanisms and models. *Environmental Pollution* **2000**, *110*, 375-391.

Mackay, D.; Puig, H.; McCarty, L. S. An equation describing the time course and variability in uptake and toxicity of narcotic chemicals to fish. *Environmental Toxicology and Chemistry* **1992**, *11*, 941-951.

Mackness, M. I.; Walker, C. H.; Rowlands, D. G.; Price, N. R. Esterase activity in homogenates of three strains of the rust red flour beetle Tribolium cast aneum (Herbst). *Comparative Biochemistry and Physiology - C Pharmacology Toxicology and Endocrinology* **1983**, *74*, 65-68.

Main, A. R. Affinity and phosphorylation constants for the inhibition of esterases by organophosphates. *Science* **1964**, *144*, 992-993.

Maxwell, D. M. The specificity of carboxylesterase protection against the toxicity of organophosphorus compounds. *Toxicology and Applied Pharmacology* **1992**, *114*, 306-312.

Maxwell, D. M.; Brecht, K. M.; Koplovitz, I.; Sweeney, R. E. Acetylcholinesterase inhibition: Does it explain the toxicity of organophosphorus compounds? *Archives of Toxicology* **2006**, *80*, 756-760.

McCarty, L. S.; Mackay, D. Enhancing Ecotoxicological Modeling and Assessment. *Environmental Science & Technology* **1993**, *27*, 1719-1728.

Mineau, P.; Fletcher, M. R.; Glaser, L. C.; Thomas, N. J.; Brassard, C.; Wilson, L. K.; Elliott, J. E.; Lyon, L. A.; Henny, C. J.; Bollinger, T.; Porter, S. L. Poisoning of raptors with organophosphorus and carbamate pesticides with emphasis on Canada, U.S. and U.K. *Journal of Raptor Research* **1999**, *33*, 1-37.

Monteiro, M.; Quintaneiro, C.; Morgado, F.; Soares, A. M. V. M.; Guilhermino, L. Characterization of the cholinesterases present in head tissues of the estuarine fish Pomatoschistus microps: Application to biomonitoring. *Ecotoxicology and Environmental Safety* **2005**, *62*, 341-347.

Mutch, E.; Williams, F. M. Diazinon, chlorpyrifos and parathion are metabolised by multiple cytochromes P450 in human liver. *Toxicology* **2006**, *224*, 22-32.

Naddy, R. B.; Klaine, S. J. Effect of pulse frequency and interval on the toxicity of chlorpyrifos to daphnia magna. *Chemosphere* **2001**, *45*, 497-506.

Newman, M. C.; McCloskey, J. T. The individual tolerance concept is not the sole explanation for the probit dose-effect model. *Environmental Toxicology and Chemistry* **2000**, *19*, 520-526.

Nuutinen, S.; Landrum, P. F.; Schuler, L. J.; Kukkonen, J. V. K.; Lydy, M. J. Toxicokinetics of organic contaminants in *Hyalella azteca*. *Archives of Environmental Contamination and Toxicology* **2003**, *44*, 467-475.

OECD OECD series on testing and assessment No. 23 - Guidance document on aquatic toxicity testing of difficult substances and mixtures. *ENV/JM/MONO(2000)6* **2000**.

OECD *OECD Guidline for Testing of Chemicals*. *Daphnia sp., Acute Immobilization Test*, 2004; Vol. 202.

Pedersen, J. A.; Yeager, M. A.; Suffet, I. H. Organophosphorus insecticides in agricultural and residential runoff: Field observations and implications for total maximum daily load development. *Environmental Science and Technology* **2006**, *40*, 2120-2127.

Poet, T. S.; Wu, H.; Kousba, A. A.; Timchalk, C. In vitro rat hepatic and intestinal metabolism of the organophosphate pesticides chlorpyrifos and diazinon. *Toxicological Sciences* **2003**, *72*, 193-200.

Pope, C.; Karanth, S.; Liu, J. Pharmacology and toxicology of cholinesterase inhibitors: Uses and misuses of a common mechanism of action. *Environmental Toxicology and Pharmacology* **2005**, *19*, 433-446.

Preuss, T. G. Personal communication

Preuss, T. G.; Hommen, U.; Alix, A.; Ashauer, R.; Van Den Brink, P.; Chapman, P.; Ducrot, V.; Forbes, V.; Grimm, V.; Schäfer, D.; Streissl, F.; Thorbek, P. Mechanistic effect models for ecological risk assessment of chemicals (MEMoRisk) - A new SETAC-Europe Advisory Group. *Environmental Science and Pollution Research* **2009**, *16*, 250-252.

Printes, L. B.; Callaghan, A. A comparative study on the relationship between acetylcholinesterase activity and acute toxicity in *Daphnia magna* exposed to anticholinesterase insecticides. *Environmental Toxicology and Chemistry* **2004**, *23*, 1241-1247.

Racke, K. D. *Degradation of organophophorus insecticides in environmental matrices*; Academic Press, Inc.: San Diego, California, 1992.

Reinert, K. H.; Giddings, J. M.; Judd, L. Effects analysis of time-varying or repeated exposures in aquatic ecological risk assessment of agrochemicals. *Environmental Toxicology and Chemistry* **2002**, *21*, 1977-1992.

Rozman, K. K.; Doull, J. Dose and time as variables of toxicity. *Toxicology* **2000**, *144*, 169-178.

Rubach, M. N.; Ashauer, R.; Buchwalter, D. B.; Lange, H. J. D.; Hamer, M.; Preuss, T. G.; Töpke, K.; Maund, S. J. Framework for traits-based assessment in ecotoxicology. *Integrated environmental assessment and management* **2010a**, *in press, available online*.

Rubach, M. N.; Ashauer, R.; Maund, S. J.; Baird, D. J.; Van Den Brink, P. J. Toxicokinetic variation in 15 freshwater arthropod species exposed to the insecticide chlorpyrifos. *Environmental Toxicology and Chemistry* **2010b**, *29*, 2225-2234.

Rubach, M. N.; Baird, D. J.; Van Den Brink, P. J. A new method for ranking mode-specific sensitivity of freshwater arthropods to insecticides and its relationship to biological traits. *Environmental Toxicology and Chemistry* **2010c**, *29*, 476-487.

Sancho, E.; Ferrando, M. D.; Andreu, E. Response and recovery of brain acetylcholinesterase activity in the European Eel, *Anguilla anguilla*, exposed to fenitrothion. *Ecotoxicology and Environmental Safety* **1997**, *38*, 205-209.

Schwarzenbach, R. P.; Gschwend, P. M.; Imboden, D. M. *Environmental organic chemistry*, 2nd ed.; John Wiley & Sons, Inc.: Hoboken, New Jersey, 2003.

Shishido, T.; Usui, K.; Sato, M.; Fukami, J. i. Enzymatic conjugation of diazinon with glutathione in rat and American cockroach. *Pesticide Biochemistry and Physiology* **1972**, *2*, 51-63.

Smedes, F. Determination of total lipid using non-chlorinated solvents. *Analyst* **1999**, *124*, 1711-1718.

Spacie, H. Alternative models for describing the bioconcentration of organiscs in fish. *Environmental Toxicology and Chemistry* **1983**, *1*, 309-320.

Stoob, K.; Singer, H. P.; Goetz, C. W.; Ruff, M.; Mueller, S. R. Fully automated online solid phase extraction coupled directly to liquid chromatography-tandem mass spectrometry: Quantification of sulfonamide antibiotics, neutral and acidic pesticides at low concentrations in surface waters. *Journal of Chromatography A* **2005**, *1097*, 138-147.

Sturm, A.; Hansen, P. D. Altered cholinesterase and monooxygenase levels in Daphnia magna and Chironomus riparius exposed to environmental pollutants. *Ecotoxicology and Environmental Safety* **1999**, *42*, 9-15.

Sultatos, L. G. *Role of Glutathione in the Mammalian Detoxication of organophosphorus Insecticides*; Academic Press, Inc.: San Diego, California, 1992.

Takimoto, Y.; Ohshima, M.; Miyamoto, J. Comparative metabolism of fenitrothion in aquatic organisms. 3. Metabolism in the crustaceans, *Daphnia pulex* and *Palaemon paucidens*. *Ecotoxicology and Environmental Safety* **1987a**, *13*, 126-134.

Takimoto, Y.; Ohshima, M.; Miyamoto, J. Comparative metabolism of fenitrothion in aquatic organisms. I. Metabolism in the euryhaline fish, Oryzias latipes and Mugil cephalus. *Ecotoxicology and Environmental Safety* **1987b**, *13*, 104-117.

Takimoto, Y.; Ohshima, M.; Miyamoto, J. Comparative metabolism of fenitrothion in aquatic organisms. II. Metabolism in the freshwater snails, Cipangopaludina japonica and Physa acuta. *Ecotoxicology and Environmental Safety* **1987c**, *13*, 118-125.

Tang, J.; Chambers, J. E. Detoxication of paraoxon by rat liver homogenate and serum carboxylesterases and A-esterases. *Journal of Biochemical and Molecular Toxicology* **1999**, *13*, 261-268.

Tsuda, T.; Kojima, M.; Harada, H.; Nakajima, A.; Aoki, S. Acute toxicity, accumulation and excretion of organophosphorous insecticides and their oxidation products in killifish. *Chemosphere* **1997**, *35*, 939-949.

Vaal, M.; Van der Wal, J. T.; Hermens, J.; Hoekstra, J. Pattern analysis of the variation in the sensitivity of aquatic species to toxicants. *Chemosphere* **1997a**, *35*, 1291-1309.

Vaal, M.; Van der Wal, J. T.; Hoekstra, J.; Hermens, J. Variation in the sensitivity of aquatic species in relation to the classification of environmental pollutants. *Chemosphere* **1997b**, *35*, 1311-1327.

Vaal, M. A.; Van Leeuwen, C. J.; Hoekstra, J. A.; Hermens, J. L. M. Variation in sensitivity of aquatic species to toxicants: Practical consequences for effect assessment of chemical substances. *Environmental Management* **2000**, *25*, 415-423.

Van den Heuvel, M. R.; McCarty, L. S.; Lanno, R. P.; Hickie, B. E.; Dixon, D. G. Effect of total body lipid on the toxicity and toxicokinetics of pentachlorophenol in rainbow trout (*Oncorhynchus mykiss*). *Aquatic Toxicology* **1991**, *20*, 235-252.

Van der Hoeven, N.; Gerritsen, A. A. M. Effects of chlorpyrifos on individuals and populations of *Daphnia pulex* in the laboratory and field. *Environmental Toxicology and Chemistry* **1997**, *16*, 2438-2447.

Van Wezel, A. P.; Opperhuizen, A. Narcosis due to environmental pollutants in aquatic organisms: Residue-based toxicity, mechanisms, and membrane burdens. *Critical Reviews in Toxicology* **1995**, *25*, 255-279.

Verhaar, H. J. M.; De Wolf, W.; Dyer, S.; Legierse, K. C. H. M.; Seinen, W.; Hermens, J. L. M. An LC50 vs time model for the aquatic toxicity of reactive and receptor-mediated compounds. Consequences for bioconcentration kinetics and risk assessment. *Environmental Science & Technology* **1999**, *33*, 758-763.

Verhaar, H. J. M.; Van Leeuwen, C. J.; Hermens, J. L. M. Classifying environmental pollutants. 1: Structure-activity relationships for prediction of aquatic toxicity. *Chemosphere* **1992**, *25*, 471-491.

Walker, C. H.; Thompson, H. M. *Phylogenetic Distribution of Cholinesterases and Related Esterases*; Elsevier: Amsterdam, London, New York, Tokyo, 1991.

Wallace, K. B. Species-selective toxicity of organophopshorus insecticides: a pharmacodynamic phenomenon. In *Organophosphates. Chemistry, Fate, and Effects*; Chambers, J. E., Levi, P. E., Eds.; Academic Press, Inc.: San Diego, California 1992.

Wallace, K. B.; Herzberg, U. Reactivation and aging of phosphorylated brain acetylcholinesterase from fish and rodents. *Toxicology and Applied Pharmacology* **1988**, *92*, 307-314.

Wallace, K. B.; Kemp, J. R. Species specificity in the chemical mechanisms of organophosphorus anticholinesterase activity. *Chemical Research in Toxicology* **1991**, *4*, 41-49.

Wang, C.; Murphy, S. D. Kinetic analysis of species difference in acetylcholinesterase sensitivity to organophosphate insecticides. *Toxicology and Applied Pharmacology* **1982**, *66*, 409-419.

Wittmer, I. K.; Bader, H. P.; Scheidegger, R.; Singer, H.; Lück, A.; Hanke, I.; Carlsson, C.; Stamm, C. Significance of urban and agricultural land use for biocide and pesticide dynamics in surface waters. *Water Research* **2010**, *44*, 2850-2862.

Xuereb, B.; Noury, P.; Felten, V.; Garric, J.; Geffard, O. Cholinesterase activity in *Gammarus pulex* (Crustacea Amphipoda): Characterization and effects of chlorpyrifos. *Toxicology* **2007**, *236*, 178-189.

Zhao, Y.; Newman, M. C. The theory underlying dose-response models influences predictions for intermittent exposures. *Environmental Toxicology and Chemistry* **2007**, *26*, 543-547.

Zöllner, N.; Kirsch, K. Über die quantitative Bestimmung von Lipoiden (Mikromethode) mittels der vielen natürlichen Lipoiden (allen bekannten Plasmalipoiden) gemeinsamen Sulfophosphovanillin-Reaktion. *Zeitschrift für Die Gesamte Experimentelle Medizin* **1962**, *135*, 545-561.

Danksagung

Nach vier Jahren Eawag möchte ich allen danken, die zum Gelingen dieser Doktorarbeit beigetragen haben und die Zeit an der Eawag so unvergesslich interessant, spannend und ereignisreich gemacht haben.

Ganz herzlicher Dank gebührt vor allem meinen beiden „Doktormüttern“ Frau Prof. Beate Escher und Frau Prof. Juliane Hollender für ihre hervorragende und sehr kompetente Betreuung und Förderung in den letzten Jahren. Nicht selbstverständlich waren ihr Vertrauen und die Geduld, mich als Doktoranden mit überwiegend physikalisch-chemischen Vorkenntnissen in der Arbeit im Ultrahochvakuum doch mit Wasserflöhen experimentieren zu lassen. Unermüdlich und trotz Zeitverschiebung zwischen der Schweiz und Australien, wo Prof. Escher seit einiger Zeit tätig ist, standen sie mir jederzeit mit Rat, Tat und Bereitschaft zur Diskussion zur Seite.

• Roman Ashauer war mir ein ausgezeichneter Berater und Mentor rund um das Thema Toxikokinetik und Toxikodynamik in Wasserfloh und *Gammarus*

• Piet Spaak und seiner Gruppe danke ich sehr für zahlreiche Diskussionen und die äußerst kollegiale Zusammenarbeit bei der Aufzucht der Daphnien, hier speziell Christine Dambone und Esther Keller

• Auch Thomas Preuss und Katrin Hoffmann von der RWTH Aachen bin ich sehr zu Dank verpflichtet, da sie mir Daphnien zur Verfügung stellten und bzgl. Umgang mit diesen immer als Ansprechpartner zur Verfügung standen.

•Kristina Hitzfeld beflügelte meine Forschungen im Rahmen eines viermonatigen Praktikums durch enorm produktive Zusammenarbeit. Tjalling Jager stand mir mit konstruktiven Gesprächen und Kommentierungen zur Seite. Andreas Focks danke ich für anregende Diskussionen.

• Der ganzen UCHEM schulde ich grossen Dank für Hilfe und Unterstützung besonders in chemisch-analytischen Fragen. Aber nicht nur im Labor, auch bei vielen außerdienstlichen geselligen Anlässen war es immer sehr lustig. Danke für die wunderbare Zeit!

• Die Abteilung UTOX unterstützte mich äußerst zuverlässig bei der Durchführung von toxikologischen Experimenten; besonderer Dank geht an Christina und die gesamte Escher-Group

• Auch der Abteilung UMIK danke ich für ihre Unterstützung im Labor.

• Special thanks to the office E22, Aurea, Damian and Luba: I thank you guys for the amazing time with you and the fishes and all the plants! This office really rocks!!

• In Erinnerung werden mir die unzähligen Aktivitäten während der Disszeit innerhalb und außerhalb der Eawag mit vielen Weggefährten bleiben, mit Holgi, Tobi, Corine, Aurea, Damian, Luba, Jörg, Holger T., Merle, Junho, Flavio, Danielle, Nadine, Christina, Anita, Roman, Thomas, Sybille, Christian, Stephan,

Judith, Etienne, Tobi D., Irene W., Irene H., Martin, Sebi, Jürgen, Phillip, Joseph, Anna, Karin, Marius, Franziska, Miguel, Simon, Benni, WG-Mitbewohner, Bandkollegen, Freunde uvm.- es ist nie langweilig geworden.

• Neben der Dankbarkeit für all die fachliche und menschliche Unterstützung gebührt mein Dank aber auch der Eawag für die finanzielle Unterstützung meiner Doktorarbeit

• An letzter Stelle sei meine Familie genannt, die in den vergangenen Jahren im Hintergrund immer für mich da war.

Curriculum Vitae

Andreas Christopher Kretschmann	born on August 5, 1979 in Nürnberg, Germany
2006 - 2010	PhD at the Swiss Federal Institute of Aquatic Science and Technology (Eawag), Dübendorf/ Swiss Federal Institute of Technology (ETH), Zurich, Switzerland
2005 - 2006	Diploma thesis at Friedrich-Alexander University Erlangen-Nürnberg: *Metallierung von Porphyrinen und Adsorption von kleinen Molekülen an Metalloporphyrinschichten auf einer Ag (111)-Oberfläche im Ultrahochvakuum*
2000 - 2006	Study of chemistry at the Friedrich-Alexander University Erlangen-Nürnberg
1999 - 2000	Alternative civilian service, Bund Naturschutz in Bayern e.V., Germany
1997 - 1999	Pirckheimer-Gymnasium Nürnberg, Germany (Abitur 1999)
1990 - 1997	Adalbert Stifter-Gymnasium Passau, Germany